

THERMAL AND MECHANICAL MANIPULATION OF IRON OXIDE
NANOPARTICLES FOR TARGETED DRUG/GENE DELIVERY AND
THERAPEUTICS

by

MERVE ZUVİN

Submitted to the Graduate School of Engineering and Natural Sciences

in partial fulfillment of

the requirements for the degree of

Doctor of Philosophy

SABANCI UNIVERSITY

JANUARY 2019

THERMAL AND MECHANICAL MANIPULATION
OF IRON OXIDE NANOPARTICLES
FOR TARGETED DRUG/GENE DELIVERY AND THERAPEUTICS

APPROVED BY:

Prof. Dr. Ali Koşar
(Dissertation Supervisor)



Prof. Dr. Devrim Gözünçak



Prof. Dr. Kürşat Şendur



Assec. Prof. Dr. Havva Yağcı Acar



Asst. Prof. Dr. Yegan Erdem



DATE OF APPROVAL: 04/01/2019

© Merve Zuvın 2019

All Rights Reserved

ABSTRACT

THERMAL AND MECHANICAL MANIPULATION OF IRON OXIDE NANOPARTICLES FOR TARGETED DRUG/GENE DELIVERY AND THERAPEUTICS

MERVE ZUVİN

Ph.D. Dissertation, January 2019

Dissertation Supervisor: Prof. Dr. Ali Koşar

Keywords: Hyperthermia, induction heating, breast cancer, superparamagnetic iron oxide nanoparticles, magnetic actuation, magnetofection

Superparamagnetic iron oxide nanoparticles provide a platform to deliver therapeutic agents to any desired group of cells in a safe fashion. These particles can be manipulated by externally applied magnetic fields, targeted to specific tissues and

heated in focused fields for cancer treatment. Hyperthermia performance of SPIONs depends on the magnetic field strength as well as the field frequency. A part of this dissertation displays the therapeutic effect of Poly(acrylic acid)-coated, anti-HER2-tagged SPIONs on breast cancer cells using a low magnetic field strength of 0.8 kAm^{-1} , which is significantly lower compared to the literature, with a frequency of 400 kHz. HER2-positive SKBR3 and MDA-MB-453 cell lines successfully internalized the nanoparticles. The particles, which were not toxic to these cell lines, led to a prominent decrease in cell proliferation and survival in MDA-MB-453 cells when subjected to hyperthermia.

Gene therapy is another developing method for the treatment of various diseases. A strong alternative is magnetofection, which involves the use of SPIONs and external magnetic field to enhance the localization of SPIONs at the target site. A new magnetic actuation system consisting of four rare earth magnets on a rotary table was designed and manufactured to have improved magnetofection. The actuation effect was revealed with green fluorescent protein DNA bearing-nanoparticle transfection to MCF7 cells. The applied magnetic field in this system increased the transfection efficiency and viability relative to traditional transfection methods. At the same time, it also reduced the transfection time (down to 1 hour) of the standard polyethylenimine transfection protocol.

ÖZET

DEMİR OKSİT NANOPARÇACIKLARIN İLAÇ/GEN TAŞINIMI VE TEDAVİ AMAÇLARI İÇİN İSİSAL VE MEKANİK MANİPÜLASYONU

MERVE ZUVİN

Doktora Tezi, Ocak 2019

Tez Danışmanı: Prof. Dr. Ali Koşar

Anahtar Kelimeler: Hipertermi, indüksiyon ısınma, meme kanseri, süperparamanyetik demir oksit nanoparçacık, manyetik eyleme, magnetofeksiyon

Süperparamanyetik demir oksit nanoparçacıklar, tedavi amaçlı kullanılacak ajanları istenen herhangi bir hücre grubuna güvenli bir şekilde ulaştırmak için bir platform sağlar. Bu parçacıklar, uygulanan manyetik alanla manipüle edilebilir, spesifik dokulara gönderilebilir ve bu alanlarda ısıtılarak kanser tedavisi için kullanılabilir. SPION'ların

hipertermi performansı, manyetik alan frekansının yanı sıra manyetik alan kuvvetine de bağlıdır. Bu tezin bir kısmında, poli (akrilik asit) ile kaplanmış, anti-HER2-etiketli SPION'ların, 0.8 kAm^{-1} 'lik bir düşük manyetik alan kuvveti ve frekans olarak 400 kHz frekanslı kullanılarak, meme kanseri hücreleri üzerindeki tedavi amaçlı etkisi gösterilmiştir. Nanoparçacıklar başarıyla HER2-pozitif SKBR3 ve MDA-MB-453 hücre hatlarına gönderilmiş ve bu hücre hatları için toksik olmayan parçacıklar, hipertermiye tabi tutulduğunda MDA-MB-453 hücrelerinde hücre çoğalmasında ve hayatta kalmada belirgin bir azalmaya yol açmıştır.

Gen terapisi, çeşitli hastalıkların tedavisi için bir başka gelişmekte olan yöntemdir. Güçlü bir alternatif, SPION'ların ve hedef alandaki lokalizasyonunu geliştirmek için harici manyetik alan kullanımını içeren manyetofeksiyondur. Döner tablada dört adet nadir toprak mıknatısından oluşan yeni bir manyetik harekete geçirme sistemi geliştirilmiş, manyetofeksiyona sahip olacak şekilde tasarlanmış ve üretilmiştir. Aktive edici etki, MCF7 hücrelerine yeşil flüoresan protein DNA taşıyan-nanoparçacık transfeksiyonu ile ortaya çıkarılmıştır. Bu sistemdeki uygulanan manyetik alan, transfeksiyon verimliliğini ve geleneksel transfeksiyon yöntemlerine göre canlılığı arttırmıştır. Aynı zamanda, standart polietilenimin transfeksiyon protokolünün transfeksiyon süresini (1 saate kadar) azaltmıştır.

To my family,

ACKNOWLEDGEMENTS

I wish to thank my thesis advisor Prof. Dr. Ali Koşar for letting me be a part of his team, and his constant support. He was more than an advisor along the way with his guidance and patience. He was the most reachable advisor anyone could have.

I thank Prof. Dr. Devrim Gözüaçık who has given the opportunity to learn cell culture and letting me perform these experiments by myself. None of that would happen if he did not give me permission.

I wish to thank Prof. Dr. Kürşat Şendur for never turning me down when I have a question and his guidance helped me a lot during my PhD period.

I am thankful to Assoc. Prof. Dr. Havva Yağcı Acar who is also our project leader for induction studies. I always felt that she was there for me any time I need. She also showed patience to all my questions and I had answers kindly and willingly everytime I need.

I would like to thank Assist. Prof. Dr. Yegan Erdem for sacrificing her time for both evaluating my thesis and defense presentation.

I wish to express my gratitude to Prof. Dr. Cem Güneri, Prof. Dr. Albert Erkip, Assoc. Prof. Kağan Kurşungöz, Dr. Şirin Kaya, and Dr. Matteo Paganin. All these years I was the part of MATH101 course and they were more than lecturers or coordinators. They were sometimes friends, sometimes mentors but all in all I am so grateful that I had the chance to spend time with them.

I would like to thank all my friends in Koşar Lab. I would like thank Dr. Ebru Demir for being there for me everytime day and night for 5 years. Dr. Zaeema Khan you are a great friend, a life-long friend. I would like to thank Yağmur Büyüköztürk for her great patience and for being a good friend. I thank Kadir Uzun for being such good friend even though we did not know each other so long, he is a great friend and such a great personality to know. I thank Mr. İlker Sevgen for being our İlker Abi in any circumstance such as helping with our setups or our discussion about life and so on. Dr. Öznur Bayraktar and Masoumeh Nedaei are also my long-time friends who taught and showed me the loyalty in friendship.

I would like to thank my family and for those who are family to me. I thank parents Hilal Zuvin and Mehmet Zuvin for their unconditional love, support and patience. I am thankful for everything they did during my PhD. I thank little my brother Safa Mert Zuvin also his support and taking me out for a coffee and for some chocolate. I would like to thank my aunt Meral Kardeřkaya for being a half mother for me all my life. I also want to thank Serap Yılmaz, Füsün Kökenler, Pınar Kızılyel and Nurřen Öztařkın for bearing my constant talk about PhD life, their advices, support and love.

Finally, I would like to thank TUBİTAK project number 213M669 for financial support.

TABLE OF CONTENTS

1	INTRODUCTION	17
	1.1. Literature Review	18
	1.1.1 Types Of Therapeutic Nanoparticles	18
	1.1.1.1. Nano-Structured Particles.....	19
	1.1.1.1.1 Polymeric particles	19
	1.1.1.1.2. Non-polymeric particles	22
	1.1.1.1.3. Lipid-based nanoparticles.....	24
	1.1.1.2. Nanocrystalline particles	25
	1.1.2. Targeted Delivery Applications of Therapeutic Nanoparticles	26
	1.1.2.1. Cancer.....	26
	1.1.2.2. Infectious Diseases	28
	1.1.2.3. Autoimmune Diseases	30
	1.1.2.4. Cardiovascular Diseases	31
	1.1.2.5. Neurodegenerative Diseases.....	32
	1.1.2.6. Ocular Diseases	34
	1.1.2.7. Pulmonary Diseases	35
	1.1.2.8. Regenerative Therapy.....	35
	1.1.3. Magnetic Nanoparticles	36
	1.1.3.1. Physicochemical Characteristics of Magnetic Nanoparticles	37
	1.1.3.1.1. Shape and Size.....	37

1.1.3.1.2 Surface Properties and Coating	38
1.1.3.1.3. Functionalization	40
1.1.3.1.4 Magnetization Characteristics of Superparamagnetic Nanoparticles	40
1.1.3.2. Biomedical Applications	41
1.1.3.2.1 Magnetic Resonance Imaging (MRI)	41
1.1.3.2.2. Magnetic Hyperthermia.....	42
1.1.3.2.3. Drug delivery.....	46
1.1.3.3. Limitations for the utility of MNPs in biomedical applications....	50
1.2 Motivation.....	52
2 THERMAL MANIPULATION OF IRON OXIDE NANOPARTICLES FOR THERAPEUTIC PURPOSES	54
2.1 Methodology.....	55
2.1.1. Materials.....	55
2.1.2 Synthesis of Nanoparticles.....	55
2.1.3. Nanoparticle Characterization.....	56
2.1.4. Experimental setup and procedure	57
2.1.5. Cell Culture	58
2.1.6. Flow cytometry analysis	58
2.1.7. Cytotoxicity assay	59
2.1.8. Immunofluorescence Analysis	59
2.1.9. Statistical Analyses	59
2.3 Results.....	59
2.4. Discussion.....	64
3 MECHANICAL MANIPULATION OF IRON OXIDE NANOPARTICLES FOR GENE DELIVERY	67
3.1. Methodology.....	68

3.1.1. Cells and Reagents	68
3.1.2. Magnetic Actuation System	69
3.1.3. PEI-SPION Synthesis and Characterization	69
3.1.4. Plasmid DNA Isolation	69
3.1.5. Cell Culture	70
3.1.6. Magnetofection	70
3.1.7. Microscopy Analysis and Transfection Efficiency	70
3.1.8. Cell Viability Assays	70
3.2. Results.....	71
3.2.1. Actuation System	71
3.2.2. Cell experiments	76
3.3. Discussion.....	78
4 CONCLUSIONS	82
5 FUTURE WORK	84
6 REFERENCES	85

LIST OF FIGURES

Figure 1.1 Classification of nanotechnology based methods	18
Figure 1.2 Different nanoparticles for therapeutic purposes.....	19
Figure 1.3 Different heating mechanisms for magnetic nanoparticles [263]	43
Figure 1.4 a) Drug loaded nanoparticles agglomerate in the tumor site only with the help of an external magnetic field, b) After drug release, the external force is removed, allowing the nanoparticles to disperse and ready to be cleared from the body.	47
Figure 1.5 Schematic representation of a) EPR effect b) active targeting c) magnetic targeting [293]	48
Figure 2.1 a) Induction coil setup, b) Schematic of the procedure	57
Figure 2.2 a) Sample TEM image of SP nanoparticles, b) VSM measurement result.....	60
Figure 2.3 Thermal camera and experimental images of SPIONs, SP01 and SP02 indicate the surfaces of measurement a) Initial temperature, no heating observed b) Final temperature, yellow color shows the heated SPIONs.....	61
Figure 2.4 Experiments with 96 well plate and image of the cells after exposure. a) Cells are seeded on one part of 96 well plate and put in induction coil for 10 min, b) Cell alignment after 10 min of magnetic field exposure, arrows show nanoparticle alignments.....	62
Figure 2.5 Toxicity and targeting analysis of nanoparticles, in SKBR3 and MDA-MB-453 cells. (a) Viability of cells treated with different concentrations of 5 to 500 μg (n=3, p<0.05) (b) Confocal microscopy analysis of Alexa-fluor-647 conjugated SP-H and SP treated MDA-MB-453 and SKBR3 cells, (c) Flow cytometry analysis of the particles after 12 h treatment ($150 \mu\text{g mL}^{-1}$).....	63

Figure 2.6 Death and viability analysis of MDA-MB-453. Cell death (%) determined by the Trypan blue exclusion assay (a), and cell viability (%) determined by MTT assay of control cells (CNT, which are not treated with nanoparticle), cells treated with 150 μgmL^{-1} SP or SP-H and subjected to inductive heating for 5 min (a, b) and 10 min (c). n=3, p value <0.05 for statistical significance 64

Figure 3.1 Actuation system and experimental procedure. a) Magnetic actuation system b) Schematic representation of experimental steps, introducing the agents - magnetic field exposure - during exposure - removing agents after exposure - gfp expressed cells after 48 hours incubation. 71

Figure 3.2 Model of the study. a) Modeling setup b) Sizes of magnets c) General view of mesh configuration d) Close up view of mesh configuration..... 72

Figure 3.3 Simulation results and 3D magnetic flux density norm patterns of the magnetic system. a) Maximum magnetic force occurs at 2 cm, b) at 2.5 cm circulation starts, c,d) non concentrated magnetic force is observed at the heights of 3 and 3.5cm, e) at the height of 6 cm magnetic fluxes are combined to an circular pattern, and the magnetic force significantly decreases. f) Red line represents densities at the distances of 2, 2.5 and 3cm, orange and yellow ones correspond to the heights of 5 and 6 cm respectively, light and dark blue represents the lowest magnetic flux density at every level..... 74

Figure 3.4 Iron dust particle experiments. a) under uniform magnetic field, dusts particles cluster near the magnets and the edges, b) under non-uniform magnetic field dusts begin to distribute throughout the plate, when the system is operational c) dusts align successively, d) lift e) roll and change direction in their own axis, f) lift again. 75

Figure 3.5 Transfection efficiency with respect to distance. PEI and PEI SPION two mag samples are used as control (a,b). After 48 hours incubation, fluorescence images of the samples for each distance are shown (c,d,e,f), Transfection performance of the device is tested at different distances between the rotary table and sample (g)... 77

Figure 3.6 Transfection Efficiency and Viability Assay. MCF7 cell lines transfected with nanoparticles were exposed to rotating magnetic field for 1h, PEI, 79

LIST OF ABBREVIATIONS

SPION	Superparamagnetic iron oxide nanoparticle
PAA	Polyacrylic acid
HER2	Herceptin2
SP	Spion PAA
SP-H	Spion/PAA/antiHER2
DMEM	Dulbecco's modified Eagle's medium
MDA-MB-453	Human breast cancer line
MCF7	Human breast cancer cell line
SPION	Superparamagnetic iron oxide nanoparticle
PEI	Polyethyleneimine
PS	PEI-SPION
PS wo	PEI-SPION without magnetic field
PS rot	PEI-SPION with rotary magnetic field
GFP	Green fluorescent protein

1 INTRODUCTION

Nanomedicine is a new approach for understanding nanotechnological systems for disease diagnosis and therapy. This branch of nanotechnology is classified into two main categories: nanodevices and nanomaterials. Nanodevices are miniature devices in nanoscale and including microarrays [1], [2], or some intelligent machines like respirococytes [3]. Nanomaterials contain nanoparticles, smaller than 100 nanometers (nm) in at least one dimension.

Recent exploration of biomedical science results in successful improvement of designing therapeutic agents in disease treatment. However, a major problem in treatment of many diseases is the delivery of therapeutic agents to the desirable site. Application of conventional agents has problems such as non-selectivity, undesirable side effects, low efficiency and poor biodistribution [4]. Therefore, the focus of current research activities is to design well-controlled and multifunctional delivery systems. Association of therapeutic agents with nanoparticles exhibiting unique physicochemical and biological properties and designing their pathways for suitable targeting is a promising approach in delivering a wide range of molecules to desired sites in the body [5]. This targeted strategy enhances the concentration of therapeutic agent in cells/tissues; thereby low doses of agent can be used, particularly if there is a contradiction between the therapeutic results or toxic effects of an agent. Moreover, increasing concentration of therapeutic agents only in-targeted area improves its therapeutic index by enhancing their efficacy and/or increasing their tolerability in

biological systems. Water-insoluble therapeutic agents can also combine with nanoparticles, which can protect them from physiological barriers and improve their bioavailability. Furthermore, association of therapeutic nanoparticles with contrast agents allows for the tracking of their pathways and imaging of their delivery site in *in vivo* systems. Figure 1.1 gives an overview of nanotechnology methods for biomedical applications

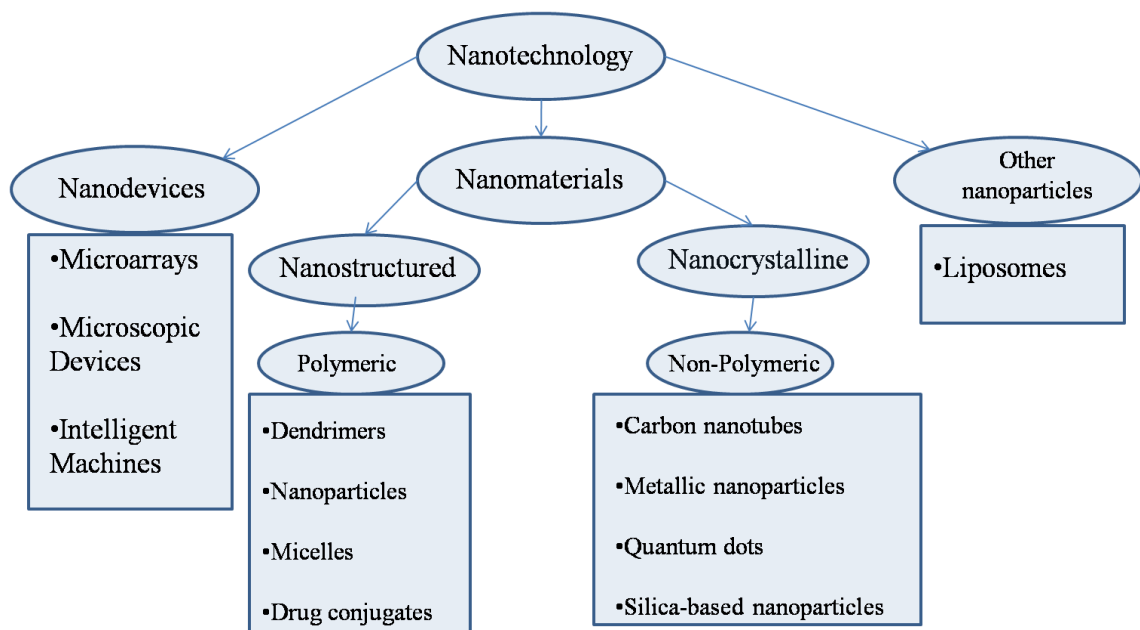


Figure 1.1 Classification of nanotechnology based methods

1.1. Literature Review

1.1.1 Types Of Therapeutic Nanoparticles

Nanomaterials can be classified into two categories: Nano-structured and nano-crystalline. Nanostructured materials can be further categorized into polymeric, non-polymeric and lipid-based categories. Polymeric nanoparticles include dendrimers, nanoparticles, micelles and drug conjugates. Non-polymeric nanoparticles include carbon nanotubes, metallic nanoparticles, quantum dots and silica-based nanoparticles. Lipid-based nanoparticles can be divided into liposomes and solid-lipid nanoparticles.

So far, most of the nanoparticles clinically approved for therapeutic use have polymeric or lipid-based components. Apart from polymeric/non-polymeric or lipid-based nano-structured particles, nano-crystalline particles that are formed by the combination of therapeutic agent in crystalline form are also used in some clinical applications. In this section, we summarized the type of clinically used nanoparticles and their specificity for therapeutic applications, as well as their current delivery strategies in challenging pathophysiological conditions. Figure 1.2 illustrates the different types of nanoparticles.

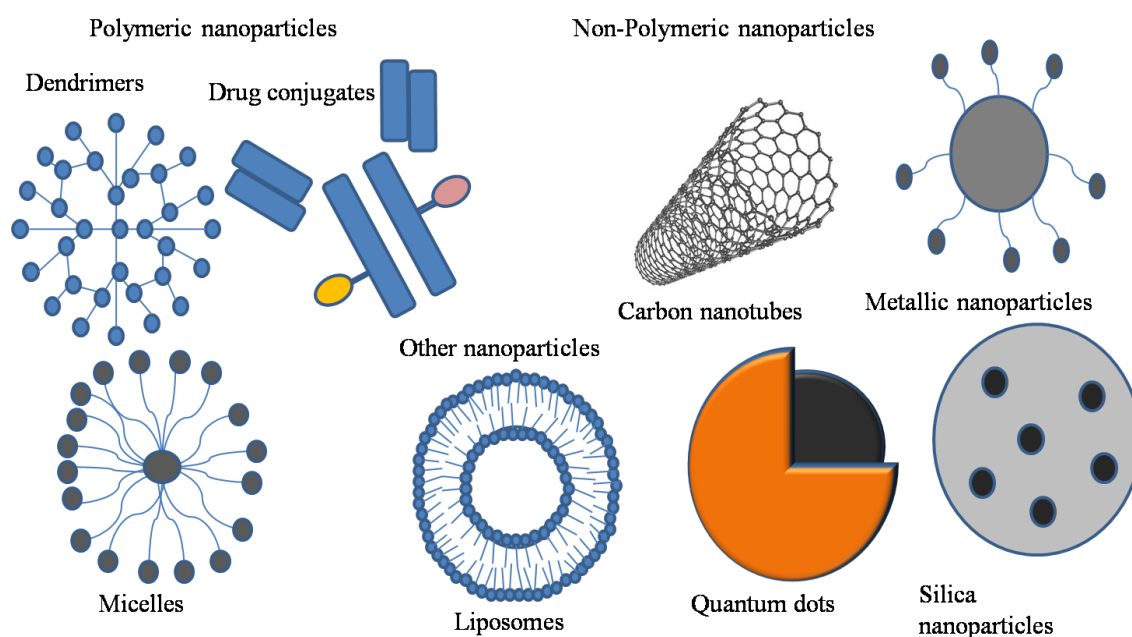


Figure 1.2 Different nanoparticles for therapeutic purposes

1.1.1.1. Nano-Structured Particles

1.1.1.1.1 Polymeric particles

1.1.1.1.1.1 Dendrimers

Dendrimers are favorable polymers in clinical applications due to their hyperbranched, compartmental and low polydispersity index. Controlling the number of branching in these polymeric nanoparticles allows to fabricate them in very small sizes (1-5 nm). They can be fabricated by polymerization in spherical shape, which leads to the formation of cavities within the dendrimer molecule, and this entrapment efficiency can be used for delivery of therapeutic agents. In addition, there are free end groups in

the structure of dendrimers that can be easily modified for conjugation of biocompatible compounds with low cytotoxicity and high biopermeability. The structure of dendrimers can also be supplied with surface functionalization allowing to improve target-specific delivery of therapeutic agents. Assembling them by either encapsulation or complexation makes dendrimers attractive vehicles for concomitant delivery of biologically active molecules such as vaccines, drugs and genes to the desired sites. Currently, single or combination of different polymers, such as polyethyleneimine, polyamidoamine, poly-(propyleneimine), chitin etc. are used for therapeutic applications in the form of dendrimers [6], [7].

1.1.1.1.2. Nanoparticles

Polymeric nanoparticles provide an alternative way for therapeutic applications, because they consist of either synthetic or natural polymers, which makes them biocompatible, non-immunogenic, non-toxic and biodegradable carriers [8]. Due to some immunogenic and toxic problems, synthetic polymers like polycaprolactone (PCL), polylactic acid (PLA) and monomers are usually used in the form of polyesters. On the other hand, natural polymer-based nanoparticles composed of chitosan, gelatin, albumin and alginate overcome toxicity problems and provide significant improvement in the efficiency of therapeutic agents compared to conventional methods. Polymeric nanoparticles are considered as a matrix system, in which the matrix is uniformly dispersed. They can be classified as nanocapsules or nanospheres depending on their composition. In nanocapsules, therapeutic agents are enclosed by a unique polymer membrane, while agents are directly dispersed throughout or within the polymer matrix in nanospheres [9]. Existence of the multitude preparation method of polymeric nanoparticles can control the release characteristics of incorporated therapeutic agents, which allows delivery of a higher concentration of agents to a desired location. Moreover, the surface of polymeric nanoparticles could be easily modified and functionalized with a specific recognition ligand, which increases the specificity of therapeutic agents in targeted area.

1.1.1.1.3. Micelles

Polymeric micelles are usually used for the systemic delivery of water-insoluble therapeutic agents. They are in <100nm size and formed in solution as aggregates. The component molecules of polymeric micelles are arranged in a spheroidal structure, in which a mantle of hydrophilic groups surrounds hydrophobic cores. The existence of hydrophilic surface contributes to their protection from nonspecific uptake by reticuloendothelial system so that their high stability within physiological systems is ensured. On the other hand, the hydrophobic core of polymeric micelles can physically trap the therapeutic agents. The component molecules can also be covalently linked to this hydrophobic core. Consequently, the dynamic structure of polymeric micelles provides a prominent delivery system for therapeutic agents, which allows versatile loading capacity, conjugation of targeted ligands and decrease in the rate of dissolution [10].

1.1.1.1.6. Drug conjugates

Conjugation of polymers with drugs is generally used for low molecular weight agents, particularly in cancer treatment. This conjugation increases the overall molecular weight of drugs, which induces the pharmacokinetic disposition of drug in cells. Polymer-drug conjugates serve as carriers with high solubility and stability, promotes EPR effect in cancer cells leading to internalization of the particles in the desired site [11]. It is also reported that covalently conjugated polymer-drugs are more reliable in terms of drug release and enhanced drug capacity [12]. There are pH sensitive polymeric drug conjugates, which accumulate in the tumor site since the tumor is considered as an acidic environment. pH sensitivity of the nanoparticle is also used for controlled drug release [13], [14]. Combination of paclitaxel and doxorubicin is extensively studied in cancer treatment, and as a result, it is reported that polymeric drug conjugates increase the bioavailability of the drug [12], [15], [16].

1.1.1.1.2. Non-polymeric particles

1.1.1.1.2.1. Carbon nanotubes

Carbon nanotubes are carbon based tubular structures in 1nm diameter and 1 to 100nm length [17]. These structures can be conceptualized by wrapping a layer of graphite called graphene into a seamless cylinder. The configuration of carbon nanotubes includes single-walled nanotubes (SWNTs), multiwalled nanotubes (MWNTs) and C₆₀ fullerenes. The size and stable geometric shape of carbon nanotubes make them an attractive non-polymeric carrier for therapeutic agents. Particularly, SWNTs and C₆₀ fullerenes have internal diameters of 1-2 nm, which is equivalent to about half of the average DNA helix diameter [18]. The SWNTs and MWNTs can enter the cells by endocytosis or by direct insertion through the cell membrane. Experiments with fullerenes have shown that they can be also used for delivery of therapeutics like antibiotics, antiviral and anticancer agents [19]–[22]. Fullerenes differ in the arrangement of their graphite cylinders and due to presence of high number of conjugated double bonds in their core structure. They can protect the injured mitochondria by providing free radicals [23]. This property allows for the tissue-selective targeting of mitochondria that can be used for delivering therapeutic agents to the desired site, particularly in cancer treatment [24].

1.1.1.1.2.2. Metallic nanoparticles

Metallic nanoparticles are nano size metals of size 1-100 nm. These particles are composed of metals such as cobalt, nickel, iron and their respective oxides like magnetite, maghemite, cobalt ferrite and chromium dioxide. Metallic nanoparticles can be synthesized and modified with versatile functional chemical groups, which allows them to be conjugated with different molecules. Combination of these nanoparticles with therapeutic agents is emerging as good delivery carrier alternative due to their magnetic properties, stability and biocompatibility. Surface functionalization can also be done, and biological molecules like peptide, protein and DNA can be stably linked onto their surface. Magnetic properties of these nanoparticles provide extra advantage for their use in therapeutic purposes because of the possibility to target them at a specific site in the body via an externally applied magnetic field. Magnetic

susceptibility, defined as ratio of induced magnetization to the applied field, is an important parameter for their medical use. For example, superparamagnetic iron oxide nanoparticles (SPIONs) have a large magnetic susceptibility, and thus, they are widely used in clinics as contrast agents in magnetic resonance imaging [25]. Likewise, superparamagnetic properties facilitate stable delivery of therapeutic agents to the body/cell and proper accumulation of the treated tissue provide a reproducible and safe treatment approach in diseases [26] [26]. When metallic nanoparticles are subjected to an alternating magnetic field, they can produce, heat and this approach is called magnetic hyperthermia, which provides another advantage for their use in the ablation of tumors in cancer treatment [27], [28].

1.1.1.1.2.3. Quantum dots

Quantum dots (QDs) are tiny particles or nanocrystals of a semiconducting material with diameters in the range of 2-10 nm. These particles consist of a semiconductor inorganic core (CdSe) and an aqueous organic coated shell (e.g., ZnS) [29]. QDs produce distinctive fluorescence colors that are partly the result of the unusually high surface-to-volume ratios for such particles. The core structure of QDs determines the color emitted, while outer aqueous shell can be used for conjugation of biomolecules such as peptides, protein or DNA [30]. QDs can also carry a cap, which improves their solubility in aqueous buffers. Due to their narrow emission, bright fluorescence and high photostability QDs can be used for tracking therapeutic agents within the cells for longer time [31]. This unique property of QDs gives an opportunity to their utilization as carriers for therapeutic vehicles such as DNA, protein, drugs or cells [32]. Although the medical use of QDs is still debated, their surfaces for versatile bioconjugation, their adaptable photophysical properties for multiplexed detection, and their superior stability for longer investigation times are the main advantages of QDs compared to other fluorescence agents, and thus, various drugs are recently developed for delivery via QDs.

1.1.1.2.4. Silica-based nanoparticles

Silica-based nanoparticles offer considerable advantages in nanotechnology because they are suitable for designing complex systems for various applications and can be easily produced with low cost. Their specific surface characteristics, porosity and capacity for functionalization make them attractive tools for therapeutic applications [33]. Silica has a large surface area covered with polar silanol groups, which is favorable for water adsorption and improves the stability of therapeutic agents. In addition, silica-based nanoparticles have ability to interact with nucleic acids, which allows their use as targeted delivery system. Their nanopores size and density can be controlled to achieve a constant delivery rate. Moreover, encapsulation of therapeutic agents with silica-based nanoparticles provides solid media for the delivery of agents. Combination of these nanoparticles with contrast agents such as gold, silver, iron oxide, organic dyes, and quantum dots facilitates their tracking in biological systems [34]. Furthermore, these nanoparticles are used as safety and biocompatible additives in pharmaceutical production, which improves the mechanical properties of powders. Eventually, silica-based nanoparticles provide advantages as biosensors [35], as well as in controlled drug release and delivery and cellular uptake [36].

1.1.1.1.3. Lipid-based nanoparticles

1.1.1.1.3.1. Liposomes

Liposomes are vesicles synthesized by hydration of dry phospholipids. They can be prepared with distinct structure, composition, size and flexibility with a variety of surface modification. One of the most important advantages of liposomes is their ability to fuse with lipid membrane of a cell and releasing its contents into the cytoplasm. Such availability of liposomes makes them suitable intelligent carrier systems for targeted delivery. They are composed of a lipid bilayer surrounded with a hollow core. The therapeutic molecules can be loaded into this hollow core for delivery to disease sites [37], [38]. Depending on the number of bilayers, they are classified into three basic types: Multilamellar, small unilamellar and large unilamellar. Multilamellar vesicles consist of several lipid bilayers separated from one another by aqueous spaces. In

contrast, unilamellar vesicles consist of a single bilayer surrounding the entrapped aqueous space having diameters smaller or larger than 100nm. These structural properties allow them to carry both hydrophobic and hydrophilic molecules. Hydrophilic molecules can be carried in the aqueous interior of the liposome, while hydrophobic molecules can be dissolved in the lipid membrane [39]. Moreover, surface modification can be obtained by either coating with a functionalized polymer or PEG chains that improve targeted delivery and increase their circulation time in biological systems [40].

1.1.1.1.3.2. Solid lipid nanoparticles (SLN)

Solid lipid nanoparticles (SLN) are form of aqueous colloidal dispersions, which comprise of lipid matrix, which is solid at room and body temperatures. Surfactants improve stability of those particles. Size of SLNs varies from 10 – 1000 nm depending on the production mechanism [41]. Lipid carriers are a sub-category of SLNs, and they have solid nanoparticle, liquid lipid matrix and improved stability and drug carrier properties [42]. SLNs have advantageous properties such as protecting the encapsulated drug and drug release control. Also, they have large surface to volume ratio and improved drug carrying capacity [43]. It is reported that SLN anticancer drugs have better properties than conventional drug formulations because of the features mentioned above [44], [45]. Moreover, they are effective carriers for pulmonary and oral drug delivery purposes [46], [47].

1.1.1.1.2. Nanocrystalline particles

Nanocrystalline particles are polycrystalline materials with crystallite size of only a few nanometers. Their small crystallite sizes reduce limitations of several therapeutic agents that are suffering from bioavailability and absorption problems. Generally, the size reduction is a suitable way to enhance the bioavailability of agents, where the dissolution velocity is the rate-limiting step. The crystalline structure leads to increased surface area and thus increases dissolution velocity. This characteristic improves the solubility, which is important especially when the therapeutic index of agent is limited due to absorption problem. Relatively, nanocrystalline particles enable the quick absorption of therapeutic agents due to their fast dissolution, offering an advantage for

agents that need to work fast. By modifying the nanocrystal surface, it is possible to achieve a prolonged or a targeted release, allowing for the use of therapeutic agents in low doses and decreasing side effects, particularly for poorly soluble agents [48].

1.1.2. Targeted Delivery Applications of Therapeutic Nanoparticles

Targeted delivery refers to the successful direction of therapeutic agent and its dominant accumulation within a desirable site. For the efficient targeted delivery, the agent-loaded system should retain in physiological system for preferable time, evade from the immunological system, target specific cell/tissue and release the loaded therapeutic agent [49]. Today, the targeted delivery of nanoparticles is mostly studied in cancer treatment. Over 20% of the therapeutic nanoparticles already in clinics or under clinical evaluation were developed for anti-cancer applications. In addition, related research has focused on nanoparticle-mediated therapy for some other diseases such as neurodegenerative, infectious, autoimmune etc. diseases. The subsequent section provides up-to-date application of therapeutic nanoparticles as targeted delivery systems in these diseases.

1.1.2.1. Cancer

Cancer is one of the major causes of death. Chemotherapy is widely used as a treatment approach for various types of cancer. However, chemotherapeutic agents suffer from the lack of aqueous solubility, exhibits dose-dependent toxicity, and their tumor specificity is inadequate [50]. Multidrug resistance is another challenge in chemotherapy, which mainly occurs due to increased efflux pumps that are responsible for export of anti-cancer agents from cell membrane [51].

Recent applications of nano-delivery system overcome these limitations such that they can be targeted directly to the cancer cell, deliver the agent at a controlled rate, and optimize the therapeutic efficacy [52]. A variety of nanoparticles has been developed for delivery of anti-cancer agents, and two major mechanisms are used to deliver them at tumor site: Passive targeting and active targeting [53]. Passive targeting is based on the accumulation of therapeutic agent in the tumors due to their different features from normal tissues. Tumors have leaky vasculature or defective lymphatic drainage, which promotes the delivery and retention of therapeutic nanoparticles; commonly referred as

the EPR effect [54]. Yet, nanoparticles encounter several obstacles in this type of targeting. Mucosal barriers or non-specific uptake of particles on the way to their target limit the efficiency. In contrast, active targeting achieves selective recognition of the targeted cells by carrying ligands at the surface of nanoparticles that bind to receptors or stimuli-based carriers [55], [56]. Currently, the majority of FDA-approved therapeutic nanoparticles is produced by re-formulation of chemotherapeutic drugs with polymeric nanoparticles. For example, PEGylated liposomal formulations of anti-cancer drug doxorubicin (Doxil®, Caelyx®) can extend the half-life of the drug dramatically and decrease the cardiotoxicity. Similarly, nanoparticle-based re-formulation of cisplatin exhibits enhanced efficiency and reduced side effects in the localized treatment of progressive breast cancer [57], [58]. The albumin-conjugated nanoparticle version of anti-cancer drug paclitaxel (Abraxane®) or re-formulation of rapamycin drug with micellar nanoparticles (Rapamune®) are another FDA-approved therapeutic nanoparticles with lower side effects and improved therapeutic indices over their drug counterparts [59]. Table 1.1 summarizes the therapeutic nanoparticles for delivery used in clinics and still under pre-clinical or clinical evaluation.

Table 1.1 Therapeutic nanoparticles for delivery and their conjugated drugs

Nanostructure	Nanoparticle	Conjugated drug	Ref
Dendrimer	polyethylene glycol (PEG)-platinum	α -cyclodextrin	[60]
Micelle	polypropylene sulfide-PEG-serine-folic acid zinc phtalocyanine	doxorubicin	[61]
Carbon nanotube	PEG diacylate-chitosan derivative single walled CNT	doxorubicin	[62]
Metallic nanoparticles	hollow mesoporous copper sulfide (HMCuSNPs) nanoparticle with iron oxides	doxorubicin	[63]
	hollw mesoporous copper sulfide (HMCuSNPs) nanoparticle with Hyaluronic acid	doxorubicin	[64]

	PEGylated MoS nanosheets		[65]
	Magnetite nanoparticles	doxorubicin	[66]
	Gold nanorods	doxorubicin-thiolated PEG-biotin-DNA	[67]
Silica based nanoparticles	Nanorod	aptamer	[68]
	mesoporous silica		[69]
	transferrin mesoporous silica	doxorubicin	[70]
	mesoporous silica	amino- β -cyclodextrin	[71]
	mesoporous silica	cytochrome C conjugated lactobionic acid-doxorubicin	[72]

1.1.2.2. Infectious Diseases

The major therapeutic approach for infectious disease is the use of anti-microbial drugs. However, pathogens can become resistant, where anti-microbial drugs become therapeutically insufficient. This requires high doses and frequent administration of drugs, which increase side effects and toxicity. Moreover, many pathogens are located intracellularly in an active or latent state, which prevents the access of anti-microbial drugs [73], [74]. The use of nano-delivery systems can overcome such problems, and currently, there is an increasing interest in their use against different pathogens such as bacteria, virus, fungi or parasites. Application of nano-delivery for the treatment of infectious disease includes both polymeric and non-polymeric nanoparticles, and liposomes that improve the anti-microbial activity of drugs [75]. Although many research articles have been published during past years, current drugs in clinical trials have sought approval for new systems (ciprofloxacin liposomes) or new applications, such as the use of Arikace™ in bronchiectasis, cystic fibrosis or chronic infection [76]. There are also clinical trials addressing the use of nanoparticles as vaccine carriers for Ebola virus (EBOV) or as antimicrobial agents in medical devices, such as AgNPs in

central venous catheters [77]. Consequently, several nano-delivery systems are today clinically available. For example, the anti-fungal liposomal carrier Ambisome® (Amphotericin B) and the SLN Nanobase® or the virosomal vaccines Inflexal® V and Epaxal® are already used in clinics for therapeutic purposes. Furthermore, there are some nanoparticles used in diagnosis or as medical devices like Verigene®, Silverline®, Acticoat™ or Endorem™ SPIONS [78]–[80]. Table 1.2 summarizes the therapeutic nanoparticles against resistant strains and some nano-delivery systems used for prevention and treatment against bacterial infection.

Table 1.2 Therapeutic nanoparticles against resistant strains

Pathogen	Nanoparticle	Conjugated Drug	Ref
C. Albicans	Metallic nanoparticle (AgNP)	Fluconazole	[81]
E. Coli	Metallic nanoparticle (AuNP and AgNP)	Ampicillin	[82]
E. Coli	Metallic nanoparticle (ZnO-PEI)	Tetracycline	[83]
Enterococci	Metallic nanoparticle (AuNP)	Vancomycin	[84]
	Liposome		[85]
HIV-infected cells	Polymeric nanoparticle (Micelle)	Nelfinavir, saquinavir	[86]
P. Aeruginosa	Liposome	Polymyxin B	[87]
P. Aeruginosa	Metallic nanoparticle (AuNP)	Ampicillin	[82]
Plasmodium sp.	Liposome	Chloroquine	[88]
S. Aureus	Chitosan NP	Vancomycin	[89]
	Metallic nanoparticle (AuNP)		[90]
	Polymeric nanoparticle (PLA NP)	Penicillin	[91]

Silica nanoparticle		[92]
Chitosan NP	Streptomycin	[93]
Liposome	β -Lactam, penicillin	[94]
Metallic nanoparticle (AuNP and AgNP)	Ampicillin	[82], [90]

1.1.2.3. Autoimmune Diseases

Treatment of autoimmune diseases by using nano-delivery systems includes therapeutic approaches for rheumatoid arthritis (RA) and Acquired Immunodeficiency Syndrome (AIDS).

RA is one of the common and severe autoimmune diseases affecting almost 1% of the world population. The cause of RA is still unknown, yet the complex interaction between immune mediators is responsible for the bone and cartilage destruction. New therapy approaches are able to improve the quality of patient's life, however, restricted administration route and requirement of repetitive long-term treatment result in systemic adverse effects [95]. Nano-delivery systems are used as a new approach for delivering therapeutic agents particularly to target inflamed tissue (synovial membrane), thereby preventing systemic and undesired effects. Certolizumab pegol (CZP) is a TNF- α inhibitor widely used in clinics [96] [93]. Nano-formulation of CZP with PEG increases its half-life to ~14 days, and its clinical trials have shown promising results for long-term treatment on RA patients [97]. Targeting inflamed tissues by using C60 fullerenes [98] or polymeric micelles [99] was also achieved in the utilization of nano-delivery systems to treat RA.

Acquired Immunodeficiency Syndrome (AIDS) is another autoimmune disease lacking treatment. Current clinical therapy is called Highly Active Anti-Retroviral Treatment (HAART), which consists of a combination of at least three anti-HIV drugs suppressing human immunodeficiency virus (HIV) replication. Although this therapeutic approach has contributed to lower mortality rate, it is not effective [100]. Recently, nano-delivery system was introduced in order to provide a target specific and

sustained release of anti-HIV drugs, thereby improving their efficiency and preventing side effects [101]. Examples of nanoparticle drugs used for AIDS therapy are summarized in the Table 1.3

Table 1.3 Drugs for AIDS therapy

Nanostructure	Nanoparticle	Conjugated Drug	Ref
Polymeric nanoparticle	Polyhexylcyanoacrylate nanoparticles	Zidovudine	[102]
	Polyisohexyl cyanate nanoparticles	Zidovudine	[103]
	Polypropyleneimine dendrimers	Efavirenz	[104]
	PPI dendrimer	Efavirenz	[105]
	PLGA nanoparticles	Ritonavir, Lopinavir, Efavirenz	[106], [107]
	PBCA and MMA-SPM nanoparticles	Stavudine, Zidovudine, Lamivudine	[108]
	Polyepsilon-caprolactone	Saquinavir	[109]
Liposome	Mannosylated and galactosylated liposomes	Stavudine	[110]

1.1.2.4. Cardiovascular Diseases

Cardiovascular disease (CVD) is a class of diseases, which affects the cardiovascular system, vascular systems of the brain and kidney, and peripheral arteries. Despite many novel therapeutic strategies such as gene delivery and cell transplantation, heart failure is still a leading reason of mortality in the world [111]. Utilization of nanoparticle-based delivery system to treat cardiovascular diseases includes approaches for treatment of vascular restenosis. Efficient targeted delivery of liposome-associated drug sirolimus has been shown in the attenuation of vascular restenosis [112]. Similarly, carrying carvedilol with liposome-based nanoparticles results in enhanced bioavailability of drug

and improves its therapeutic effect [113]. Angiogenic therapy of myocardial ischemia with vascular endothelial growth factor (VEGF) is a convenient approach to overcome hypoxia-dependent side effects. Polymeric particles loaded with VEGF have been proposed as a promising system to improve vasculogenesis and tissue remodeling in an acute myocardial ischemic model [114], [115]. Moreover, oral bioavailability of cardio-protective resveratrol is enhanced by using nano-delivery systems based on lipid nanoparticles [116]. Furthermore, targeting nano-delivery system in atherosclerosis is achieved to visualize and treat atherosclerotic lesions by using magneto-fluorescent nanoparticles or ligand-binding polymeric micelles [117].

1.1.2.5. Neurodegenerative Diseases

Neurodegenerative diseases (NDs) are characterized via the progressive loss of the function of neurons, which subsequently causes the neuronal death. Patients with NDs, such as Alzheimer's disease (AD), Parkinson's disease (PD), and multiple sclerosis (MS), have symptoms related to movement, memory, and dementia due to the gradual loss of neurons. Although significant progress is achieved in the treatment of NDs, the therapeutic strategies are limited because of the restrictive structure of blood-brain-barrier (BBB). BBB is a highly selective semipermeable membrane barrier, which separates the circulating blood from the brain and prevents the passage of most circulating molecules so that central nervous system homeostasis is maintained [118]. Due to highly selective nature of BBB, most of the therapeutic drugs cannot reach to the brain, which requires high doses leading to adverse effects in the body. Nanoparticle-based therapeutic approach in NDs mainly focuses on targeted delivery and sustained local release of therapeutic agents into the diseased area of brain by crossing the BBB [119], [120].

The aggregation of the amyloid- β (A β) peptide into amyloid plaques is the main pathological feature of AD, and current treatments include cholinesterase inhibitors (donepezil, rivastigmine, galantamine), N-methyl-D-aspartate (NMDA) receptor antagonists (memantine) [121]. Re-formulation of clinically used drugs with polymeric nanoparticles, non-polymeric quantum dots or lipid-based nanoparticles enables them passing through BBB and reduces the side effects compared to free drug administration [122]–[127]. Concerning nano-delivery systems, there are also other attempts to cross

the BBB and to reduce A β aggregates by using several neuroprotective compounds like metal chelators, various NMDA antagonists of anti-amyloids [128], [129].

Parkinson's disease (PD) is another type of neurodegenerative disease characterized by the selective degeneration of dopaminergic neurons and by the existence of α -synuclein as well as protein inclusions in neurons termed Lewy bodies [130]. Dopamine replacement therapies are presently the mostly used strategy for PD treatment, since this class of drugs can help to improve the symptoms in motor neurons and is able to slow down the progression of diseases. However, the effect of these drugs on behavior and cognition is still debated [131]. Recent research activities in nano-delivery focus on development of therapeutic nanoparticles based on different strategies. Targeted delivery of dopamine using polymeric nanoparticles or liposomes is one of the nanoparticle-based therapeutic approaches in PD treatment [132]. Several studies use various drugs (Ropinirole, Bromocriptine, Mitoapocynin, apomorphine) encapsulated with liposomes or polymeric nanoparticles in order to improve sustained release of drugs and to reduce undesired effects of conventional PD therapy [133]–[135]. Anti-inflammatory strategies are also developed by using polymeric nanoparticles or PEGylated liposomes to prevent neuronal cell death in PD [136]–[138]. As a neurotrophic strategy, PEGylated nanoparticles loaded with h-GDNF (Glial cell-derived neurotrophic factor) improve locomotor activity and decrease the loss of dopaminergic neurons, which results in enhanced dopamine levels [139], [140]. Moreover, polymer-based biodegradable nanoparticles have been engineered as cell therapeutics allowing stem cells to repair damaged nerves [141]. Furthermore, several groups proposed a therapeutic nano-system for delivery of genetic material, such as DNA, RNA, and oligonucleotides, which inhibits undesired gene expression or synthesizes therapeutic proteins in PD models [142]. Although significant improvement in clinical symptoms is observed in advanced PD patients taken gene therapy, this approach is still a contradictive issue because of the heterogenic pathology of PD [143].

Despite many research articles in the development of novel therapeutic nanoparticles published for AD and PD; only few approaches have been reported for other neurodegenerative diseases, like Amyotrophic lateral sclerosis (ALS), Multiple Sclerosis (MS). ALS is a progressive neurodegenerative disease affecting motor neurons responsible for controlling voluntary muscle movements (chewing, walking,

and talking) in the brain and spinal cord. Clinically, progressive muscle weakness results in death due to respiratory failure. To date, the only agent approved for treating ALS is Riluzole. Loading Riluzole on lipid-based nanoparticles promotes the efficiency of the drug, and targeted delivery into the brain is achieved with lower undesirable biodistribution [144], [145]. MS is characterized by the destruction of the protective coating (myelin sheath) on nerves of the central nervous system, which causes a faulty relay of instructions from the brain to the body. The conjugation of a glutamate receptor antagonist with a non-polymeric fullerene derivative nanoparticle is able to rescue the clinical progression of chronic MS in in vivo model [146].

1.1.2.6. Ocular Diseases

Current therapy for ocular diseases includes mydriatics or cycloplegics miotics, anti-infective, anti-inflammatory, diagnostics, and surgical adjuvants. However, blood-retina barrier has made the eye impermeable for the most therapeutic agents. Targeted nano-delivery system offers advantages in ocular disease therapy by lowering eye irritation or enhancing ocular tissue compatibility [147]. The most widely used nano-delivery systems consist of polymeric nanoparticles and liposomes developed for targeting of drugs at the diseased area, which enhances corneal permeability, increases the residence period and bioavailability [148], [149]. Nano-formulation of the drug pranoprofen with polymeric PLGA (poly (lactic-co-glycolic acid) and its ophthalmic delivery significantly promote the local anti-inflammatory and analgesic results of the drug [150]. Moreover, chitosan-based polymeric nanoparticles encapsulated with cefuroxime, diclofenac or dexamethasone improve ocular bioavailability of the drugs [151]. These nanoparticles are able to interact with both ocular surface and drug and thus protect the drug from metabolic degradation leading to extended pre-corneal residence [152]. Similarly, lipid-based nanoparticles loaded with brimonidine was used to treat an ophthalmic disease, glaucoma [153], [154]. Immunologic graft rejection is a challenge in the corneal transplantation. PLGA- or PEG- based polymeric nanoparticles of dexamethasone and curcumin prevent the rejection of corneal graft by the sustained release of the corticosteroids [155], [156].

1.1.2.7. Pulmonary Diseases

Pulmonary lung diseases include asthma, chronic obstructive pulmonary disease (COPD), cystic fibrosis, pulmonary tuberculosis and idiopathic pulmonary fibrosis (IPF) [157]. These diseases are often fatal, and there is no effective treatment for completely restoring lung functions. Nano-delivery of therapeutic agents at the diseased area is the main strategy for effective treatment of lung diseases. For this purpose, natural polymeric nanoparticles such as gelatin, chitosan, and alginate, as well as synthetic polymers like poloxamer, PLGA, and PEG are widely used [158], [159]. Moreover, polyamidoamine (PAMAM) dendrimers assembled with anti-asthma beclometasone dipropionate (BDP) were effectively used for pulmonary inhalation [160]. Furthermore, lipid-, polysaccharide- or polymer- based nanoparticles and metallic or carbon-based nanoparticles were utilized for carrying vaccine or for pulmonary immune hemostasis [161].

1.1.2.8. Regenerative Therapy

Regenerative therapy focuses on the design and application of biocompatible materials, which can enhance the repair and regeneration of tissues by making use of their natural cellular mechanisms. Stem cell-based therapy is one strategy for promoting tissue's natural repair or regeneration mechanism.

Over the years, there has been increased interest in the development and direct administration of therapeutic nanoparticles to promote bone regeneration [162]. The most commonly used nano-delivery systems for bone regeneration are synthetic polymers (PLA or PLGA) or natural polymers (collagen, gelatin, albumin and chitosan). Besides the polymeric ones, various formulations of non-polymeric nanoparticles (silica-based, metallic) have also been used as nano-delivery systems for bone regeneration. For example, calcium phosphate-based non-polymeric nanoparticles are mostly used due to their similarities to human bone [163]–[165]. Delivering several growth factors is one of the nanoparticle-based therapeutic strategies based on the stimulation of osteoblasts for bone formation [166]–[169]. Moreover, nano-delivery of synthetic molecules is used as other therapeutic strategy in bone tissue, which could suppress the bone-resorbing cells, the osteoclasts. The bisphosphonate drugs promote

osteoclasts apoptosis and are thus widely used for osteoporosis treatment. Several types of polymeric or non-polymeric metallic nanoparticles have been used to deliver bisphosphonate drugs [170], [171]. Another strategy for the use of therapeutic nanoparticles in bone tissue is reducing inflammation, particularly in the case of large wounds. Synthetic or natural polymeric nanoparticles loaded with anti-inflammatory agents are delivered into the infected area, which could inhibit both the inflammation and osteoblast resorption [172], [173]

1.1.3. Magnetic Nanoparticles

Advances in nanotechnology led to a significant progress in applications in diagnostics, drug delivery, and sensor technology, research topics of which are of cardinal importance [174]–[180]. As a branch of nanotechnology, the use of nanoparticles has increasingly attracted the attention of researchers from various scientific fields because of their dimensions, biocompatibility, electronic, optical, and magnetic properties [181]–[183]. For example, nanoparticle properties are exploited in nanomedicine for use in early diagnosis and therapy of serious diseases such as cancer [184]–[189]. In addition, this approach has the potential to reduce side effects typical of conventional drugs, while also acting as a contrast agent for early diagnosis [190]–[195]. Thus, for the above-mentioned purposes, magnetic field-assisted methods involving magnetic nanoparticles (MNPs) are widely tested [196]. Magnetic nanoparticles have properties such as superparamagnetism and high saturation field since each particle has a narrow and final size distribution and area that affects magnetic properties. When the particle of a ferromagnetic material is under a critical dimension (< 15 nm), it contains single magnetic domains and has a uniform magnetic field within any field [197], [198]. The magnetic behavior of these particles over a certain temperature (i.e. blocking temperature) is similar to atomic paramagnets apart from their higher susceptibility values, which is superparamagnetism and therefore very high moments are concerned [akb 46]. Magnetic Resonance Imaging (MRI), and drug delivery are considered as major application areas [199]–[202]. To improve the efficacy of chemotherapy and reduce side effects, the use of nanoparticles in drug delivery systems has been extensively investigated [203]. Conventional cancer treatments such as chemotherapy are non-specific, cytotoxic, and damage to healthy cells as well [204], [205]; thus, MNPs present a great potential to circumvent this. Drugs can be loaded

onto MNPs, which in turn can be used in tumor therapy [206]–[208]. Stable delivery of iron oxides to the body/cell and proper accumulation of the treated tissue will provide reproducible and safe treatment [209] and targeted drug delivery with MNPs might present a significant alternative for conventional chemotherapy in the future since the nanoparticles have the potential to mainly localize at cancerous sites and lead to a local increase in drug concentrations while leaving the other sites unaffected [210]. Gene delivery with nanoparticles has also been intensively studied [211], [212]. Specificity and transfer efficacy challenges exist but they can be overcome and gene delivery benefits might be further amplified [213]. Using magnetic nanoparticles may reduce surgical intervention in treatment. So that tumors of different and complex shapes can be effectively treated, helping to minimize the damage that may occur to nearby cells. Due to their unique properties, MNPs enable researchers to work at the cellular or molecular scales [214], [215]. These MNPs are made generally of a metal core that is covered by polymeric structures and/or organic/inorganic components. Suitable surface coatings allow maintenance of stability, biocompatibility and functionality [216]–[218]. MNPs can also be manipulated externally by magnetic fields and can be guided to any desired site of interest [219]. Commonly used ions include the magnetite Fe_3O_4 and the maghemite $\gamma\text{-Fe}_2\text{O}_3$.

1.1.3.1. Physicochemical Characteristics of Magnetic Nanoparticles

1.1.3.1.1. Shape and Size

The shape and size of nanoparticles influence their usage in biomedical applications; thus precision in their fabrication is of great importance [220], [221]. Furthermore, targeted delivery is facilitated by particle size [214]. Sufficiently small nanoparticles possess the ability to withstand an external magnetic field without becoming demagnetized. Measurement of this resistance is called coercivity, and in order to achieve superparamagnetic properties, the particle size must be at such a point that coercivity becomes zero [222]. Quantum mechanical effects become dominant when the particle size decreases and superparamagnetism is achieved due to the single domain of particles [223], [224]. The general approach involves attaching a therapeutic agent to a magnetic nanoparticle or capturing it inside a polymer and then exposing it to magnetic fields. In addition to iron oxides, nickel and cobalt may be used for nanoparticle formulation, but due to their biocompatibility properties, iron oxides have

found more applications for drug delivery [225]. Size and magnetic properties of nanoparticles are tabulated in Table 1.4.

Table 1.4 Size differences of iron oxide nanoparticles

Property	Size
Bulk materials	cm size range
Ferromagnetic materials	Multi domain nps
Superparamagnetic iron oxide nanoparticles (SPIONs)	50 to 180 nm
Ultra small SPIONs	10 to 50 nm
Very small SPIONs	< 10 nm

1.1.3.1.2 Surface Properties and Coating

Most iron oxide based-nanoparticles exhibit superparamagnetic behavior and they are biocompatible, but they might be easily oxidized, resulting in a reduction of their magnetic moment. However, bare iron oxide nanoparticles (IONPs) might be toxic since they might trigger reactive oxygen species (ROS) production by cells. Their use in biomedical applications requires surface modifications because of their dissolution and agglomeration tendency [226]. The surface coating is also important for improving nanoparticle stability and circulation time in the blood [227]. Commonly used materials are dextran, PEG (polyethylene glycol), and amino silanes [228], [229]. PEG is a suitable coating material because of its chemical properties, solubility, and biocompatibility [213], [230] since polymer-coated nanoparticles offer a better solution for stability and oxidation resistance [231], [232]. Aviles et al. studied capillary tissue magnetic nanoparticle capturing with dextran coatings. They used dextran-coated nanoparticles as seeds and poly divinylbenzene magnetite particles as magnetic drug carrier particles (MDCPs). Seed particles were then magnetized, resulting in a local magnetization enhancement that favors a more efficient MDCP magnetization and captures in the targeted area. They suggested that this system resulted in a more efficient magnetization compared to the use of magnet only [233]. Next, Xu et al.

demonstrated coating of Fe₃O₄ nanoparticles with PEG by the alkaline coprecipitation method. They modified the particles with 3-APTES (3-aminopropyltriethoxysilane) which gives an NH₂ functional group, making them suitable for use as an agent to immobilize proteins, while also suggesting that these particles can be used for potential separation and transportation of specific proteins [234]. Likewise, Gupta et al. reported the engineering of particle surfaces with PEG to increase biocompatibility due to protein adsorption resistance and uptake enhancement. They modified the superparamagnetic iron oxide particles with PEG and investigated the effects of this modification in terms of adhesion, viability, uptake, and morphology in human dermal fibroblasts. Cells incubated with the PEG-coated nanoparticles were not significantly different from those of the uncoated control group. Morphological analysis by SEM confirmed low toxicity and normal morphology of coated particles, while uncoated particles resulted in abnormal cell morphology. The authors confirmed that PEG-coated particles did not affect the cytoskeletal arrangement of fibroblasts [235]. Moreover, Cao et al. suggested a superparamagnetic Fe₃O₄/aminosilane core shell for drug delivery and bioseparation [236]. In addition, Lin et al. synthesized water soluble micelles incorporating IONPs and modified them with several polymers to demonstrate their usage and efficiency as diagnosis and imaging agents [237]. Finally, Cheng et al. synthesized carboxy-terminated poly (D,L-lactide-co-glycolide)-block poly(ethylene glycol) (PLGA-b-PEG-COOH) nanoparticles and investigated their size-dependent biodistribution in prostate cancer cell lines. They suggested that controlling nanoparticles size, together with targeted delivery, may result in favorable biodistribution and might lead to the development of clinically-relevant targeted therapies [238]. Nadeem et al. (2016) coated iron oxide nanoparticles (ionps) with polyvinyl alcohol (PVA) and used doxorubicin (DOX) as a therapeutic agent. They concluded that 3 % wt is ideal for controlling ionps via external magnetic field and at a high concentration one might lose the control over their usage for drug delivery purposes [239]. Khalkhali et al. (2015) synthesized SPIONs and stabilized them with dextran, chitosan, and methoxy polyethylene glycol polycaprolactone (mPEG-PCL). They obtained high colloidal stability in the expense of losing the magnetic property. However, when they analyzed the data they observed that saturation magnetizations were reduced for coated particles compared to naked superparamagnetic iron oxide nanoparticles (SPIONs) but the saturation magnetization values were still in the range

that could be used for biomedical applications such as MRI contrast agents [240]. The use of glyceryl monooleate (GMO) as a coating material has also been reported in the literature. The three groups working with this particle looked at drug activity and analyzed the IC₅₀ levels that we could define as the amount of drug needed to break down a biological process. Dilnawaz et al. have shown the ability to use paclitaxel and rapamycin as drugs and to kill GMO-coated, Her2-labeled magnetic nanoparticles in MCF7 cells, both individually and in combination. Another group using paclitaxel as a drug was Trickler et al. and they synthesized GMO/chitosan nanoparticles and investigated their uptake to MDA-MB-231 cells. Accordingly, they received 4 times more cellular uptake and a 1000-fold reduction in IC₅₀ levels for paclitaxel [241].

1.1.3.1.3. Functionalization

Functionalization of nanoparticles with an amino group, silica, and polymers enhances their effect and provides improved physical and chemical properties for biomedical applications. Commonly used metals are iron-iron oxides and gold-silver. Iron oxides are typically used as the core material while gold is used as the shell material [242]. Yu et al. synthesized mPEG-poly(ι -Asparagine) magnetite nanoparticles and modified them with imidazole and doxorubicin (DOX). Resulting nanoparticles were applied to breast cancer cells. They showed that changes in pH and magnetic property had an effect on particle internalization and drug release, affecting its anti-tumoral [243].

1.1.3.1.4 Magnetization Characteristics of Superparamagnetic Nanoparticles

Adequately small ferromagnetic materials are good candidates for superparamagnetics [244]. Due to their superior magnetic properties, superparamagnetic IONPs are preferred in biomedical applications [245] and are generally used in core shell structures [246]. Usage of a particle as a drug carrier require low toxicity, high carrier capacity, and synergistic effects when in combination therapeutic agents [247], [248], as well as high oxidation stability of the core shell structure and high dispersion capacity of drug-loaded particles, and all these properties can be constructed with superparamagnetic IONPs [246], [249]. Also, they have no remnant magnetization after the external magnetic field is removed. Thus, with the usage of SPIONs consequential

toxicity of particle agglomeration after the procedure is prevented [250]. Additionally, increasing magnetization positively affects manipulation [248], and to achieve superparamagnetism, a small particle size is necessary. Magnetite Fe_3O_4 and hematite Fe_2O_3 are commonly used IONPs due to their small size of 3 – 20 nm [251], [252].

1.1.3.2. Biomedical Applications

1.1.3.2.1 Magnetic Resonance Imaging (MRI)

MRI is a useful tool for the diagnosis of various diseases. Its working principle relies on the forced alignment of water molecules in the body with the direction of the applied magnetic field. Then, with a radio frequency pulse, the molecules can be excited to change their net magnetization. After the field is removed, the molecules turn back to their original state and emit photons. A scanner detects these photons and generates an image of the body. To distinguish normal cells from abnormal ones, contrast agents are used. There are two relaxation times: T_1 and T_2 . In most applications involving T_1 relaxation, gadolinium-based contrast agents are used. However, this relaxation time can be shortened by using paramagnetic agents. For T_2 relaxation, dextran-coated IONPs are commonly used. These T_2 -weighted images result in darker pixels for solid tissues (e.g. muscle, fat etc.) and brighter pixels for water. T_2 contrast agents are typically used as a negative contrast for darker images of a region of interest [242]. When a magnetic field is applied, MNPs induce faster relaxation times, resulting in a non-homogeneous magnetic field. This phenomenon allows MNPs to be suitably used as MRI contrast agents [253], [254].

Jain et al. investigated oleic acid-coated iron oxide and pluronic-stabilized MNPs in drug delivery and MRI. Their results showed a 74 and 95% efficiency with doxorubicin and paclitaxel loading, separately and in combination, respectively. The cells were analyzed in a magnetic nanoparticle-containing medium. The drug combination indicated an anti-proliferative effect on breast cancer cells [255]. Furthermore, Xie et al. used lactoferrin-conjugated SPIONs (Lf-SPIONs) *in vivo* to detect gliomas in a rat model. They administered the nanoparticles at a dose of 12 mg Fe/kg and then made observations for 2 to 48 h. As a contrast agent, Lf-SPIONs enhanced the T_2 -weighted images of gliomas; thus these results suggested that Lf-SPIONs can be used as contrast agents for glioma diagnosis due to their sensitivity and

specificity [256]. Additionally, Rumenapp et al. reviewed the usage of SPIONs in MRI imaging for diagnostic purposes and analyzed the effect of these particles on T_1 and T_2 relaxation times and R_1 and R_2 relaxation rates. Relaxation rates expressed as $1/T_1$ and $1/T_2$ formulas. Molecular structures affect relaxation rates because they are influenced by proton diffusion velocity. For example, oil has a wider molecular structure than water, which means a slower diffusion rate. This leads to more relaxation rate and shorter relaxation time [257]. Yazdani et al. used mebrofenin functionalized silica coated magnetite nanoparticles for liver targeting. MRI results showed that these nanoparticles increased the R_2 value to provide enough contrast for imaging [258]. Huang et al. investigated T_2 weighted images of mice using doxorubicin loaded FA (folic acid) SPIONs and concluded that T_2 relaxation time is shortened thus liver appeared darker in T_2 weighted images. This result can also be interpreted as an increase in R_2 [259]. Moreover, Weinstein et al. reviewed the MRI imaging of central nervous system tumors, trauma, inflammation, stroke, carotid atherosclerosis, autoimmune system disorders, and epilepsy, using ultra-small superparamagnetic iron oxide (USPIOs having 10 to 50nm size) nanoparticles. Gadolinium based contrast agents (GBCAs) are generally used as an MRI contrast agent in brain imaging. Although neovascularization is not possible, however, micrometastases may not be detected with these particles because blood brain barrier (BBB) is preserved. Because the permeability of blood tumor brain (BTB) may vary from tumor to tumor, and this permeability may cause nanoparticles to leak out of the blood vessel. This means that you cannot get contrast in image. USPIOs gave more intense MRI images than GBCAs in imaging using ferumoxytol and ferumoxtran10 in relation to their larger size than GBCAs. They concluded that although there is no perfect contrast agent, USPIOs can compensate for the limitations of GBCAs [225]. Finally, Rosen et al. reviewed targeting capabilities of SPIONs with different types of functionalization, such as targeting with monoclonal antibodies, arginyl glycy l aspartic acid peptides, folic acid, and transferrin, and concluded that those methods have potential for future therapy applications [260].

1.1.3.2.2. Magnetic Hyperthermia

Hyperthermia therapy is a medical technique generally used for cancer treatment. For this technique, the tumor tissue is exposed to slightly higher temperatures in order to damage or kill cancer cells. This treatment is also used to sensitize cancer cells to the

effects of radiation or to certain anti-cancer drugs. Magnetic hyperthermia is based on the production of heat from MNPs when subjected to an alternating magnetic field. In this method, targeted MNPs (e.g. antibody labeled ferrofluid form of SPIONs) penetrate and attach inside the tumor tissue. Since the heating mechanisms are different for particles, size is very important especially for hyperthermia applications. There are three heating mechanisms: eddy currents (bulk materials), hysteresis losses (ferromagnets >100 nm) and Neel and Brownian relaxations (superparamagnets <100 nm) (Figure 1.3). Since most of the superparamagnetic nanoparticles have a single domain and are very small only Neel and Brownian relaxation mechanisms will be valid for hyperthermia [261], [262].

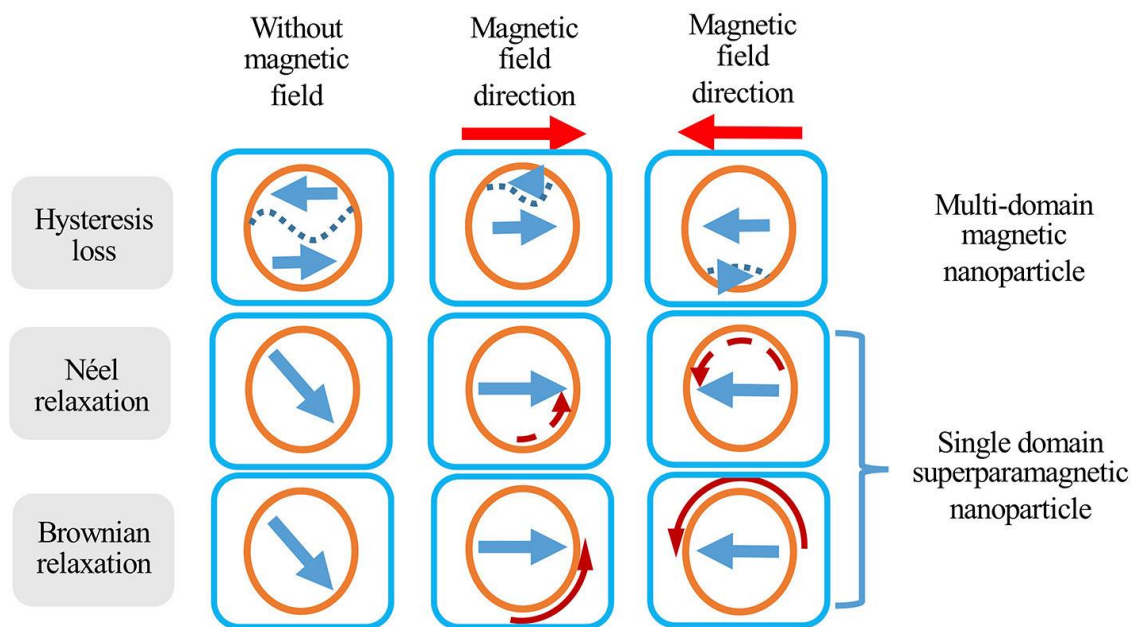


Figure 1.3 Different heating mechanisms for magnetic nanoparticles [263]

SPIONs may induce hyperthermia in the presence of an alternating magnetic field, which rapidly changes direction. Hysteresis losses are valid for particles larger than 100 nm, which is out of scope for superparamagnetic nanoparticles. Heating due to eddy currents is for centimeter size and bigger materials. Besides, eddy currents depend on the electrical resistivity of the materials. Since most iron based nanoparticles have high electrical resistivity, eddy current loss will be very low [264]. This property of SPIONs is often used for dimensions below 100 nm. Thus, the relaxation theory is more appropriate to explain the heating mechanism of nanoparticles in alternating magnetic field. For SPIONs, magnetic moments of the particles in the suspension are in their

equilibrium positions. If a magnetic field is strong enough, the magnetic moments of the particles move away from their equilibrium positions. When the magnetic field is removed or changed, the magnetic moments revert to their original positions, and local heating occurs, which is associated with the Neel relaxation mechanism. Accordingly, Neel relaxation time is given as:

$$\tau_N = \frac{\tau_0}{2} \sqrt{\pi \frac{kT}{KV}} \exp \frac{KV}{kT} \quad (1)$$

where V is the volume of the nanoparticle, T is temperature, K is the anisotropy constant, k is Boltzmann constant, and τ_0 is the relaxation time constant (order of 10^{-9} s). If the particle is activated in the liquid due to the applied magnetic field, the magnetic anisotropy of the particle is strong enough to overcome the viscous and inertial effects. Then, the thermal energy is transferred to the liquid by shear stress, which is linked with the Brownian relaxation mechanism. Brownian relaxation time is given as:

$$\tau_B = \frac{3\eta V_H}{kT} \quad (2)$$

where V_H is the hydrodynamic volume of the particle, and η is the viscosity of the liquid. Depending on the relaxation theory, the frequencies around 100-500 kHz are sufficient enough to induce hyperthermia [261], [265]. The temperatures between 39-45°C are generally referred as hyperthermia. It is reported that these temperatures only affects cancerous cells not the healthy ones [266]. For this purpose, magnetic nanoparticles are used to induce hyperthermia for cancer cells. The temperatures above 46°C correspond to thermal ablation applications [266]–[268], which is out of scope for this article. The heating performance of nanoparticles depends on the structure and magnetic properties of the particle as well as on the frequency and magnitude of the applied magnetic field. However, there are some limitations in biomedical aspects regarding the increase in frequency and magnitude. Because the alternative magnetic field application might create eddy currents in tissues, it is possible that not only the cancerous tissue but also the healthy tissue near the cancerous region might be affected. Therefore, to avoid such undesirable cases, there exists a $H.f \leq C$ criterion called as the ‘Brezovich criterion’ [209], [266]. For biomedical applications, C is taken as

$5.10^9 \text{ Am}^{-1}\text{s}^{-1}$, and Hergt et al. suggested that the frequency of 400 kHz and amplitude of 10 kAm^{-1} constitute the best combination for a high hyperthermia performance [269].

Another important limitation is the size and aggregation of SPIONs. In the *in vivo* studies, the overall hydrodynamic size (aggregated particle size) influences the biodistribution, and large particles, which would respond to external magnetic field faster, are quickly cleared from the blood circulation. Hence, if molecular targeting is desired, SPIONs need to be small (less than 150 nm), and if possible ultrasmall (less than 50 nm).

In this thesis highly functional, colloidally stable, ultrasmall SPIONs coated with poly(acrylic acid) are used and it is investigated whether the Neel relaxation mechanism could be triggered by these ultrasmall SPIONs via applying a magnetic field with a frequency of 400 kHz and a low magnitude of 0.8 kAm^{-1} , which is small enough to avoid any eddy current in tissues. Further, we have investigated the efficiency of this treatment in HER2-positive breast cancer cells by using antiHER2 tagged SPIONs *in vitro* using MDA-MB-453 and SKBR3 cells. These cells were found to be high expressors of the HER2 receptor on their cell surface. Both cell lines were used for the demonstration of receptor-mediated targeting of the SPIONs, while MDA-MB-453 cells were used for hyperthermia experiments. anti-HER2 antibody conjugated SPIONs targeted and killed HER2 overexpressing cancer cells by hyperthermia generated by induction under magnetic field strengths at low magnitudes. As a result, the utilized nanoparticles served as safe, biocompatible, targeted therapy agents in low magnetic field. We showed that cell death as well as reduced cell proliferation could be successfully achieved by heating the nanoparticles in the designed and developed system without using any additional therapeutic agent.

Application of an alternating magnetic field of well-chosen amplitude and frequency increases the temperature in the targeted region. When the direction of the magnetic field is changed, heat can be regulated by adjusting the magnetic field exposure time and duration [270]. Balivada et al. showed that hyperthermia reduces the size of tumors in mouse melanoma tumor grafts via intratumoral injection [271]. Furthermore, Hernandez et al. designed mesoporous silica-coated maghemite nanoparticles conjugated with DNA. They used hyperthermia as an on-off mechanism

for drug release. SPION loaded exosomes have also great potential for nanoparticles to induce hyperthermia. Exosomes are nano structures ranging in size from 30 to 200 nm. The presence of exosomes in the nanometric size allows them to enter and interact with any distant tissue. According to which exosomes can be used to transport carcasses to tumors and conjugation of them with SPIONs can be used for MRI contrast agent and therapeutic purposes by preventing agglomeration and using the nanoparticle benefits many applications can be performed including hyperthermia. [272]–[274]. Almaki et al. investigated targeting using PEG and Trastuzumab conjugated magnetic nanoparticle for hyperthermia treatment of breast cancer and increased the therapeutic effect both in vitro and in vivo treatments [275] .

1.1.3.2.3. Drug delivery

The working principle of drug-loaded MNPs relies on the basis of applying an external magnetic field [230], [276]. As shown in Figure 1.4, superparamagnetic particles can be manipulated to localize to diseased sites such as tumors. Then their local concentrations may increase when a magnetic field is applied. Following delivery, they are reverted to their original state when the magnetic field is removed. Vainauska et al. used a dynamic gradient magnetic field and obtained a 21% higher transfection efficiency with liposomal magnetofection [277]. Oral et al. studied the effect of varying magnetic fields on transfection using PEI coated superparamagnetic iron oxide nanoparticles (PEI-SPION). They used green fluorescent protein (GFP) tagged nanoparticles and rotor system as an external magnetic force generator. They obtained high transfection efficiencies with high viability. With usage of PEI coated nanoparticles toxicity of using only PEI was eliminated [212].

Targeted drug delivery systems allow tissue-specific delivery of drugs or drug-like molecules permitting achievement of local high therapeutic concentrations in diseased sites. Other important goals include timed-release, prolongation of drug release, protection of neighboring normal tissues and self-elimination of particles without having side effects. Targeted systems can be classified into two groups. First, if the delivery is performed via binding of a therapeutic agent to a tissue or cell-specific ligand with a specific recognition mechanism, it is called “active targeting” [278]–[282]. Second, if the delivery is accomplished by encapsulating drugs into especially high molecular weight polymers and guided through the tissue by enhanced

permeability and retention (EPR), it is called as “passive targeting”; here the properties of the carrier remain unchanged [283]–[288]. Active targeting involves antibodies as recognition tools. Passive targeting via EPR-dependent targeting relies on the abnormal neovascularization of tumor tissues. These new vessels are fenestrated and more permeable to macromolecules than normal and healthy blood vessels. The EPR also allows SPIONs to accumulate inside tumor tissues rather than being extravasated in normal tissue sites. Since tumors have a poor lymphatic drainage system, once SPIONs enter the tumor, they are difficult to eliminate, and can diffuse to the tumor core and remain there for long periods [260], [289], [290].

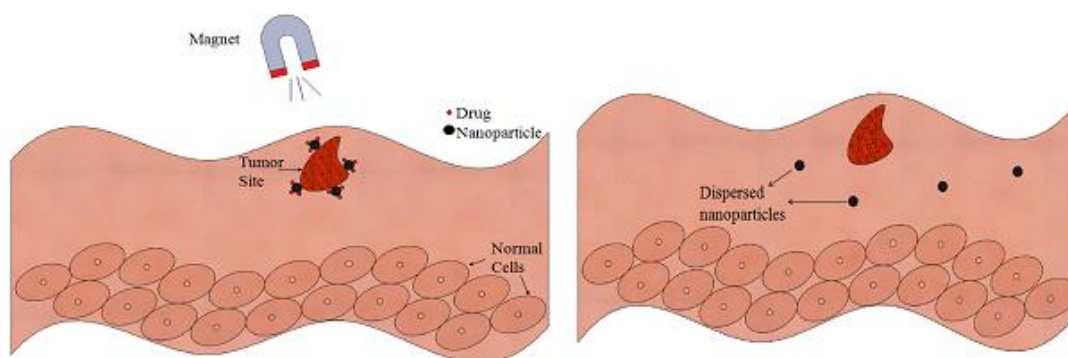


Figure 1.4 a) Drug loaded nanoparticles agglomerate in the tumor site only with the help of an external magnetic field, b) After drug release, the external force is removed, allowing the nanoparticles to disperse and ready to be cleared from the body.

Lee et al. reported that since the mechanisms that the nanoparticles encountered in the body after the injection are the same, i.e. blood circulation and extravasation around the tumor, the conjugating the particle with a ligand or an antibody will not create a difference in the number of particles reaching the targeted area and suggested that separating the targeting mechanisms as active and passive should not be used [251]. Arias et al. demonstrated the use of poly cyanoacrylate nanospheres magnetic core shell as antitumor drugs, and the EPR effect was suggested as the cause of nanoparticle concentration inside tumor tissues rather than in normal tissues [291]. Gravel et al. synthesized polymerized micelles from amphiphile unimers via photopolymerization and then loaded them with imaging agents for MRI or positron emission tomography for

diagnostic and therapy purposes. Polydiacetylene micelles were investigated for a drug delivery system, and the results demonstrated an EPR-mediated tumor accumulation for all micelles. Since PEG2000-coated micelles gave the best uptake in tumors, they were chosen for drug delivery and loaded with paclitaxel. *In vitro* studies with PEG2000-coated micelles indicated they had low cytotoxicity, while *in vivo* studies revealed significant inhibition of tumor growth, suggesting that these micelles can be used as a tool for real-time monitoring and diagnostics[292].

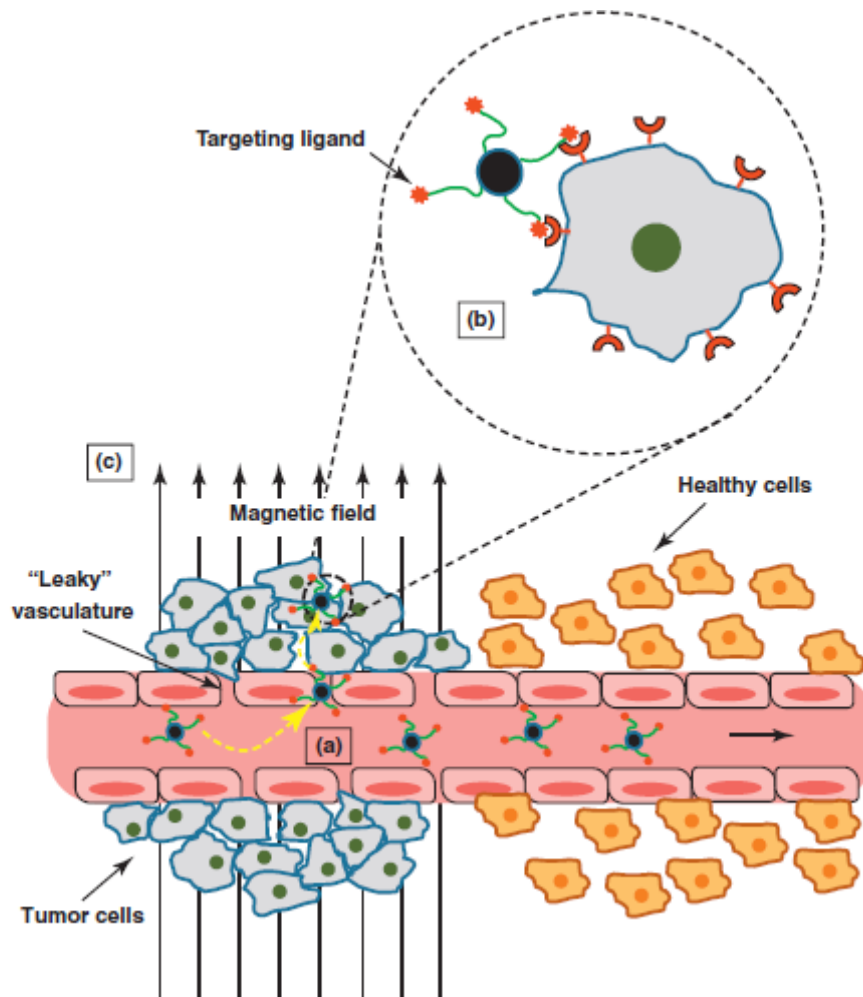


Figure 1.5 Schematic representation of a) EPR effect b) active targeting c) magnetic targeting [293]

Cole et al. synthesized long circulating PEG-modified cross-linked starch MNPs (PEG-MNPs) for brain tumor therapy. They investigated the biodistribution patterns of these nanoparticles in the rat brain, as well as in organs such as the kidney, spleen, lung, and liver. They showed a 15-fold improvement in drug delivery performance in brain

tumors [294]. Park et al. chose SKOV3 human adenocarcinoma cells which do not have extravasating nature like most of the cancer cells. They utilized polymer iron oxide nanocomposites for drug delivery via a magnet and concluded that their particles are suitable for drug delivery purposes despite the poor EPR effect [295]. Figure 1.5 shows the schematic of both active and passive targeting mechanisms.

Since the polymer coating of magnetic nanoparticles facilitates the addition of functional materials, drug and fluorescent dye can be added as well, which can help monitor where the particle's route. They are also very suitable for theranostic applications since simultaneous treatment can be performed when the magnetic property is also activated.

Lübbe et al. demonstrated targeting pancreatic cancer with epirubicin-loaded MNPs. The authors also reported the first clinical liver cancer therapy trial involving manipulation of magnetic microspheres to introduce epirubicin to patients via magnetic fields. It was observed that magnetically imposed epirubicin was well tolerated and up to 50 mg of epirubicin did not result in any toxicity [296]. Chertok et al used IONPs to deliver cancer drugs to glioma cells and monitoring it by MRI [297]. They intravenously injected nanoparticles into rats and applied 0 to 0.4 T magnetic fields at 1 h intervals for 4 h. They obtained a 3.6 times enhancement of nanoparticle accumulation in glioma cells compared to normal cells [297]. Furthermore, Ito et al. showed both in *in vitro* and *in vivo* experiments that MNPs could be taken orally and then targeted with magnetic fields for esophageal cancer treatment [298]. With these findings, the authors conducted a phase I clinical trial in patients with advanced and unsuccessfully pretreated cancers or sarcomas. They reported a successful usage of MNPs as drug delivery agents [299]. Huang et al. synthesized nanoparticles coated with PEG and PEI; functionalized with folic acid and attached with doxorubicin. They performed experiments on nude mice MCF7 and concluded that for MCF7 cells and xenograft their treatment resulted in improved efficiencies for tumor growth inhibition [259] Results of selected research articles using MNPs as drug carriers are summarized in Table 1. Examples of clinical trials using MNPs are tabulated in Table 2. The use of nanoparticles in drug delivery is not limited to cancer alone. In addition to cancer, Alzheimer's and Parkinson's diseases have also been reported. Busquet et al reviewed the use of SPIONs in Alzheimer's disease and reported that magnetic nanoparticles

could be used as proper agents to diagnose amyloid beta plaques. In addition, it can be said that SPIONs may also be used as theranostic agents because they have been shown to delay the fibrillation process [300], [301]. When it comes to Parkinson's disease, one of the causes of this disease is alpha synuclein accumulation. Niu et al. have concluded that SPIONs can be a therapeutic agent for Parkinson's disease by showing the reduction of alpha synuclein expression using oleic acid-coated magnetite nanoparticles [125], [302].

1.1.3.3. Limitations for the utility of MNPs in biomedical applications

SPIONs are promising tools for diagnostics (imaging, contrast agents) and therapy (targeted drug delivery systems) due to their inherent properties such as low cytotoxicity, functionalization, modifiable structure, and morphology according to the application. However, there are limitations for excessive use of SPIONs in a clinical setting.

Jurgons et al. used phosphated starch polymer-covered iron oxide particles to investigate their distribution after intra-arterial infusion. They investigated the stability of IONPs in deionized water containing NaCl and reported an increased instability of the artery model as well as the decomposition of nanoparticle suspension under a magnetic field. They concluded that this instability and agglomeration may raise the safety concerns about the usage of these particles. Thus, the stability of nanoparticles under physiological conditions should be maintained in order to be widely used of them in the clinics for cancer therapy purposes [303].

The blood brain barrier is a result of a semi-permeable and tight lining of endothelial cells in the brain capillary vessels, making them selectively permeable for many substances circulating in the rest of the body [304]. Blood brain barrier block passage to the central nervous system of nanoparticles as well. Therefore, SPIONs should be functionalized with a surface coating to gain access through the blood-brain barrier. Brain tumors might also be detected and treated by MNPs following functionalization [305]–[307].

The use of superparamagnetic IONPs offers advantages over conventional methods. However, since they are inorganic and chemically produced, they may cause

problems for the body in *in vivo* as well as *in vitro* applications. Therefore, cytotoxic properties of these nanoparticles should be investigated and assessed carefully. Wang et al. designed cell penetrating FITC-MNPs and FITC-Tat peptides conjugated to an MNP system and compared the uptake efficiencies of these two peptides in Caco-2 cell lines. They observed that FITC-Tat MNPs accumulated in the cytoplasm and nucleus while FITC-MNPs accumulated in the cell membrane. Cytotoxicity tests showed that FITC-Tat MNPs resulted in insignificant cell death, suggesting that these particles can be further used for therapeutic drug and gene delivery purposes [308]. Masoudi et al. synthesized Fe/Fe-oxide core shell nanoparticles and characterized CuK α radiation X-Ray diffraction (XRD) and transmission electron microscopy (TEM) for imaging the spherical shape. They performed a cell death-survival assays on mouse fibroblast cells and demonstrated that when iron concentration increases, cytotoxicity also increases [254]. Gupta et al. synthesized magnetic polymeric nanoparticles having a magnetic core and polymeric shell via microemulsion polymerization. They prepared PEG-modified superparamagnetic particles in aqueous sodium bis(2-ethylhexyl sulfosuccinate) (AOT)/hexane solutions and characterized them with TEM, Atomic Force Microscopy, and UV visible spectrometry. After PEGylation of nanoparticles via an inverse microemulsion polymerization process, the resulting nanoparticles will have a hydrophilic shell. TEM results showed that the core shell nanoparticle structure is spherical, and has a size of 40–50 nm. Cytotoxicity studies showed that such nanoparticles are nontoxic and suitable for use in *in vivo* and *in vitro* studies [309]. Furthermore, Fonseca et al. prepared poly(lactic-co-glycolic acid) (PLGA) nanoparticles loaded with paclitaxel via interfacial deposition. They investigated the incorporation of paclitaxel onto the nanoparticles while also using spherically shaped nanostructures as a drug delivery agent for human small-cell lung cancer cell lines. When the authors combined these particles with various drugs, a decrease in cell viability and an increase in cytotoxicity is observed. Additionally, the paclitaxel-loaded PLGA nanoparticles also yielded high anti-tumoral efficacy [310]. Chan et al. demonstrated the synthesis of a biodegradable core shell nanoparticle system via nanoprecipitation with self-assembly. They characterized these particles in terms of stability in drug release and cytotoxicity. These structures had a hydrophobic core, PLGA and soybean lecithin monolayer, and PEG shell. Finally, the authors also encapsulated the chemotherapy drug docetaxel and tested its cytotoxicity in cancer cell

lines in vitro [311]. Couto et al. investigated the effects of polyacrylic acid (PAA) coated iron oxide nanoparticles on biological systems as well. They also confirmed accumulation of these particles in liver, spleen, and lungs. They analyzed liver, spleen, and lungs separately and reported no severe damage to organs. However, when they analyzed liver they observed hepatic lipid peroxidation and concluded that although these particles have no catastrophic effect they might cause oxidative stress and suggested further investigation in this area [312].

Recent advances in magnetic drug delivery systems have led to improvements in selective and specific targeting as well as biocompatibility. These developments have resulted in novel systems involving the nanoformulation of metallic/polymeric nanoparticles. The improvements have significantly increased the efficacy of treatments compared to conventional therapies. Moreover, a combination of these novel approaches with conventional treatment strategies might reduce drug doses and minimize side effects. Superparamagnetic IONPs are promising candidates as drug carriers as well as diagnostic agents. Drugs can be loaded onto them and be directed to the desired site using an external magnetic field. Thus, extensive research is currently underway to improve its efficiency for clinical use.

1.2 Motivation

Hyperthermia is a technique mostly used as an additional therapy with cancer drugs. In most of the studies, large magnetic field strengths are used. However, they might be harmful for tissues or organs because of the excessive current generation. In this dissertation we report a drugless direct method for cancer therapy at a small magnetic field strength and high frequency.

For gene delivery, magnetofection is a strong non-viral alternative to viral methods. Among non-viral methods, it yields greater efficiencies compared to conventional ones. In this dissertation, polyethyleneimine (PEI) transfection and PEI coated nanoparticle mediated magnetofection is compared. A system which gives higher efficiencies than the standard PEI protocol could be achieved.

The objectives of this dissertation are as follows:

- To achieve hyperthermia with small strengths via high frequency induction heating,
- To propose a targeted therapeutic method for breast cancer,
- To design, and build an experimental system for gene delivery,
- To overcome the limitations of conventional transfection methods,
- To search for the transfection possibilities,
- To propose a fast, safe, new method for gene delivery via magnetofection.

The following research plan was implemented to achieve the objectives:

- Cancer cell lines were selected and cultured for experiments,
- A hyperthermia experimental system was designed and produced,
- Magnetic field duration was optimized for cancer cell death via hyperthermia,
- A rotary magnetic actuation system for gene delivery was designed and produced,
- Velocities of rotary table and the distance between the sample and the table were optimized,
- Transfection time was optimized to achieve increased efficiency and fast procedure time.

2 THERMAL MANIPULATION OF IRON OXIDE NANOPARTICLES FOR THERAPEUTIC PURPOSES

With the advances in nanotechnology, alternatives to chemotherapy have been explored in cancer treatment. Chemotherapy does not only affect cancerous tissues or cells but also has systemic side-effects on all tissues and cell types in an organism. Hence, it is important to develop selective, local therapeutic strategies affecting only the desired locations and tissues in the body. Nanoparticles could be used as effective tools for the development of targeted therapies. Since the tumor tissues have rather leaky vasculatures compared to healthy counterparts, some nanoparticles may have a tendency to naturally accumulate more in the tumors (the Enhanced Permeability and Retention (EPR) effect)[284]. While the EPR effect might facilitate passive targeting, this feature cannot guarantee elimination of drugs from other sites. Alternatively, an active targeting approach, in which nanoparticles are decorated with a specific antibody or molecule selectively binding to cell surface receptor, seems more promising [279], [281]. Hyperthermia emerged as a valuable alternative to chemotherapy or mostly as an adjuvant therapy. Locality of the treatment is one of the most important features of the method. Among the nanostructures used for hyperthermia, the superparamagnetic iron oxide nanoparticles (SPIONs) have attracted much attention due to their ability to respond to external magnetic field coupled with the potential of molecular targeting or encapsulation of a therapeutic cargo as well as due to their biocompatibility[313]–[317]. In breast cancer studies, specificity could be achieved using differentially expressed cell

surface receptors such as *ERBB2* (HER2)[318]. Studies showed that anti-HER2 antibody conjugated to polymer-coated iron-oxide nanoparticles successfully targeted HER2 overexpressed breast cancer cells and resulted in effective hyperthermia under magnetic fields with different coatings (polyvinylpyrrolidone – polylactic co-glycolic acid (PVP-PLGA)), polyethylene glycol(PEG)), magnetic field exposure times and strengths (30 min, 280 kHz) and particle sizes [275], [319], [320]. S

2.1 Methodology

2.1.1. Materials

FeCl₃.6H₂O and FeCl₂.4H₂O were purchased from Merck (U.S.A). Ammonium hydroxide (26%), poly(acrylic acid sodium salt), Bradford reagent, bovine serum albumin (BSA) standard and Potassium Phosphate dibasic anhydrous were purchased from Aldrich (U.S.A.). Phosphate buffer saline (PBS) and 2-(N-morpholino)ethanesulfonic acid (MES) monohydrate buffers were purchased from Biomatik (Canada). Ethylenediaminetetraacetic acid (EDTA) disodium salt was purchased from Multicell (U.S.A.). Potassium Phosphate monobasic was purchased from Riedel-de Haën (U.S.A.) Ethyl-3-(3-dimethylaminopropyl)carbodiimide (EDC), N-hydroxysulfosuccinimide (sulfo-NHS), DyLight 650 NHS ester, Traut's Reagent and Slide-A-Lyzer 10k, 20k dialysis cassettes were purchased from Thermo Scientific (U.S.A.). antiHER2 (BMS 120) was purchased from Bio-Rad Antibodies. Maleimide and amine heterobifunctionalized polyethylene glycol (Mal-PEG-NH₂) (2K) was purchased from Nanocs (U.S.A.). Vivaspin 20 MWCO 30,000 polyethylenesulfonate (PES) filters were purchased from Sartorius (Germany). Float-A-Lyzer MWCO 300,000 was purchased from Spectrumlabs (U.S.A). N-N dimethylformamide (DMF) was purchased from Merck-Milipore (U.S.A.)

2.1.2 Synthesis of Nanoparticles

Poly(acrylic acid) coated SPIONs (SP) were synthesized in water with the precursor molar ratio of [PAA]: [Fe²⁺]: [Fe³⁺]: [OH⁻] 3:2:1:6 under argon atmosphere and at 85°C for 1 h. After the reaction, mixture was cooled down to RT, placed on 0.3 Tesla magnetic field overnight to remove any precipitate if there was any, and finally the black colloidal suspension was washed with ultracentrifugation using 10 kDa MWCO PES filter and DI water. The elemental iron content in nanoparticle suspension

was determined by ICP-MS method. ICP samples (100 μ l of nanoparticle dispersion) was etched with 250 μ L of H₂SO₄ and 250 μ L H₂NO₃. This sample was diluted to 10 ml for the analysis with DI water.

antiHER2 conjugation to SP was carried out by thiol-maleimide chemistry. Before the thiol-ene conjugation, antiHER2 was fluorescently labelled with commercially available NHS active dye (Dylight 650[®]). Dye was dissolved in DMF in 0mg/mL concentration and mixed with antiHER2 antibody in sodium borate buffer at pH 8.55 in the molar ratio of [antiHER2] : [Dye] = 1:10 at room temperature for 1h. Dye labelled antiHer2 antibody was purified with dialysis using 20 kDa MWCO dialysis cassette (Slide-A-Lyzer) against phosphate/EDTA buffer (pH:8.5) at +4°C. Dialysis was continued for 12 h with buffer refreshment in every 3 h. Next, Dye labelled antiHer2 was mixed with Traut's Reagent at pH 8 at the molar ratio of [1:100] at room temperature for 2h. Thioled antibody was purified with dialysis in 10k MWCO dialysis cassette at +4°C for 4h with 6 buffer refreshments in PBS/EDTA.

Parallel to this procedure, SPION/PAA was mixed with 3 mg of NH₂-PEG-Mal (2000 da) for 48h at +4°C and quenched with excess hydroxylamine. Product was purified using ultracentrifugation with 10kDa MWCO Amicon filter at +4°C. Freshly prepared antiHER2-dye-SH was mixed with maleimide functionalized SP in PBS/EDTA at pH 7.2 for 1h at room temperature and overnight at +4°C. The overall product was purified with the dialysis (300 kDa MWCO dialysis device membrane) at +4°C with 4 times buffer refreshment every 3 h in PBS.

2.1.3. Nanoparticle Characterization

Dynamic light scattering (DLS) experiments were conducted with Zetasizer Nano Series ZS at room temperature with 173° backscattered angle. Functional groups were investigated using the dried samples and Thermo Scientific Nicolet iS10 ATR-IR. Transmission electron microscopy (TEM) images were taken by Techani G2 F30 at brightfield high resolution (HR) TEM (acceleration voltage 200 kV) using samples deposited on carbon coated Cu-grid from dilute solutions. Vibrating Sample Magnetometry (VSM) measurements were conducted with Cryogenic limited PPMS under ambient conditions. ICP MS measurement was carried out with Agilent 7700x.

2.1.4. Experimental setup and procedure

A horizontal induction coil having 10 windings, which have a diameter of 5.4 cm, with a magnetic field frequency of 400 kHz was used. The system was operated at 5A maximum current, and the magnetic field had an amplitude of 0.8 kAm^{-1} . The device consists of a DC power supply to generate power for magnetic field generation, an inverter, an amperemeter to measure the current passing through the coil, a coil to generate magnetic field, and a thermometer for the maintenance of the system at the ambient temperature as shown in Figure 2.1a.

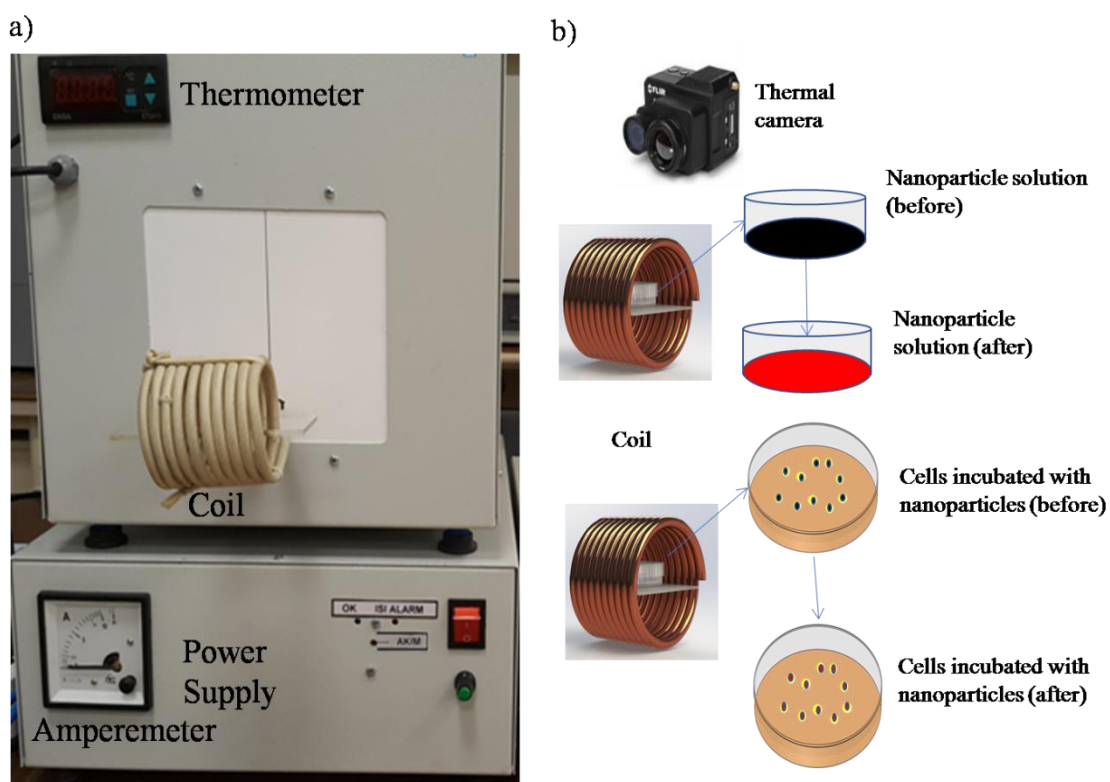


Figure 2.1 a) Induction coil setup, b) Schematic of the procedure

The direction of magnetic field generated by the coil is from the center to outside. Current-driven heating of the coil is prevented by a chiller during the experiments, which is capable of cooling the coil to avoid any interference of heat (generated by the coil) with the samples.

In order to be able to apply magnetic field to breast cancer cells, the cell culture plate was placed on a plexiglass sheet, which keeps the plate at the center of the coil.

Hyperthermia treatments were performed with a current of 5 A, which is the maximum current in the system, for 5 and 10 minutes. Figure 2.1b is the schematic representation of the experiment. Trypan blue staining for the death cell analysis was used after 5 and 10 min exposure and 48 h incubation time [216], [321]. Since the coil in this study was rather small, the 96 well plate was cut with the laser cutting system, and the cells were seeded into these wells.

2.1.5. Cell Culture

SK-BR-3 (isolated by Trempe and Old; ATCC number HTB-30) human breast cancer/mammary gland cells, derived from metastatic site: pleural effusion MDA MB 453 (isolated by R. Cailleau; ATCC number HTB-131) human breast cancer/mammary gland cells, derived from metastatic site: pericardial effusion. MDA-MB-453 and SKBR3 cells were incubated with Dulbecco's modified Eagle's medium (DMEM, Biological Industries, #BI01-050-1A) supplemented with 10 % (v/v) fetal bovine serum (FBS, PAN, #P30-3302), antibiotics (Penicillin/streptomycin, Biological Industries, #BI03-031-1B) and L-Glutamine (Biological Industries, #BI03-020-1B) in a 5 % CO₂ humidified incubator at 37°C. Cell lines were incubated with 150 µg mL⁻¹ SPION/PAA (SP) or SPION/PAA/antiHER2 (SP-H) for 12 hours, and then exposed to the magnetic field for 5 or 10 minutes. After the procedure, cells were incubated for an additional 36 hours. Cell viability was analyzed using trypan blue exclusion or MTT assays.

2.1.6. Flow cytometry analysis

Alexa-fluor-647 conjugated nanoparticles were used to demonstrate targeting of the HER2 expressing cells. MDA-MB-453 and SKRB3 cells were seeded in 12-well plates and treated with nanoparticles at defined time intervals. After washing twice with 1 x PBS, cells were trypsinized and fixed with ice-cold 70% ethanol. Alexa-fluor-647 positive cells were detected using a BD FACSCanto™ device and analyzed with the Flow Jo software. 10.000 event populations were collected for each sample, and cellular debris was excluded from the counts. Nanoparticles, which do not have anti-HER2 on their surface, were also combined with Alexa-fluor-647 and used as controls.

2.1.7. Cytotoxicity assay

The toxic effects of nanoparticles on cells were investigated using the 3-(4,5-dimethylthiazol-2-yl)-2,5-diphenyl tetrazolium bromide (MTT) assay. MDA-MB-453 cells were seeded in 96-well plates, and after 12 hours incubation, cells were treated with nanoparticles for an additional 48 hours period. Then, 10 μ l MTT reagent was added onto 100 μ l of medium and cells were incubated at 37°C for 4 hours. Following removal of the medium, formazan crystals were solublized in DMSO for 10 min at RT. The absorbance of the solution was determined at 570 nm using a Microplate absorbance reader (Biorad, iMark) and a 650 nm reference filter. Cell viability for each group was expressed as percentage of viable cells over untreated control cells.

2.1.8. Immunofluorescence Analysis

The cells were cultured on coverslides in the presence of 150 μ g nanoparticle suspension and subsequently fixed in 4% ice-cold paraformaldehyde (PFA). After staining with the Hoechst 33342 dye (Invitrogen, 31716W), coverslides were analyzed under a Carl Zeiss LSM 710 confocal microscope under 63 x magnification (Zeiss, Germany).

2.1.9. Statistical Analyses

Statistical analyses were carried out by One-Way Anova, and p values smaller than 0.05 were considered as significant.

2.3 Results

Colloidally stable ultra-small SPIONs with about 4 nm crystal, 17 nm hydrodynamic size (number based average measured by DLS) (Figure 2.2a) and -19meV zeta potential were successfully obtained in a single step, aqueous synthetic route. Iron content of the PAA coated SPIONs was determined as 20% by ICP-MS analysis. VSM analysis indicated that particles did not reach saturation even at 1T possibly due to ultra-small size of the SPION cores. However, a magnetization of 21.6 emu per gram is obtained at 1 T for total amount of nanoparticle (Figure 2.2b) while magnetization was 43.7 emu per gram for iron content.

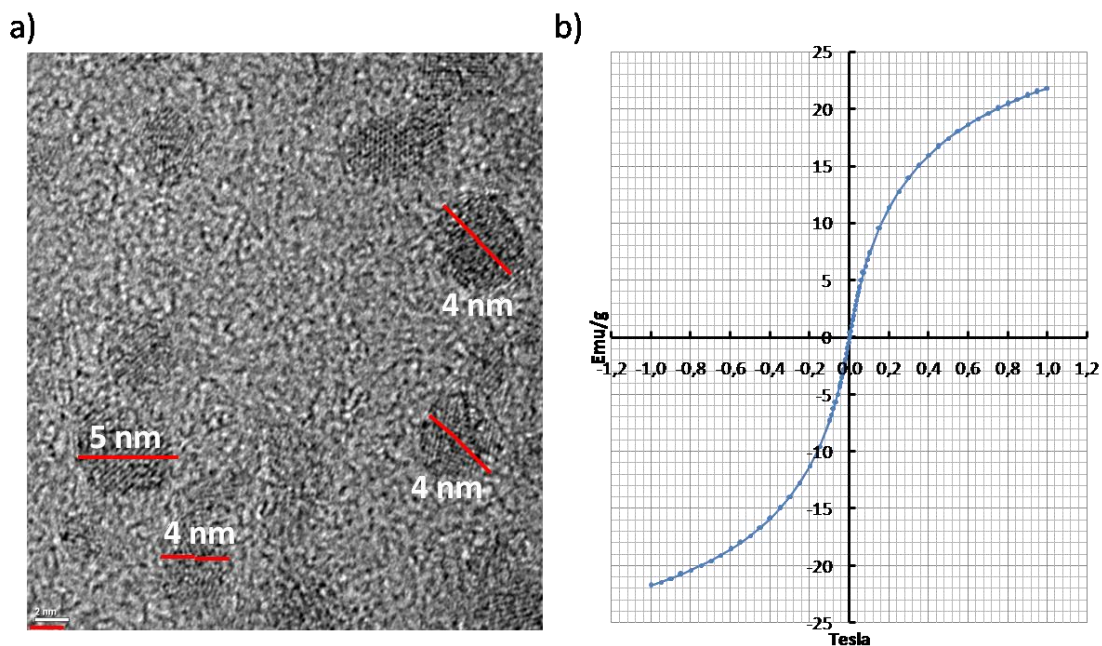


Figure 2.2 a) Sample TEM image of SP nanoparticles, b) VSM measurement result

We first performed inductive heating of concentrated Lauric acid (LA) coated nanoparticle solution. The temperature increase in LA coated nanoparticles was measured by a FLIR thermal camera for less than 2 min inductive heating. For this experiment, 1 ml of the SPION solution was placed into the plates, which were put into the induction heating device. A temperature of 41.5°C was reached within less than 2 minutes along with a current drop from 5 to 1.5A. Based on the thermal camera image, it was confirmed that the system could successfully heat SPIONs (Figure 2.3). However, these nanoparticles are not suitable for targeted drug delivery applications. Therefore, the experiments continued with biocompatible PAA coated iron oxide nanoparticles tagged with HER2 (SP-H) antibody. Since, a low amount of SP-H nanoparticles targeted the cells, the thermal camera could not capture the heating of individual nanoparticles for local heating. Therefore, cell death analysis was utilized as the local heating indicator for cell culture experiments.

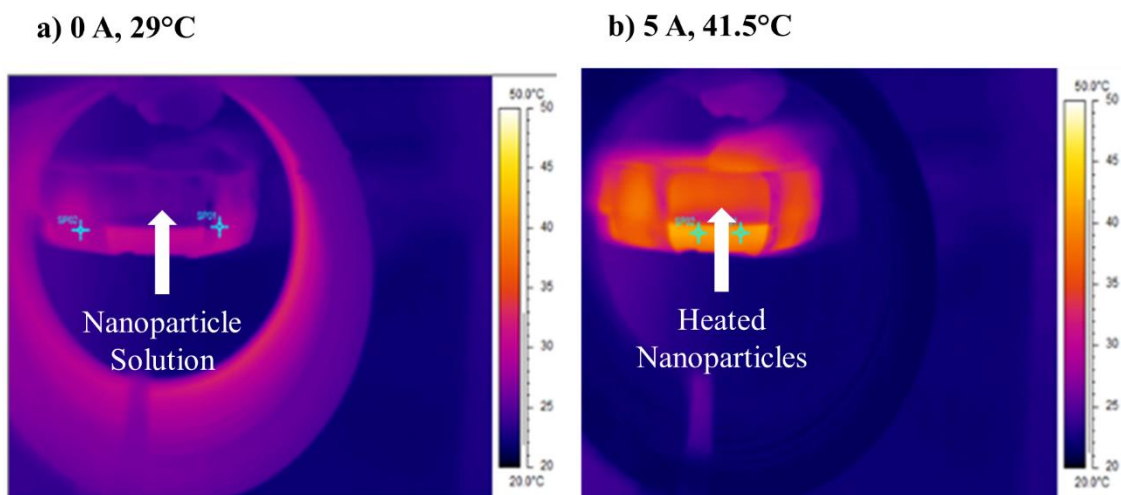


Figure 2.3 Thermal camera and experimental images of SPIONs, SP01 and SP02 indicate the surfaces of measurement a) Initial temperature, no heating observed b) Final temperature, yellow color shows the heated SPIONs

Magnetic hyperthermia was tested with the SP-H in the cell culture. Initially, MDA-MB-453 cells were treated with $150 \mu\text{g mL}^{-1}$ SP and SP-H for 12h, un-internalized nanoparticles were washed, and the plate was placed in the coil (5A, 10 min, Figure 2.4a). Since the amount of internalized nanoparticles is small, the thermal camera could not capture the heating of the fixed cells but an alignment was observed for the cells, which were incubated with SP-H (labeled as Np in Figure 2.4b). This alignment could be attributed to the relaxation mechanism, and cells containing nanoparticles were aligned at locations with larger magnetic field after they died/sensitized because of the exposure and detachment from the plate surface.

In vitro cell viability analysis was performed as an alternative indicator of hyperthermia. Initially, SP and SP-H were incubated with SKBR3 and MDA-MB-453 cells with different nanoparticle doses between $5 \mu\text{g}$ to $500 \mu\text{g}$. MTT assay was carried out to assess the toxicity of nanoparticles on cells after 48 h of treatment. As shown in Figure 2.5a, these particles were not toxic to these cell lines.

In order to demonstrate the targeting ability of the SP-H particles, a fluorophore, Alexa-fluor-647, was attached to the SP-H and on SP nanoparticles (Figure 2.5b). Microscopy analyses of SKBR3 and MDA-MB-453 cells showed that SP-H nanoparticles, but not the SP particles, accumulated on the surface of cells, indicating an

anti-HER2-dependent targeting ability of SP-H. This was also confirmed by flow cytometry analysis. The signal of the SKBR3 and MDA-MB-453 cells incubated with SP-H shifted to the right, while the signals of the SKBR3 and MDA cells that were incubated with SP or control stayed the same. This signal shift confirmed SP-H attachment/uptake in HER2-positive cells (Figure 2.5c). This is quite critical to accumulate effective SPION dose at the target.

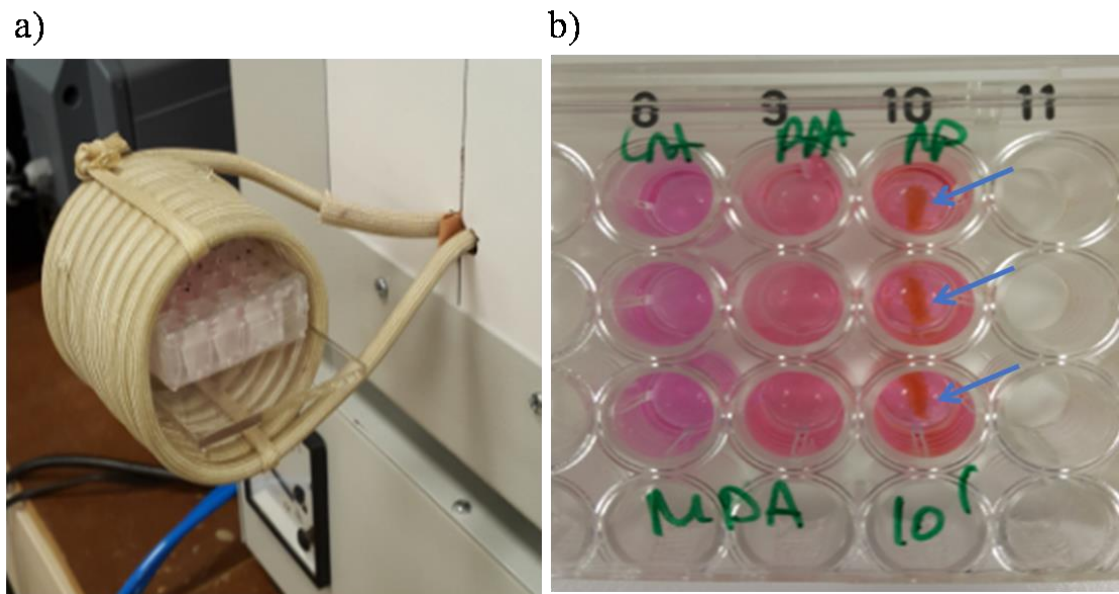


Figure 2.4 Experiments with 96 well plate and image of the cells after exposure. a) Cells are seeded on one part of 96 well plate and put in induction coil for 10 min, b) Cell alignment after 10 min of magnetic field exposure, arrows show nanoparticle alignments.

Lastly, MDA-MB-453 cells that were treated with SP or SP-H and control samples were exposed for 5 or 10 min to the magnetic field. Cell death was measured with trypan blue exclusion test, cell viability was measured by MTT assays. According to trypan blue exclusion tests, cells that were incubated with nanoparticles cause significantly more cell death than the control (Figure 2.6a). Less than 10% mortality in control cells (not treated with nanoparticles) implies that the magnetic field alone did not kill the cells. On the other hand, SP-H caused a higher mortality than the SP-treated cells following 5 min magnetic field exposure (Figure 2.6a). Cell viability assay results show that 10 min exposure is more suitable for reducing cell proliferation compared to the 5 min exposure (Figure 2.6b & c). Also, SP particles cause decreased viability,

which suggests that even though particles are not internalized by these cells in significant amount (based on Figure 2.5b & c), nanoparticle and magnetic field combination affects the proliferation. SPIONS were tagged with red fluorophore to track them optically in the in vitro studies.

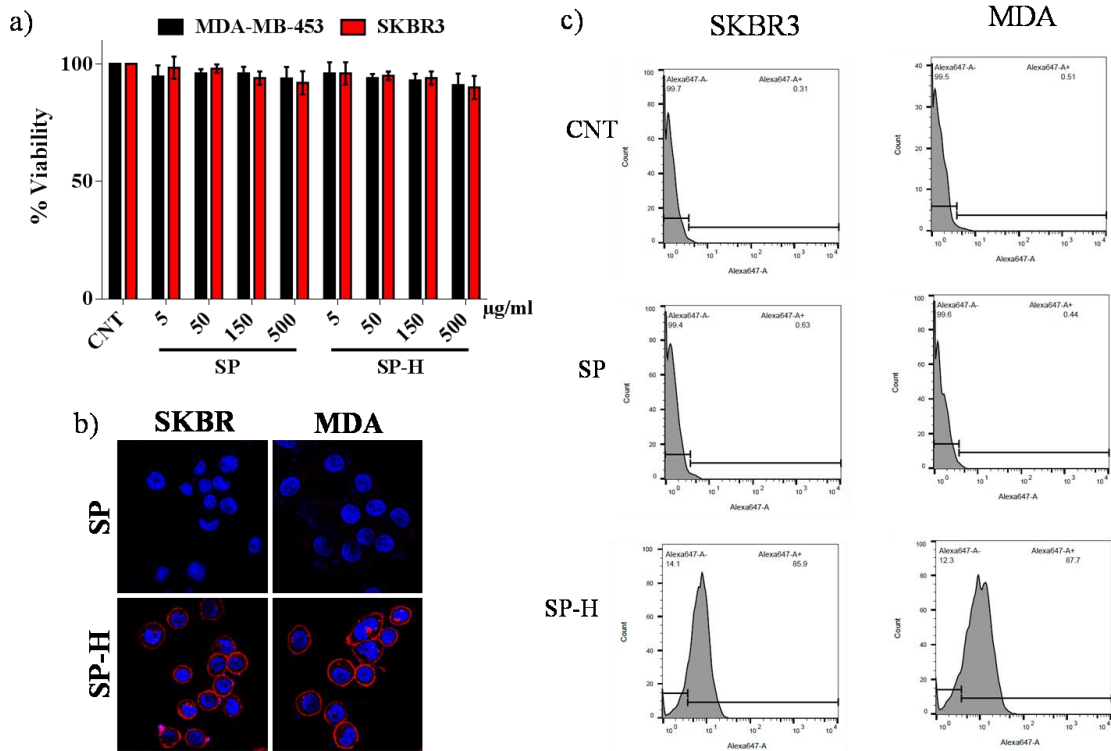


Figure 2.5 Toxicity and targeting analysis of nanoparticles, in SKBR3 and MDA-MB-453 cells. (a) Viability of cells treated with different concentrations of 5 to 500 μg ($n=3$, $p<0.05$) (b) Confocal microscopy analysis of Alexa-fluor-647 conjugated SP-H and SP treated MDA-MB-453 and SKBR3 cells, (c) Flow cytometry analysis of the particles after 12 h treatment (150 $\mu\text{g/mL}^{-1}$).

Consequently, SPION internalized cells present red fluorescence either in cell membrane or in the cell. Both Figure 2.5b (confocal microscopy analysis) and Figure 2.5c (FACS analysis) represent the percentage of the cells, which were targeted either way and confirm the internalization of SPIONS by these cells. Hence, this information coupled with the toxicity results presented in Figure 2.6 confirms cell heating in the realization of SPION-based magnetic hyperthermia.

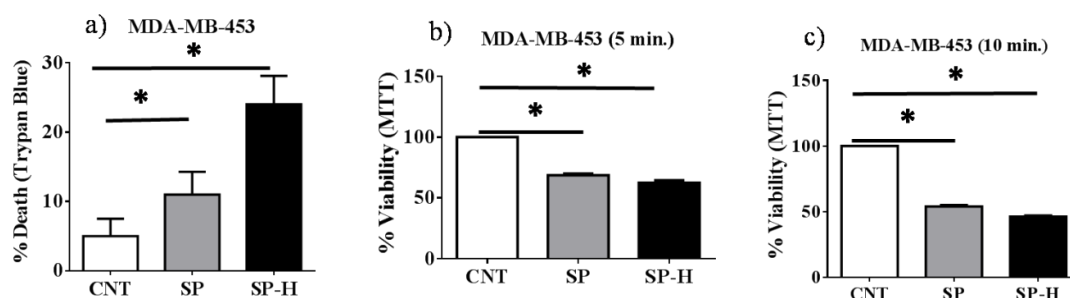


Figure 2.6 Death and viability analysis of MDA-MB-453. Cell death (%) determined by the Trypan blue exclusion assay (a), and cell viability (%) determined by MTT assay of control cells (CNT, which are not treated with nanoparticle), cells treated with $150 \mu\text{g mL}^{-1}$ SP or SP-H and subjected to inductive heating for 5 min (a, b) and 10 min (c). $n=3$, p value <0.05 for statistical significance

2.4. Discussion

To determine, whether these small SP-H (antiHer2 targeting) and SP (no targeting feature) nanoparticles are able to suppress the growth of breast cancer cells or kill them via magnetic hyperthermia at low field and high frequency within short operational times, two different HER2-positive breast cancer cell lines (SKBR3, MDA-MB-453) were treated by these nanoparticles in a dose dependent manner. No significant cytotoxic effect was observed even at higher levels of nanoparticle concentration, which proves that SP and SP-H nanoparticles could be used as biocompatible cancer therapy agents. Via fluorescent microscopy and FACS analysis, selective and higher uptake of SP-H particles compared to SP by these HER2 expressing cancer cell lines was demonstrated in vitro. Indeed, although SPIONs are considered as good MRI contrast agents, fluorescent tagging allows for optical tracking, especially valuable in the in vitro studies. Such effective targeting of cancer cells is invaluable for the diagnosis of cancer and also for the local and/or target specific treatment via hyperthermia.

This hypothesis was tested using the SP and the SP-H nanoparticles decorated with tumor specific antiHER2 antibody in vitro using the MDA-MB-453 cells, which have a higher HER2 receptor expression than SKBR3 cells (unpublished data). The control cells (no nanoparticle treatment) and the cells treated with either nanoparticle were exposed to magnetic field at 5A for 5 and 10 min after 12 h incubation. The

current read from the plates of SP-H treated cells fell from 5A to values below 2.5 A during the experiment, while no change was detected in the control group or SP treated cells, which is attributed to the targeting ability of SP-H, resulting in higher uptake of nanoparticles and hence greater hyperthermia effect. This trend may be also linked to generation of eddy current, even though our particles are not within the effective size range suggested for eddy current generation. If we generated eddy currents, even though the small magnetic flux (1.01mT) and strength (0.8 kAm^{-1}) were smaller than in the literature[322], we would have been still below the toxicity limit for eddy current generation :

$$H.f = 0.8 \times 10^3 \times 400 \times 10^3 = 3.2 \times 10^8 \text{ Am}^{-1} \text{ s}^{-1} \leq 5 \times 10^9 \text{ Am}^{-1} \text{ s}^{-1} \quad (3)$$

Indeed, in vitro tests also confirm that our system, and inductive heating procedure does not kill the cells if they lack SPIONs. The cancer cells treated with SPIONs and subjected to inductive heating showed cell death, and dead cells are detached from the plate surface and are aligned towards to magnetic field because they contain SPIONs in their cytoplasm (Figure 2.4b). This behavior also serves for an experimental proof for superparamagnetic property of nanoparticles, where magnetization does not exist without any external magnetic field[270]. It is important to note here that the death and reduced proliferation of cancer cells treated with nanoparticles could be observed despite of the small magnetic field strengths used in the experiments, which can be explained with frequency dependency of the relaxation times. Our homemade system has a higher frequency compared to the most of the systems used in the literature [262].

Attaching an antibody to the nanoparticle provides site specific targeting and is shown to be effective for hyperthermia as well. Almaki et al.[275] used PEG coated HER2 tagged magnetic nanoparticles in hyperthermia for 20 min at 230 kHz, while Pala et al.[320] synthesized dextran coated aptamer tagged nanoparticles for 30 min+30 min intervals at 280 kHz. They both have lower frequencies than our system. Also, Pala et al. used a higher magnetic field magnitude. Vivek et al.[319] utilized PVP-PLGA coated nanoparticles conjugated with an anticancer drug Tam and showed cytotoxic effects of both hyperthermia and drug. In our system, PAA coated SPIONs were used at a frequency of 400 kHz. Drug-less cytotoxicity and proliferation reduction via hyperthermia at a low magnetic field magnitude were achieved. Our in vitro studies

showed both significant reduction in cell viability and dramatic cell death in SPION treated cells subjected to inductive heating with some differences between the two assays. Briefly, SP-H increased cell death (determined by trypan blue assay) much more dramatically than SP after inductive heating, which confirms that antiHER2 antibody enhanced cellular uptake of SP-H due to receptor-targeting, hence provided higher hyperthermia and more cell death. On the other hand, MTT assay indicates a decrease in viability of cells with no significant difference between SP or SP-H treated cells subjected to inductive heating. This may suggest that the amount of SP nanoparticles, which are internalized through diffusion, is lower than the SP-H, but still enough for hyperthermia-induced prevention of proliferation, however does not provide enough temperature increase to cause dramatic cell death. Higher concentration of nanoparticles per cell would cause higher temperature increase under magnetic field. Besides, in 5 min inductive heating, the cell viability drops to about 50%, which drops below this value in 10 min treatment.

3 MECHANICAL MANIPULATION OF IRON OXIDE NANOPARTICLES FOR GENE DELIVERY

With the development of nanotechnology, gene therapy applications for diagnosis and treatment have gained both variety and importance. Gene therapy involves replacing a gene, which is losing its function, or introducing an exogenous gene to re-functionalize the damaged gene [323]–[326]. The exogenous gene needs to be transported to the cell in vectors, which are classified as viral and non-viral vectors. Commonly used viral vectors are adenovirus, lentivirus, and adeno-associated viruses [327]–[329]. While viral vectors are efficient carriers, they might cause damage to the targeted cell and the surrounding tissue because of their toxicity. On the other hand, non-viral vectors emerged as an alternative thanks to their reduced toxicity. Cationic lipids and polymers are commonly used non-viral vectors [330]. They are regarded as suitable carriers for genes since they can be conjugated with different particles and be functionalized with coatings [9]-[10]. Magnetic nanoparticles are good candidates for this task [171], [333], [334]. Iron oxide nanoparticles are considered as advantageous among magnetic nanoparticles for drug/gene delivery in therapeutics and diagnostics of various diseases because of their biocompatibility, functionality and physical properties [335]–[338]. Since they are in the superparamagnetic regime, they are effective, when an external magnetic field is applied, and upon the removal of magnetic field, they can be removed from the environment/body because they will have no remnant magnetization [339].

Transferring genes via nanoparticles using magnetic fields is called magnetofection [213], [340], [341]. Such nanoparticles are generally coated with cationic polymers for DNA binding and are sent to the cell. Then, they interact with the

cell membrane and are dispersed into cytoplasm through endosomal escape. In this case, the particles remain in cellular vesicles and are taken up by endocytosis. The expression takes place after internalization [340], [342]. Polyethyleneimine is the conventional and well established transfection agent. However, it is known to be harmful to the cell [338], [341]. Coating nanoparticles with polyethyleneimine and using them with magnetic fields increase the transfection efficiency while reducing the toxicity effects [336], [343].

Oral et al. showed that polyethyleneimine coated superparamagnetic nanoparticles (PEI-SPIONs) can efficiently transfer green fluorescent protein tagged DNA (GFP-DNA) under varying magnetic fields. In that study, the transfection agents remained on the cells with an 8 hour incubation, while the device was in operation. The viability was improved, but the transfection yield was still lower than the PEI. In this chapter, interventions, which could be introduced to the transfection protocol, were investigated using MCF7 cells, which we reported as resistant to transfection [212]. Accordingly, the transfection time of 8 hours was reduced to 1 hour, and the necessity of an incubator during the experiment was eliminated. The viability also significantly increased when the transfection agents were washed out from the cells at the end of 1 hour of actuation. When the transfection efficiencies were examined, it was proven that efficient transfection could be performed even within a short time (1 hour) with the developed new generation actuation system. Accordingly, GFP-DNA transfer to MCF7 cell line with high efficiency was achieved with magnetofection.

3.1. Methodology

3.1.1. Cells and Reagents

The pmax-GFP mammalian expression vector was supplied by Amaxa (Amaxa, Lonza, Switzerland). Branched PEI (MW 25,000) was purchased from Sigma- Aldrich (408727-USA). Dulbecco's modified Eagle's medium (DMEM) was purchased from Sigma-Aldrich (D5671-Germany). L-glutamine (BIO3-020-1B), Penicillin/Streptomycin (BIO3-031-1B) and Trypsin-EDTA (BIO3-050-1A) were purchased from Biological Industries (Israel). Fetal Bovine Serum (FBS) was purchased from BioWest (S1810-USA). Phosphate Buffered Saline (PBS-17-516F) without

calcium or magnesium was purchased from Lonza (USA). Breast cancer (MCF-7, HTB-22) cell line was obtained from American Type Culture Collection (ATCC, USA).

3.1.2. Magnetic Actuation System

The system consists of a rotary table, which has four rare earth magnets, a 12 V DC motor, power cables, and adjustable plexiglass stages for placing 10 cm petri dishes (Figure 3.1). The magnets were placed in such a way that their poles pull each other. Rotation of the table was provided with the 12V DC motor. The parts of the system were fabricated with the laser cutting and 3D printing techniques. Magnetic field fluxes of the magnets and the variation of magnetic field depending on the distance between table and sample were measured by a gaussmeter (Hirst Magnetic Instruments Ltd.). Air surrounding, magnets and plexiglass table are also modeled AC/DC module of the COMSOL Multiphysics 5.2a software for simulating the magnetic fluxes exerted to the sample at different distances.

3.1.3. PEI-SPION Synthesis and Characterization

PEI coated SPIONs were prepared by using a ligand exchange method as explained in our previous work [212]. This sample was directly used for DLS (Dynamic Light Scattering) and zeta potential measurements. AFM (Atomic Force Microscopy) analysis was performed on a Bruker Dimension Icon in ScanAsyst mode in air with ScanAsyst-Air cantilever (Bruker, USA, $k = 0.4$ N/m, frequency 70 kHz). The samples were diluted with ethanol, sonicated and drop cast on silicon wafer for analysis. 80% of total product mass (PEI-SPION) was determined as PEI by thermo-gravimetric analysis performed on dried samples.

3.1.4. Plasmid DNA Isolation

Plasmid DNA isolation was performed with plasmid DNA purification kit according to manufacturer's instructions (Nucleobond Xtra Midi/Maxi, Macherey-Nagel, Germany). pmax-GFP plasmid was used for transfection experiments.

3.1.5. Cell Culture

MCF-7 human breast cancer cells were cultured in DMEM supplemented with 10% fetal bovine serum (FBS) and antibiotics (Penicillin–Streptomycin). 1.2×10^6 cells were seeded on 10 cm culture plates in 8 ml cell culture medium. Cells were incubated at 37 °C in a humidified incubator with a 5% CO₂ atmosphere.

3.1.6. Magnetofection

60 µg of branched PEI or PEI-SPION solutions, which carried 60 µg PEI, were added into Eppendorf tubes containing 200 µL DMEM (without serum and antibiotics). In another Eppendorf tube, 10 µg of pmax-GFP was mixed with 200 µL DMEM (without serum and antibiotics). Contents of the tubes were mixed and vortexed for 15 s. Following 10 min incubation at room temperature, the mixture was dropwise added onto culture plates. Cells were concomitantly exposed to magnetic field for 1h, and they were put into the incubator for additional 11 – 5 – 2h, while the transfections agents were still interacting with the cells. Thereby, cells were exposed to transfection agents for 12 – 6 – 3 hours before removing the agents. Then, they were washed with PBS, and then, the culture was maintained in DMEM for an additional 48 h. For 1h experiment, cells carrying the PEI-SPION solution were put onto the device. Then, they were immediately washed with PBS to remove the agents, and fresh medium was added and put into incubator for 48h.

3.1.7. Microscopy Analysis and Transfection Efficiency

At 48 h post-transfection, transfection efficiency was observed using an inverted fluorescent microscope (Olympus IX70) with 10x magnification. Transfection efficiencies were determined from the microscopy images. Accordingly, 900 cells were counted for each sample.

3.1.8. Cell Viability Assays

Cancer cells transfected with PEI or PEI-SPION in the presence or absence of rotating magnetic field conditions were evaluated for cell viability. Non-transfected

cells were used as control and were treated in the same way as their transfected counterparts. Cells were harvested at 48 h post-transfection, and viability was assessed using the trypan blue exclusion technique. Here, loss in membrane integrity was determined by the uptake of the trypan blue dye, to which cells were normally impermeable.

3.2. Results

3.2.1. Actuation System

A varying magnetic field was generated by rotating the system consisting of 4 magnets on a table as shown in Figure 3.1a while Figure 3.1b illustrates the cell experiment steps. Each individual magnet had a magnetic field flux of 230 mT. The magnetic flux values of the system were utilized in the numerical model with air as the surrounding, 4 magnets, and a plexiglass table (

Figure 3.2a). The system was modeled to prove the non-uniform magnetic field distribution throughout the rotary table.

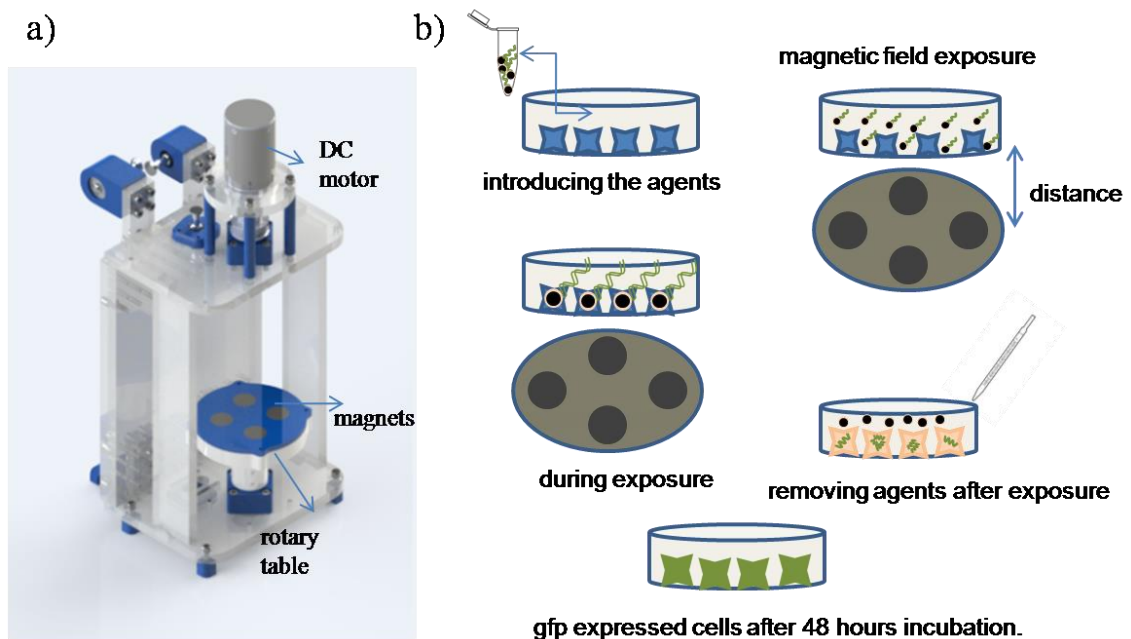


Figure 3.1 Actuation system and experimental procedure. a) Magnetic actuation system b) Schematic representation of experimental steps, introducing the agents - magnetic field exposure - during exposure - removing agents after exposure - gfp expressed cells after 48 hours incubation.

Simulations were performed using a workstation of Intel(R)Core(TM) i7-3630QM CPU with 2.40 GHz processor. The diameter and height of the magnets were 2.5 cm and 0.5 cm, respectively (

Figure 3.2b). The plexiglass table was 9 cm wide and 0.5 cm thick. An extremely fine free tetrahedral mesh configuration (1151002 domain, 33178 boundary and 1072 edge elements) were used (

Figure 3.2c & d). The governing equations are as follows:

$$\nabla \times \mathbf{H} = \mathbf{J} \quad (4)$$

$$\nabla \times \mathbf{A} = \mathbf{B} \quad (5)$$

$$\mathbf{J} = \sigma \mathbf{E} \quad (6)$$

Here, \mathbf{H} is the magnetic field strength, \mathbf{B} is the magnetic field, \mathbf{A} is magnetic vector potential [344], \mathbf{J} is current (in our case is 0), \mathbf{E} is electric field (in our case is 0), σ is electrical conductivity. The magnetic flux value was utilized in the multiphysics software COMSOL5.2a using a configuration of 4 magnets and plexiglass surrounding.

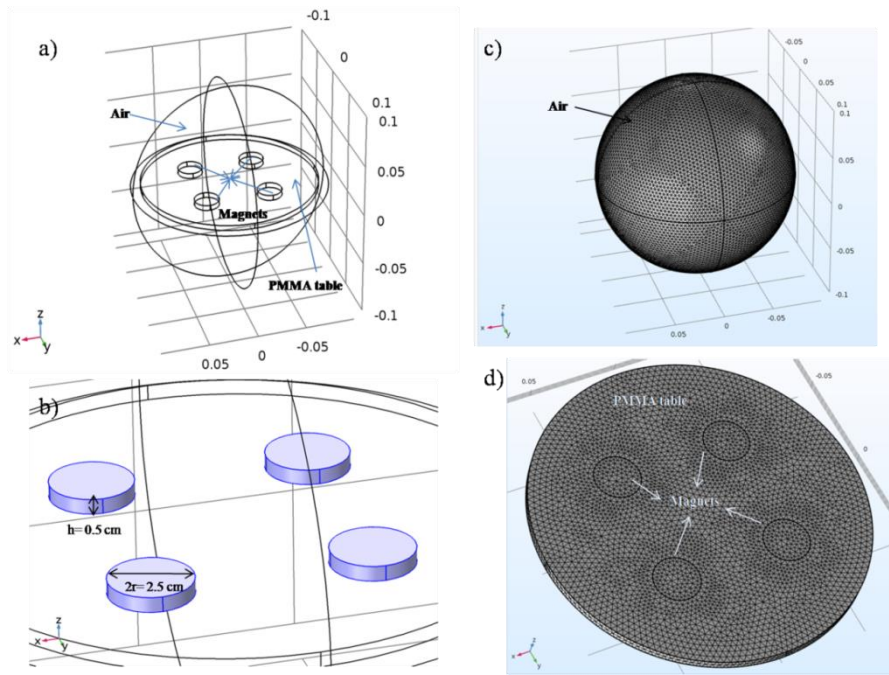


Figure 3.2 Model of the study. a) Modeling setup b) Sizes of magnets c) General view of mesh configuration d) Close up view of mesh configuration

According to the simulation results maximum magnetic force values are obtained at a distance of 2 cm for a diameter of 2.5 cm in parallel lines of the experiments (Figure 3.3a). Furthermore, as the distance between the sample and the magnet system increases, the magnetic force decreases. However, the fluxes exerted from magnets are distributed in such a way that their magnetic forces move in a circular pattern around the center of these 4 magnets. Thus, the circulating effect initiates at the height of 2.5cm (Figure 3.3b), and it neither leads to small forces at larger distances nor the forces are concentrated at smaller distances. As a result, the distance of 2.5cm is chosen as the best option for both magnetic force and uniformity for iron dust particle experiments. At the distances of 3 and 3.5 cm, less concentrated magnetic patterns are observed, and smaller forces are generated (Figure 3.3c-e). All the magnetic flux density patterns regarding Figure 3.3a-e are combined to a single 3D illustration (Figure 3.3f).

This system generated a non-uniform magnetic field with fluxes varying from 2mT to 60 mT through the rotary table, which were experimentally measured. To visualize the effect of distance between the sample and rotary table, iron dust particles were used. It can be observed that iron dust particles are influenced by the magnets' own field and aggregate on individual magnets as expected, when the petri dish

containing iron dusts is placed on the magnets and clustered near the edges (Figure 3.4a). When the petri dish is slowly removed upwards (from the table), the magnets work together, and the dusts are evenly distributed to the plate (Figure 3.4b). Then, the effect of the rotation of the system on dusts is investigated. Accordingly, when the behaviour of dust particles at different distances are examined, and it can be seen for a 2.5 cm distance dust particles arrange successively, the particles are continuously lifted from a one side and roll around the center. (Figure 3.4c-f). In a permanent magnetic actuation system, the particles experience a lifting force given as

$$F = \frac{\mu_0 M^2 A}{2} = \left(\frac{(\mu_0 M^2) A}{2\mu_0} \right) \quad (7)$$

where F is the lifting force of a permanent magnet, μ_0 is magnetic permeability ($4\pi \times 10^{-7}$), M magnetization, $(\mu_0 M)$ is the saturation magnetization A is the area of magnetization (area of rotary table) [345]. In our system saturation magnetization of a single magnet is 223 mT. Therefore the generated lifting force is 971.26 kN.

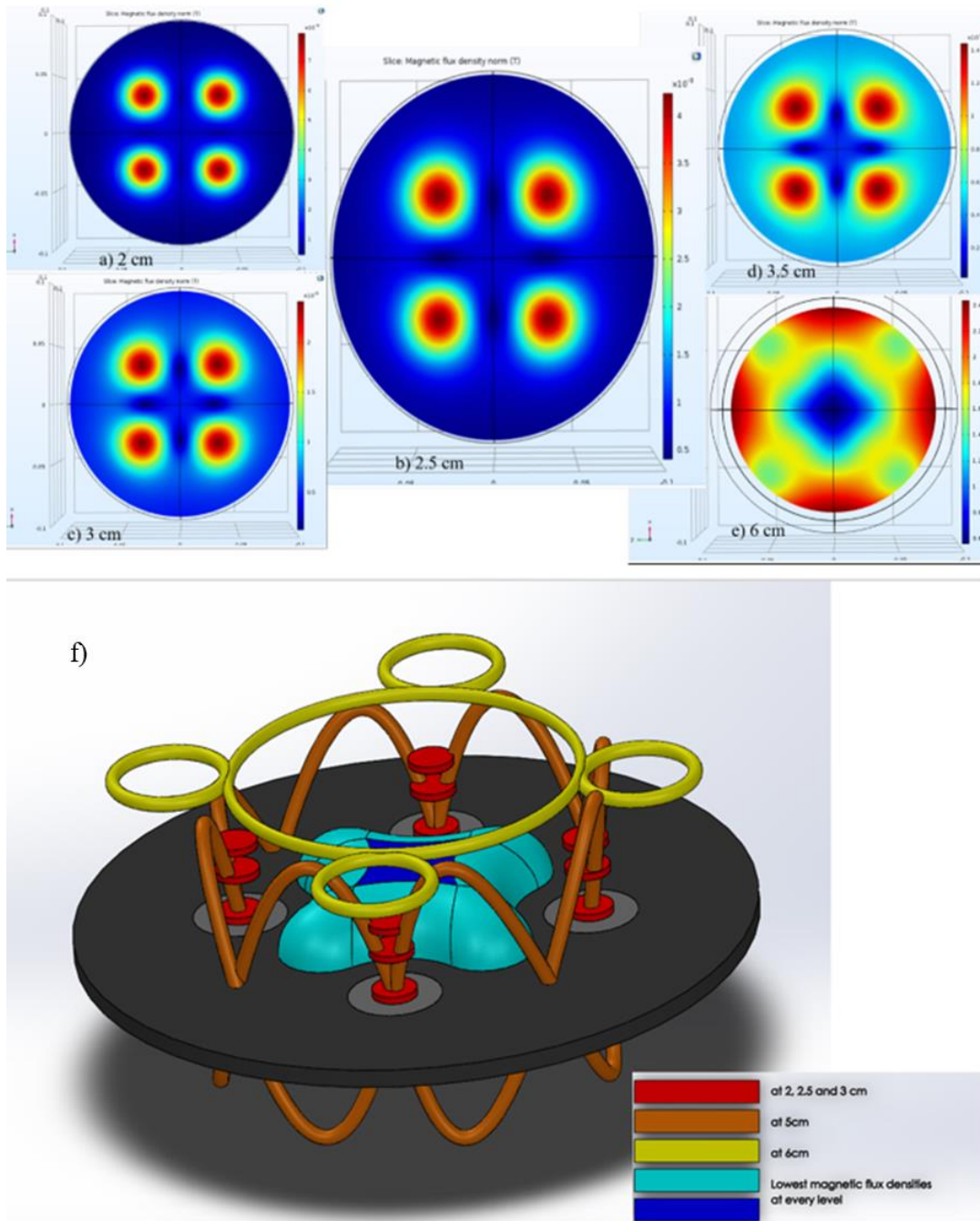
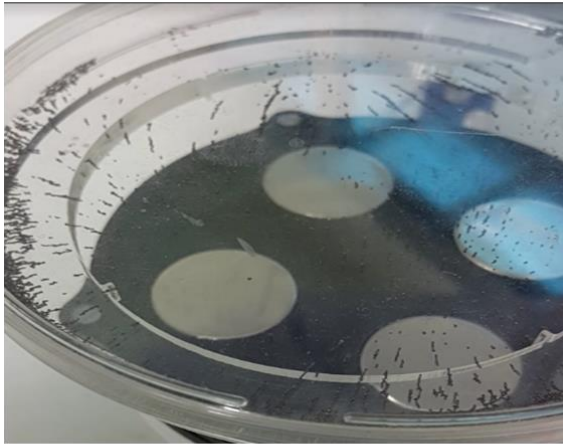
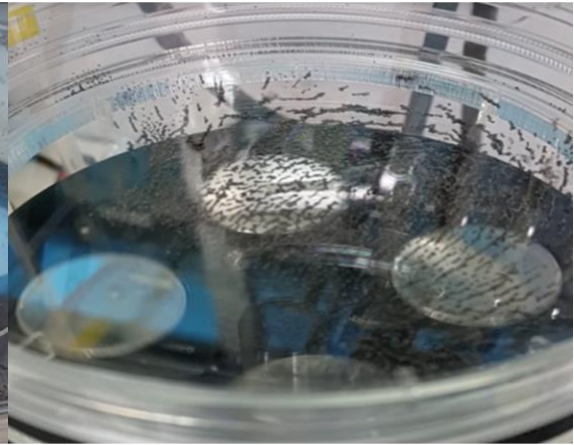


Figure 3.3 Simulation results and 3D magnetic flux density norm patterns of the magnetic system. a) Maximum magnetic force occurs at 2 cm, b) at 2.5 cm circulation starts, c,d) non concentrated magnetic force is observed at the heights of 3 and 3.5cm, e) at the height of 6 cm magnetic fluxes are combined to an circular pattern, and the magnetic force significantly decreases. f) Red line represents densities at the distances of 2, 2.5 and 3cm, orange and yellow ones correspond to the heights of 5 and 6 cm respectively, light and dark blue represents the lowest magnetic flux density at every level.

a) Clustered particles



b) Distributed particles



d) Aligned particles



c) Lifted particles



e) Rolled particles around their axis



f) Lifted particles



Figure 3.4 Iron dust particle experiments. a) under uniform magnetic field, dusts particles cluster near the magnets and the edges, b) under non-uniform magnetic field dusts begin to distribute throughout the plate, when the system is operational c) dusts align successively, d) lift e) roll and change direction in their own axis, f) lift again.

Because of strong magnetic field (in the light of simulations) is at this distance, 2 – 2.5 – 3 – 3.5 cm distances are examined for the cell experiments. The objective of the rotating system is to allow as many nanoparticles as possible to enter into the cells, which are attached to the plate.

3.2.2. Cell experiments

The cell experiments were carried out with 3 different samples, namely polyethyleneimine (PEI), polyethyleneimine coated superparamagnetic iron oxide nanoparticle without magnetic field (PS wo) and polyethyleneimine coated superparamagnetic iron oxide nanoparticle under rotary magnetic fields (PS rot). First, the effect of transfection time is investigated. In viability experiments, the control cell line is added among PEI, PS wo and PS rot. To increase the viability, 6 – 3 – 1h transfection times and 120 and 60 rpm velocities for the rotation are investigated. 3h of transfection and 6V are enough to obtain decreased cell death and efficient transfection. Also, the effect of distance between table and the petri dish is investigated to obtain a uniform distribution. For this purpose, 2 – 2.5 – 3 – 3.5 cm distances are explored (Figure 3.5a-f). After the experiments, 300 cells are counted from each plate, and the transfection efficiencies are examined (Figure 3.5g). Then, 1h of transfection time is investigated and further enhancement of cell viability and efficient transfection can be achieved (Figure 3.6a-f). According to results, 1h of transfection efficiency of PEI is remained low (around 2%), while that of PS rot at 3.5 cm is 45 % (Figure 3.6e).

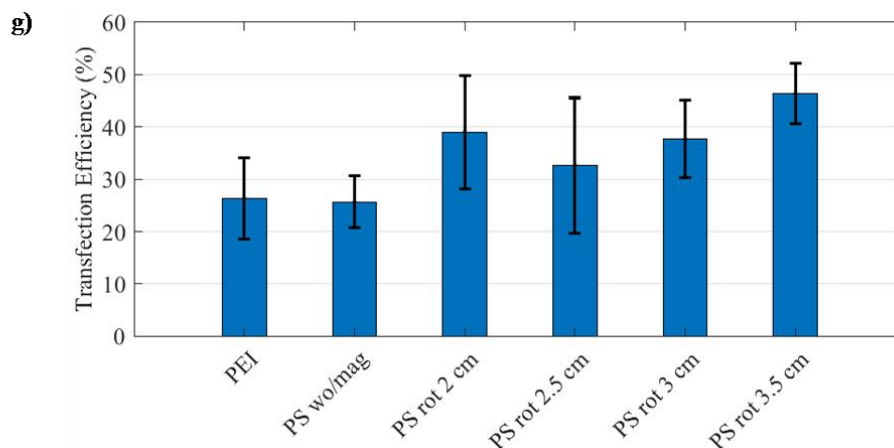
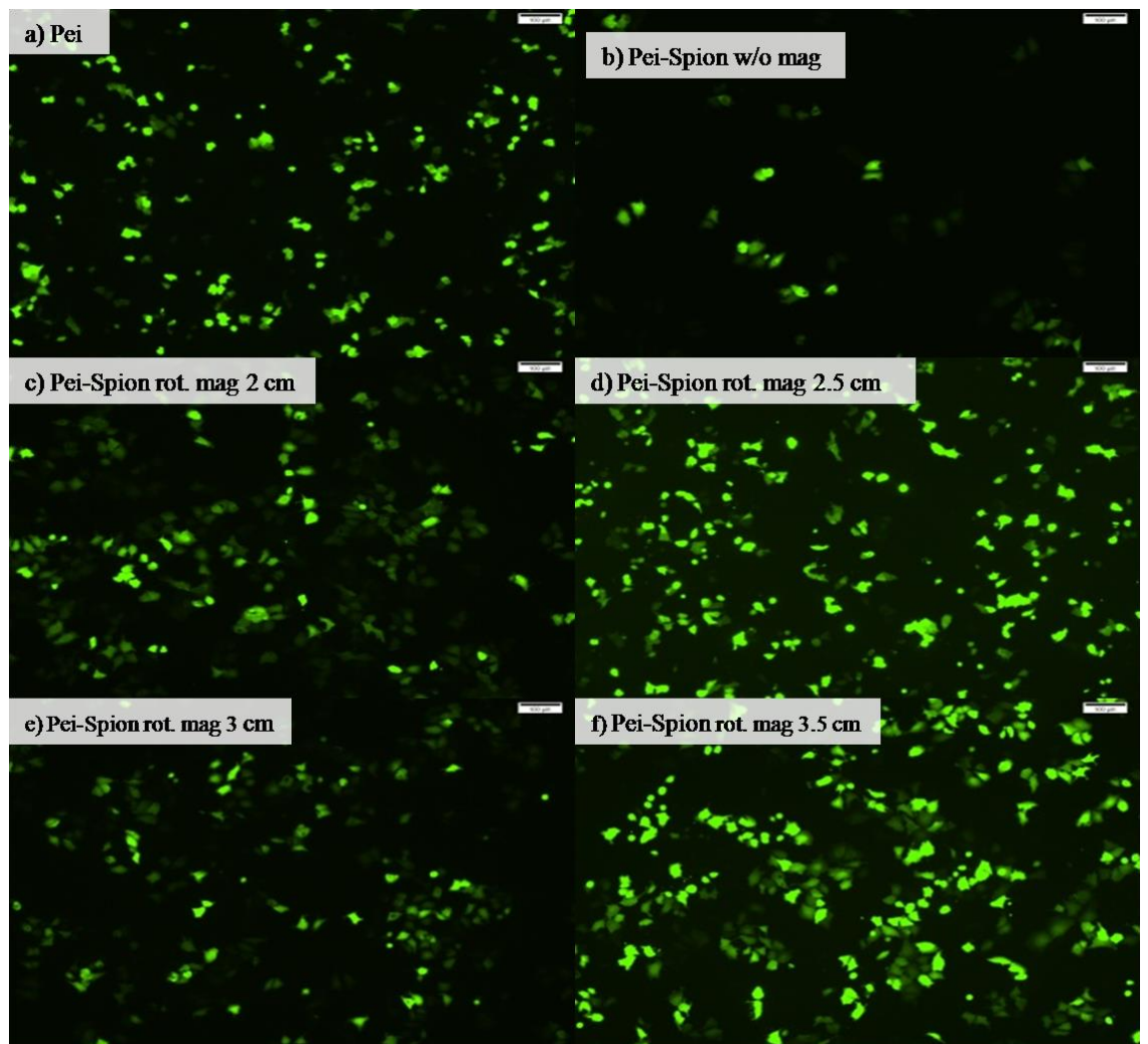


Figure 3.5 Transfection efficiency with respect to distance. PEI and PEI SPION wo mag samples are used as control (a,b). After 48 hours incubation, fluorescence images of the samples for each distance are shown (c,d,e,f), Transfection performance of the device is tested at different distances between the rotary table and sample (g).

without magnetization, and rotating magnetic field exposed samples were used to determine the transfection efficiencies, 60 μg PEI conjugated with 10 μg green fluorescent protein (GFP) tagged DNA was used, after 48 hours transfected cells were visualized using a fluorescent microscope (a-e) (10x magnification), Viability is tested after 48 hours (f). p-values smaller than 0.05 were accepted as significant.

3.3. Discussion

Many different magnetic systems are being used for gene transfer. Popular ones are oscillating magnet arrays, placing magnets under the culture plates and magnet arrays [343], [346], [347]. McBain et al.[346] used a oscillating magnet array and reported that human lung epithelial cells were effectively transfected. They reported positive effects of the system on viability. In our study, magnetic field application significantly raised the viability. In addition, the transfection time was reduced to 1 hour, since all the transfection agents were removed from the cells at the end of 1 hour.

Lu et al. [347] used a staggered magnet array and placed two magnets underneath the culture plates. Two adjacent magnets interfered with each other and had a negative effect on transfection. Because the two magnets were affected by each other, they claimed that the efficiency was more in between. Accordingly, the cells, which were located above the magnets, experienced a uniform magnetic field, while the cells in the other wells of the plate were exposed to non-uniform magnetic fields. The group concluded that the non-uniform magnetic field was more suitable for in vivo studies. However, in our system, we benefit from the condition of the interaction of two magnets with each other. In order to investigate the uniformity of the generated magnetic field are shown that a uniform transfection can be obtained under non-uniform magnetic field by finding the appropriate distance between the magnets and culture plate. Cell experiments at various distances were performed for this task. At the smallest distance of 2 cm, a more concentrated cell population was seen around the magnet, and a cell population was found distributed throughout the entire 10 cm plate at 3.5 cm distance. Furthermore, Kozlov et al. [348] explained how a similar system distributed nanoparticles to the plate depending on the speed of rotation. Accordingly, while stagnant particles accumulate around the magnet, they computationally showed that the particles were uniformly distributed when the velocity is increased. In our study, experiments were conducted at high speeds, and there was also a decrease in viability

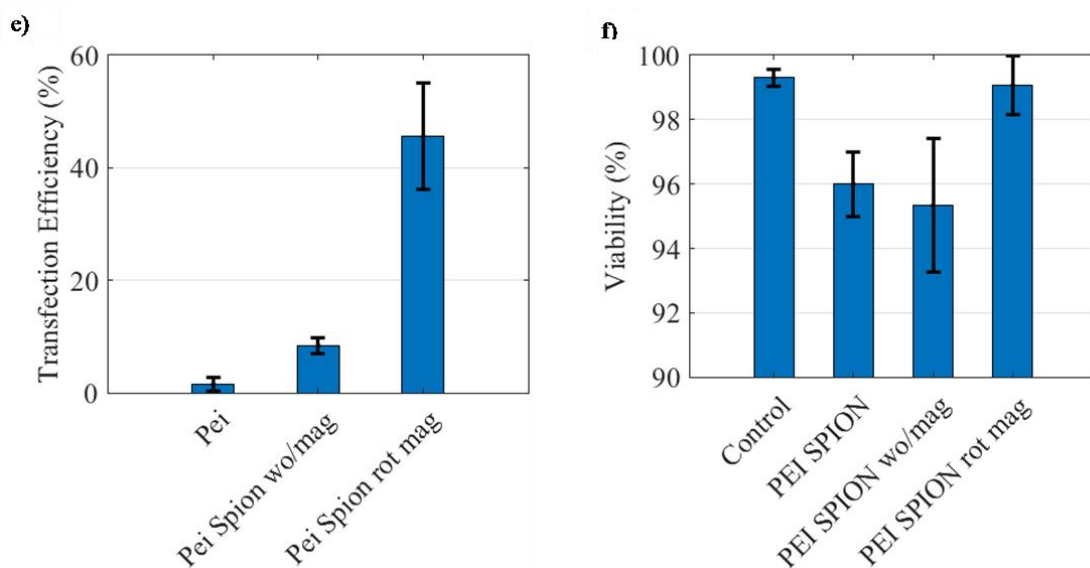
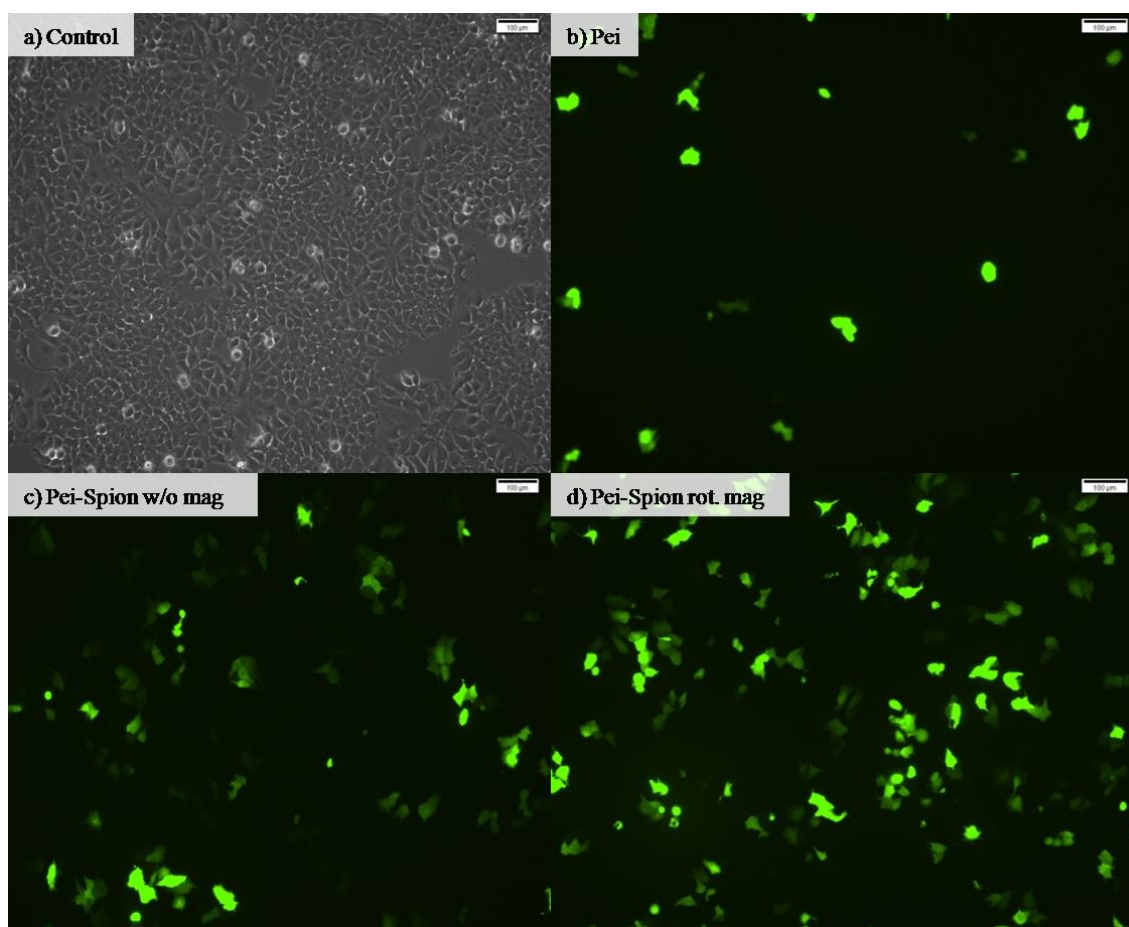


Figure 3.6 Transfection Efficiency and Viability Assay. MCF7 cell lines transfected with nanoparticles were exposed to rotating magnetic field for 1h, PEI,

when the distance between magnets and culture plate was kept small. This is attributed to the fact that nanoparticles lifted the cells by twisting and might have damaged them by tearing the cell membrane at 12 V, since the particles are attracted closer to the surface and prefer to gather at the place, where the magnets are located. Accordingly, the speed is decreased, while the distance is increased in the performed experiments. The distance is increased to 3.5 cm, and the transfection times are kept as 3h and 1h. As a result, an efficient transfection is achieved.

PEI is an effective agent for transfection. Some studies with PEI reported that free PEI is needed for high transfection efficiencies, and its effects on transfection were investigated [342]. The results showed that nanoparticles could not enter into the cell nucleus but free PEI in the medium helped sending the plasmids to the nucleus. In other words, since a sufficient number of nanoparticles could not be directed to the core, excess PEI was concentrated in the cell. Although PEI is an effective agent, the toxicity of the material is a known fact. Therefore, it is important that the cells should be in contact with carriers containing PEI for short periods and in sufficient quantities. In our study, the particles were sent to the cells in a total amount of 60 μg PEI bearing nanoparticle solution, and the transfection times were changed proving the sufficiency of the amount used in the experiments. In addition, when the duration of transfection is short, the efficiency of the transfection is significant because of the capability of the actuation system.

Huth et al. examined the nanoparticle uptake of HeLa cells [349]. They found that the PEI coated nanoparticles were close to the cell membrane at the 5th minute, on the cell surface at the 10th minute and in the cell at the 15th minute. Motivated by this finding, the purpose in our study is benefitting from a rotating, i.e non-uniform magnetic field, to allow more particles to enter the cell, thereby increasing the number of particles the cell can encounter. In this regard, we show that efficient transfection can be obtained even within a short transfection time of 1h.

Although PS is known to be effective for magnetic transfection [212], [343], it is not very clear whether the success of the transfection is due to the magnetic field effect or whether the known method is to be used because of the presence of PEI in the medium. In the related studies, where a cell plate containing PS solution was placed in the incubator for 8 hours, it could be transfected because of PEI [212]. Transfection

time experiments are also conducted in our study to investigate this phenomenon. Accordingly, efficient transfection can be achieved using nanoparticles with our new generation actuation system even within 1 hour period when PEI transfection was not successful. Thus, the viability could be increased, and efficient gene transfer could be ensured with our actuation system.

4 CONCLUSIONS

In this dissertation thermal and mechanical manipulation mechanisms of iron oxide nanoparticles are studied. For thermal manipulation, a heating coil, which operates at low amplitude of 0.8 kAm^{-1} and a frequency of 400 kHz magnetic field is developed. The system did not cause any cell death in the absence of a sensitizer, namely superparamagnetic iron oxide nanoparticle (SPION). Moreover, we prepared ultra-small, colloidally stable and highly cytocompatible, poly(acrylic acid) coated SPIONs decorated with dye-labeled antiHER2 antibody to target HER2 overexpressing tumor cells and achieved local, tumor specific, highly efficient hyperthermia. Overall, we showed that both non-targeting SP (SPION/PAA) and targeting SP-H (SPION/PAA/antiHER2) nanoparticles can significantly inhibit the proliferation of cancer cells, and SP-H nanoparticles effectively kill cancer cells when exposed to inductive heating even at low magnitudes. Motivated by the promising results of this study, these nanoparticles and the inductive heating coil and protocol will be used for in vivo applications.

Due to their adverse effects, viral and non-viral chemical vectors should not be favored in gene therapy. In addition to their biosafety problems, such vectors have limited amount of access for transporting exogenous DNA. Accordingly, research outputs in nanotechnology recommend new techniques such as using magnetic nanoparticles in gene therapy, especially in transfection process. Due to many advantages such as manipulation capability and less toxicity, their utilization in biotechnology has an increasing trend. In this thesis, we developed a safe transfection

method with a short operation time. Using this method, we investigated magnetofection under non-uniform magnetic fields with the aim of high cell viability and high transfection rate. Based on the results on MCF-7 cell line and PEI-SPIONs, we achieved short transfection time and high transfection rates without having cell death.

In the light of the known success of PEI in causing exogenous DNA to enter the cells resulting transfection, we determined the PEI group as control. Accordingly, different with or without magnetic field experiments were conducted on PEI-SPIONs with cells, and their efficiency was assessed. GFP-DNA transfer to MCF7 cells was obtained. Longer transfection time such as 8 h resulted in higher rate of cell death due to longer exposure to agents. Fast disc rotating speed resulted in decreased cell viability. The application of variable magnetic field to PEI-SPIONs showed resemblance to the cells, to which we have applied PEI agent solely without magnetic field. After 48 hours of incubation (for expression to occur), the viability and transfection tests were performed at the end of the incubation period. The results showed that the magnetic field exposure increased cell viability as well as increased transfection efficiency with nanoparticles. At an optimum distance, which leads to uniform magnetic field in cell culture plate with a diameter of 10 cm, a uniform distribution was obtained and in vitro gene transfer was shown.

The employment of PEI coated SPIONs under magnetic fields in nucleic acid delivery was investigated to overcome the disadvantages of conventional methods of transfection by gene therapy. In this regard, with our developed system, better tissue localization and higher transfection efficiency could be achieved, and our system could be easily tested in both vitro and in vivo studies.

5 FUTURE WORK

In this thesis, *in vitro* hyperthermia and gene delivery methods were proposed. The results of hyperthermia experiments revealed that with the system we produced, cancer cells could be killed after iron nanoparticle internalization. This system can be well adapted to *in vivo* tests. Since, the nanoparticles have antibodies on their surfaces, targeted delivery is achieved in *in vivo* tests. Since, the strength of this system is safe for animal testing *in vivo* hyperthermia will be conducted in the future. To be able to perform such experiments there are few approaches such as changing the size of the coil specific to the animal we will use. If the coil size is decreased the magnetic field strength will be increased and frequency will be adjusted to a lower value accordingly. Moreover, effect of higher frequencies can be explored in terms of triggering death mechanism of cells.

For gene delivery, efficient DNA magnetofection to breast cancer cells was proven. Efficiency of the actuation system on different cell types will be also tested. In the future the magnet arrangement of the system will be altered and the magnetic field characteristics will be studied. Also, miRNA or siRNA based therapeutic nucleic acids will be conjugated with nanoparticles, and their magnetofection efficiency and therapeutic features can be explored.

A joint therapy hyperthermia can be also performed following the actuation process.

6 REFERENCES

- [1] R. V. Chandrasekhar S, Iyer LK, Panchal JP, Topp EM, Cannon JB, “Microarrays and microneedle arrays for delivery of peptides, proteins, vaccines and other applications,” *Expert Opin. Drug Deliv.*, vol. 10, no. 8, pp. 1155–1170, 2013.
- [2] P. Rabl, S. J. Kolkowitz, F. H. L. Koppens, J. G. E. Harris, P. Zoller, and M. D. Lukin, “A quantum spin transducer based on nanoelectromechanical resonator arrays,” *Nat. Phys.*, vol. 6, no. 8, pp. 602–608, 2010.
- [3] V. L. B. A. jasmine R. Shabnashmi PS NKS, Vithya V., “Therapeutic applications of Nanorobots- Respirocytes and Microbivores,” *J Chem Pharm Res*, vol. 8, no. 5, pp. 605–609, 2016.
- [4] R. S. Kadam, D. W. A. Bourne, and U. B. Kompella, “Nano-advantage in enhanced drug delivery with biodegradable nanoparticles: Contribution of reduced clearance,” *Drug Metab. Dispos.*, vol. 40, no. 7, pp. 1380–1388, 2012.
- [5] S. T. Jahan, S. M. A. Sadat, M. Walliser, and A. Haddadi, “Targeted Therapeutic Nanoparticles: An Immense Promise to Fight against Cancer,” *J. Drug Deliv.*, vol. 2017, no. iv, pp. 1–24, 2017.

- [6] H. J. Hsu, J. Bugno, S. R. Lee, and S. Hong, "Dendrimer-based nanocarriers: a versatile platform for drug delivery," *Wiley Interdiscip. Rev. Nanomedicine Nanobiotechnology*, vol. 9, no. 1, pp. 1–21, 2017.
- [7] L. P. Mendes, J. Pan, and V. P. Torchilin, "Dendrimers as nanocarriers for nucleic acid and drug delivery in cancer therapy," *Molecules*, vol. 22, no. 9, pp. 1–21, 2017.
- [8] C. I. C. Crucho and M. T. Barros, "Polymeric nanoparticles: A study on the preparation variables and characterization methods," *Mater. Sci. Eng. C*, vol. 80, pp. 771–784, 2017.
- [9] K. Letchford, R. Liggins, K. M. Wasan, and H. Burt, "In vitro human plasma distribution of nanoparticulate paclitaxel is dependent on the physicochemical properties of poly(ethylene glycol)-block-poly(caprolactone) nanoparticles," *Eur. J. Pharm. Biopharm.*, vol. 71, no. 2, pp. 196–206, 2009.
- [10] H.-B. Ahmad, Zaheer; Shah, Afzal; Siddiq, Muhammad; Kraatz, "Polymeric micelles as drug delivery vehicles," *RSC Adv.*, vol. 4, pp. 17028–17038, 2014.
- [11] E. Markovsky, H. Baabur-Cohen, and R. Satchi-Fainaro, "Anticancer polymeric nanomedicine bearing synergistic drug combination is superior to a mixture of individually-conjugated drugs," *J. Control. Release*, vol. 187, pp. 145–157, 2014.
- [12] R. Yang, G. Mondal, D. Wen, and R. I. Mahato, "Combination therapy of paclitaxel and cyclopamine polymer-drug conjugates to treat advanced prostate cancer," *Nanomedicine Nanotechnology, Biol. Med.*, vol. 13, no. 2, pp. 391–401, 2017.
- [13] X. Pang, Y. Jiang, Q. Xiao, A. W. Leung, H. Hua, and C. Xu, "PH-responsive polymer-drug conjugates: Design and progress," *J. Control. Release*, vol. 222, pp. 116–129, 2016.
- [14] S. Lv *et al.*, "Well-defined polymer-drug conjugate engineered with redox and pH-sensitive release mechanism for efficient delivery of paclitaxel," *J. Control. Release*, vol. 194, pp. 220–227, 2014.
- [15] Z. Chen *et al.*, "Controlled release of free doxorubicin from peptide-drug

- conjugates by drug loading,” *J. Control. Release*, vol. 191, pp. 123–130, 2014.
- [16] Y. Tu and L. Zhu, “Enhancing cancer targeting and anticancer activity by a stimulus-sensitive multifunctional polymer-drug conjugate,” *J. Control. Release*, vol. 212, pp. 94–102, 2015.
- [17] I. S., “Helical microtubules of graphitic carbon,” *Nature*, pp. 56–58, 1991.
- [18] R. M. Reilly, “Carbon Nanotubes: Potential Benefits and Risks of Nanotechnology in Nuclear Medicine,” *J. Nucl. Med.*, vol. 48, no. 7, pp. 1039–1042, 2007.
- [19] P. Mroz *et al.*, “Functionalized fullerenes mediate photodynamic killing of cancer cells: Type I versus Type II photochemical mechanism,” *Free Radic. Biol. Med.*, vol. 43, no. 5, pp. 711–719, 2007.
- [20] G. P. Tegos *et al.*, “NIH Public Access,” vol. 12, no. 10, pp. 1127–1135, 2011.
- [21] S. Bosi, T. Da Ros, S. Castellano, E. Banfi, and M. Prato, “Antimycobacterial activity of ionic fullerene derivatives,” *Bioorganic Med. Chem. Lett.*, vol. 10, no. 10, pp. 1043–1045, 2000.
- [22] H. Ji *et al.*, “Antiviral activity of nano carbon fullerene lipidosome against influenza virus in vitro,” *J. Huazhong Univ. Sci. Technol. - Med. Sci.*, vol. 28, no. 3, pp. 243–246, 2008.
- [23] X. Cai *et al.*, “Polyhydroxylated fullerene derivative C(60)(OH)(24) prevents mitochondrial dysfunction and oxidative damage in an MPP(+)-induced cellular model of Parkinson’s disease,” *J. Neurosci. Res.*, vol. 86, no. 16, pp. 3622–34, 2008.
- [24] Z. Markovic and V. Trajkovic, “Biomedical potential of the reactive oxygen species generation and quenching by fullerenes (C60),” *Biomaterials*, vol. 29, no. 26, pp. 3561–3573, 2008.
- [25] A. G. Cuenca, H. Jiang, S. N. Hochwald, M. Delano, W. G. Cance, and S. R. Grobmyer, “Emerging implications of nanotechnology on cancer diagnostics and therapeutics,” *Cancer*, vol. 107, no. 3, pp. 459–466, 2006.
- [26] C. Fan *et al.*, “Tumor selectivity of stealth multi-functionalized

- superparamagnetic iron oxide nanoparticles,” *Int. J. Pharm.*, vol. 404, no. 1–2, pp. 180–190, 2011.
- [27] G. Andocs, H. Renner, L. Balogh, L. Fonyad, C. Jakab, and A. Szasz, “Strong synergy of heat and modulated electromagnetic field in tumor cell killing,” *Strahlenther. Onkol.*, vol. 185, no. 2, pp. 120–6, 2009.
- [28] N. G. Shetake, M. M. S. Balla, A. Kumar, and B. N. Pandey, “Magnetic Hyperthermia Therapy: An Emerging Modality of Cancer Treatment in Combination with Radiotherapy,” *J. Radiat. Cancer Res.*, vol. 7, no. 1, pp. 13–17, 2016.
- [29] H. Kim *et al.*, “Multifunctional Photonic Nanomaterials for Diagnostic, Therapeutic, and Theranostic Applications,” *Adv. Mater.*, vol. 30, no. 10, pp. 1–33, 2018.
- [30] A. M. Iga, J. H. P. Robertson, M. C. Winslet, and A. M. Seifalian, “Clinical potential of quantum dots,” *J. Biomed. Biotechnol.*, vol. 2007, 2007.
- [31] C. T. Matea *et al.*, “Quantum dots in imaging, drug delivery and sensor applications,” *Int. J. Nanomedicine*, vol. 12, pp. 5421–5431, 2017.
- [32] R. E. Bailey, A. M. Smith, and S. Nie, “Quantum dots in biology and medicine,” *Phys. E Low-Dimensional Syst. Nanostructures*, vol. 25, no. 1, pp. 1–12, 2004.
- [33] F. Chen, G. Hableel, E. R. Zhao, and J. V. Jokerst, “Multifunctional nanomedicine with silica: Role of silica in nanoparticles for theranostic, imaging, and drug monitoring,” *J. Colloid Interface Sci.*, vol. 521, pp. 261–279, 2018.
- [34] E. Bagheri *et al.*, “Silica based hybrid materials for drug delivery and bioimaging,” *J. Control. Release*, vol. 277, no. January, pp. 57–76, 2018.
- [35] M. Mathelié-Guinlet *et al.*, “Silica Nanoparticles Assisted Electrochemical Biosensor for the Detection and Degradation of Escherichia coli Bacteria,” *Procedia Eng.*, vol. 168, no. 0, pp. 1048–1051, 2016.
- [36] J. G. Croissant, Y. Fatieiev, A. Almalik, and N. M. Khashab, “Mesoporous Silica and Organosilica Nanoparticles: Physical Chemistry, Biosafety, Delivery Strategies, and Biomedical Applications,” *Adv. Healthc. Mater.*, vol. 7, no. 4, pp.

1–75, 2018.

- [37] S. E. Leucuta, “Nanotechnology for Delivery of Drugs and Biomedical Applications,” *Curr. Clin. Pharmacol.*, vol. 5, no. 4, pp. 257–280, 2010.
- [38] E.-A. A. Buse J, “Properties, engineering and applications of lipid-based nanoparticle drug- delivery systems: current research and advances,” *Nanomedicine*, vol. 5, pp. 1297–1260, 2010.
- [39] A. Sharma and U. S. Sharma, “Liposomes in drug delivery: Progress and limitations,” *Int. J. Pharm.*, vol. 154, no. 2, pp. 123–140, 1997.
- [40] A. Gabizon *et al.*, “Prolonged circulating time and enhanced accumulation in malignant exudates of doxorubicin encapsulated in polyethylene- glycol coated liposomes,” *Cancer Res.*, vol. 54, pp. 987–992, 1994.
- [41] M. B. De Jesus and I. S. Zuhorn, “Solid lipid nanoparticles as nucleic acid delivery system: Properties and molecular mechanisms,” *J. Control. Release*, vol. 201, pp. 1–13, 2015.
- [42] S. Doktorovova, E. B. Souto, and A. M. Silva, “Nanotoxicology applied to solid lipid nanoparticles and nanostructured lipid carriers - A systematic review of in vitro data,” *Eur. J. Pharm. Biopharm.*, vol. 87, no. 1, pp. 1–18, 2014.
- [43] J. E. N. Dolatabadi, H. Valizadeh, and H. Hamishehkar, “Solid lipid nanoparticles as efficient drug and gene delivery systems: Recent breakthroughs,” *Adv. Pharm. Bull.*, vol. 5, no. 2, pp. 151–159, 2015.
- [44] E. Rostami, S. Kashanian, A. H. Azandaryani, H. Faramarzi, J. E. N. Dolatabadi, and K. Omidfar, “Drug targeting using solid lipid nanoparticles,” *Chem. Phys. Lipids*, vol. 181, pp. 56–61, 2014.
- [45] H. Shen, S. Shi, Z. Zhang, T. Gong, and X. Sun, “Coating solid lipid nanoparticles with hyaluronic acid enhances antitumor activity against melanoma stem-like cells,” *Theranostics*, vol. 5, no. 7, pp. 755–771, 2015.
- [46] S. Weber, A. Zimmer, and J. Pardeike, “Solid Lipid Nanoparticles (SLN) and Nanostructured Lipid Carriers (NLC) for pulmonary application: A review of the state of the art,” *Eur. J. Pharm. Biopharm.*, vol. 86, no. 1, pp. 7–22, 2014.

- [47] Y. Luo, Z. Teng, Y. Li, and Q. Wang, "Solid lipid nanoparticles for oral drug delivery: Chitosan coating improves stability, controlled delivery, mucoadhesion and cellular uptake," *Carbohydr. Polym.*, vol. 122, pp. 221–229, 2015.
- [48] V. B. Junyaprasert and B. Morakul, "Nanocrystals for enhancement of oral bioavailability of poorly water-soluble drugs," *Asian J. Pharm. Sci.*, vol. 10, no. 1, pp. 13–23, 2015.
- [49] M. E. Davis, Z. Chen, and D. M. Shin, "Nanoparticle therapeutics: An emerging treatment modality for cancer," *Nat. Rev. Drug Discov.*, vol. 7, no. 9, pp. 771–782, 2008.
- [50] C. Moorthi, R. Manavalan, and K. Kathiresan, "Nanotherapeutics to overcome conventional cancer chemotherapy limitations," *J. Pharm. Pharm. Sci.*, vol. 14, no. 1, pp. 67–77, 2011.
- [51] A. A. Stavrovskaya, "Cellular mechanisms of multidrug resistance of tumor cells.," *Biochemistry. (Mosc.)*, vol. 65, no. 1, pp. 95–106, 2000.
- [52] B. Mishra, B. B. Patel, and S. Tiwari, "Colloidal nanocarriers: a review on formulation technology, types and applications toward targeted drug delivery," *Nanomedicine Nanotechnology, Biol. Med.*, vol. 6, no. 1, pp. 9–24, 2010.
- [53] F. Danhier, O. Feron, and V. Préat, "To exploit the tumor microenvironment: Passive and active tumor targeting of nanocarriers for anti-cancer drug delivery," *J. Control. Release*, vol. 148, no. 2, pp. 135–146, 2010.
- [54] H. Maeda, G. Y. Bharate, and J. Daruwalla, "Polymeric drugs for efficient tumor-targeted drug delivery based on EPR-effect," *Eur. J. Pharm. Biopharm.*, vol. 71, no. 3, pp. 409–419, 2009.
- [55] R. Tong, H. D. Hemmati, R. Langer, and D. S. Kohane, "Photoswitchable nanoparticles for triggered tissue penetration and drug delivery," *J. Am. Chem. Soc.*, vol. 134, no. 21, pp. 8848–8855, 2012.
- [56] F. U. Din *et al.*, "Effective use of nanocarriers as drug delivery systems for the treatment of selected tumors," *Int. J. Nanomedicine*, vol. 12, pp. 7291–7309, 2017.

- [57] R. Misra, S. Acharya, and S. K. Sahoo, "Cancer nanotechnology: Application of nanotechnology in cancer therapy," *Drug Discov. Today*, vol. 15, no. 19–20, pp. 842–850, 2010.
- [58] S. M. Cohen *et al.*, "Efficacy and toxicity of peritumoral delivery of nanoconjugated cisplatin in an in vivo murine model of head and neck squamous cell carcinoma," *JAMA Otolaryngol. - Head Neck Surg.*, vol. 139, no. 4, pp. 382–387, 2013.
- [59] W. J. Gradishar, "Albumin-bound paclitaxel: a next-generation taxane," *Expert Opin. Pharmacother.*, vol. 7, no. 8, pp. 1041–1053, 2006.
- [60] X. Wang, C. Wang, Q. Zhang, and Y. Cheng, "Near infrared light-responsive and injectable supramolecular hydrogels for on-demand drug delivery," *Chem. Commun.*, vol. 52, no. 5, pp. 978–981, 2016.
- [61] L. Dai *et al.*, "Photosensitizer enhanced disassembly of amphiphilic micelle for ROS-response targeted tumor therapy in vivo," *Biomaterials*, vol. 104, pp. 1–17, 2016.
- [62] Y. Qin *et al.*, "Near-infrared light remote-controlled intracellular anti-cancer drug delivery using thermo/pH sensitive nanovehicle," *Acta Biomater.*, vol. 17, pp. 201–209, 2015.
- [63] Q. Feng *et al.*, "Programmed near-infrared light-responsive drug delivery system for combined magnetic tumor-targeting magnetic resonance imaging and chemo-phototherapy," *Acta Biomater.*, vol. 49, pp. 402–413, 2017.
- [64] Q. Feng *et al.*, "Tumor-targeted and multi-stimuli responsive drug delivery system for near-infrared light induced chemo-phototherapy and photoacoustic tomography," *Acta Biomater.*, vol. 38, pp. 129–142, 2016.
- [65] T. Liu *et al.*, "Drug Delivery with PEGylated MoS₂ Nano-sheets for Combined Photothermal and Chemotherapy of Cancer," *Adv. Mater.*, vol. 26, no. 21, pp. 3433–3440, 2014.
- [66] F.-H. Chen, L.-M. Zhang, Q.-T. Chen, Y. Zhang, and Z.-J. Zhang, "Synthesis of a novel magnetic drug delivery system composed of doxorubicin-conjugated

- Fe₃O₄ nanoparticle cores and a PEG-functionalized porous silica shell,” *Chem. Commun. (Camb)*., vol. 46, no. 45, pp. 8633–8635, 2010.
- [67] W. Zhang *et al.*, “PH and near-infrared light dual-stimuli responsive drug delivery using DNA-conjugated gold nanorods for effective treatment of multidrug resistant cancer cells,” *J. Control. Release*, vol. 232, pp. 9–19, 2016.
- [68] X. Yang, X. Liu, Z. Liu, F. Pu, J. Ren, and X. Qu, “Near-infrared light-triggered, targeted drug delivery to cancer cells by aptamer gated nanovehicles,” *Adv. Mater.*, vol. 24, no. 21, pp. 2890–2895, 2012.
- [69] Z. Luo *et al.*, “Mesoporous silica nanoparticles end-capped with collagen: Redox-responsive nanoreservoirs for targeted drug delivery,” *Angew. Chemie - Int. Ed.*, vol. 50, no. 3, pp. 640–643, 2011.
- [70] X. Chen, H. Sun, J. Hu, X. Han, H. Liu, and Y. Hu, “Transferrin gated mesoporous silica nanoparticles for redox-responsive and targeted drug delivery,” *Colloids Surfaces B Biointerfaces*, vol. 152, pp. 77–84, 2017.
- [71] Q. Zhang *et al.*, “Multifunctional mesoporous silica nanoparticles for cancer-targeted and controlled drug delivery,” *Adv. Funct. Mater.*, vol. 22, no. 24, pp. 5144–5156, 2012.
- [72] L. Huang, Q. Zhang, L. Dai, X. Shen, W. Chen, and K. Cai, “Phenylboronic acid-modified hollow silica nanoparticles for dual-responsive delivery of doxorubicin for targeted tumor therapy,” *Regen. Biomater.*, no. January 2017, p. rbw045, 2017.
- [73] H. Hillaireau and P. Couvreur, “Nanocarriers’ entry into the cell: Relevance to drug delivery,” *Cell. Mol. Life Sci.*, vol. 66, no. 17, pp. 2873–2896, 2009.
- [74] P. Sendi and R. A. Proctor, “Staphylococcus aureus as an intracellular pathogen: the role of small colony variants,” *Trends Microbiol.*, vol. 17, no. 2, pp. 54–58, 2009.
- [75] H. Zazo, C. I. Colino, and J. M. Lanao, “Current applications of nanoparticles in infectious diseases,” *J. Control. Release*, vol. 224, pp. 86–102, 2016.
- [76] “U.S. National Institutes of Health,” 2015. [Online]. Available:

<https://clinicaltrials.gov/ct2/results?cond=ebola&term=&cntry=&state=&city=&dist=>. [Accessed: 10-May-2018].

- [77] “U.S. National Institutes of Health,” 2015. [Online]. Available: <https://clinicaltrials.gov/ct2/results?cond=arikace&term=&cntry=&state=&city=&dist=>. [Accessed: 10-May-2018].
- [78] G. Bozzuto and A. Molinari, “Liposomes as nanomedical devices,” *Int. J. Nanomedicine*, vol. 10, pp. 975–999, 2015.
- [79] S. G. Beal *et al.*, “Evaluation of the nanosphere verigene gram-positive blood culture assay with the versaTREK blood culture system and assessment of possible impact on selected patients,” *J. Clin. Microbiol.*, vol. 51, no. 12, pp. 3988–3992, 2013.
- [80] V. Weissig, T. K. Pettinger, and N. Murdock, “Nanopharmaceuticals (part 1): products on the market,” *Int. J. Nanomedicine*, vol. 9, pp. 4357–4373, 2014.
- [81] C. Longhi *et al.*, “Combination of fluconazole with silver nanoparticles produced by *Fusarium oxysporum* improves antifungal effect against planktonic cells and biofilm of drug-resistant *Candida albicans*,” *Med. Mycol.*, vol. 54, no. 4, pp. 428–432, 2016.
- [82] A. N. Brown, K. Smith, T. A. Samuels, J. Lu, S. O. Obare, and M. E. Scott, “Nanoparticles functionalized with ampicillin destroy multiple-antibiotic-resistant isolates of *Pseudomonas aeruginosa* and *Enterobacter aerogenes* and methicillin-resistant *Staphylococcus aureus*,” *Appl. Environ. Microbiol.*, vol. 78, no. 8, pp. 2768–2774, 2012.
- [83] S. Chakraborti, A. K. Mandal, S. Sarwar, P. Singh, R. Chakraborty, and P. Chakrabarti, “Bactericidal effect of polyethyleneimine capped ZnO nanoparticles on multiple antibiotic resistant bacteria harboring genes of high-pathogenicity island,” *Colloids Surfaces B Biointerfaces*, vol. 121, pp. 44–53, 2014.
- [84] N. Shimizu, K. Otsuka, H. Sawada, T. Maejima, and S. Shirotake, “Bacteriolysis by vancomycin-conjugated acryl nanoparticles and morphological component analysis,” *Drug Dev. Ind. Pharm.*, vol. 40, no. 6, pp. 813–818, 2014.

- [85] H. Gu, P. L. Ho, E. Tong, L. Wang, and B. Xu, "Presenting vancomycin on nanoparticles to enhance antimicrobial activities," *Nano Lett.*, vol. 3, no. 9, pp. 1261–1263, 2003.
- [86] W. F. Shaik, Naveed Pan, Guoyu Elmquist, "Interactions of Pluronic Block Copolymers on P-gp Efflux Activity: Experience With HIV-1 Protease Inhibitors," *Pharm Sci.*, vol. 97, no. 12, pp. 5421–5433, 2008.
- [87] M. Alipour, M. Halwani, A. Omri, and Z. E. Suntres, "Antimicrobial effectiveness of liposomal polymyxin B against resistant Gram-negative bacterial strains," *Int. J. Pharm.*, vol. 355, no. 1–2, pp. 293–298, 2008.
- [88] N. P. Aditya, P. G. Vathsala, V. Vieira, R. S. R. Murthy, and E. B. Souto, "Advances in nanomedicines for malaria treatment," *Adv. Colloid Interface Sci.*, vol. 201–202, pp. 1–17, 2013.
- [89] S. P. Chakraborty, S. K. Sahu, P. Pramanik, and S. Roy, "In vitro antimicrobial activity of nanoconjugated vancomycin against drug resistant *Staphylococcus aureus*," *Int. J. Pharm.*, vol. 436, no. 1–2, pp. 659–676, 2012.
- [90] G. Zhao *et al.*, "HHS Public Access," vol. 82, no. 1, pp. 34–44, 2013.
- [91] E. Turos *et al.*, "Penicillin-bound polyacrylate nanoparticles: Restoring the activity of β -lactam antibiotics against MRSA," *Bioorganic Med. Chem. Lett.*, vol. 17, no. 12, pp. 3468–3472, 2007.
- [92] L. Wang *et al.*, "Functionalised nanoparticles complexed with antibiotic efficiently kill MRSA and other bacteria," *Chem. Commun.*, vol. 50, no. 81, pp. 12030–12033, 2014.
- [93] S. Hasan and H. Al, "and antibacterial studies of a novel streptomycin chitosan magnetic nanoantibiotic Synthesis , characterization , controlled release , and antibacterial studies of a novel streptomycin chitosan magnetic nanoantibiotic," no. August 2016, pp. 549–557, 2014.
- [94] S. C. Abeylath, E. Turos, S. Dickey, and D. V. Lim, "Glyconanobiotics: Novel carbohydrate nanoparticle antibiotics for MRSA and *Bacillus anthracis*," *Bioorganic Med. Chem.*, vol. 16, no. 5, pp. 2412–2418, 2008.

- [95] J. Falconer *et al.*, “Synovial cell metabolism and chronic inflammation in rheumatoid arthritis,” *Arthritis Rheumatol.*, 2018.
- [96] and Y.-S. H. Heejin Lim, Sang Hyung Lee, Hyun Tae Lee, Jee Un Lee, Ji Young Son, Woori Shin, “Structural Biology of the TNF α Antagonists Used in the Treatment of Rheumatoid Arthritis,” *Int J Mol Sci.*, vol. 19, no. 3, 2018.
- [97] E. P. Horton S, Walsh C, “Certolizumab pegol for the treatment of rheumatoid arthritis,” *Expert Opin Biol Ther*, vol. 12, no. 2, pp. 235–249, 2012.
- [98] K. Yudoh, R. Karasawa, K. Masuko, and T. Kato, “Water-soluble fullerene (C60) inhibits the development of arthritis in the rat model of arthritis,” *Int. J. Nanomedicine*, vol. 4, pp. 217–225, 2009.
- [99] B. K. Lee, Y. H. Yun, and K. Park, “Smart nanoparticles for drug delivery: Boundaries and opportunities,” *Chem. Eng. Sci.*, vol. 125, pp. 1–7, 2014.
- [100] S. de Castro and M. J. Camarasa, “Polypharmacology in HIV inhibition: can a drug with simultaneous action against two relevant targets be an alternative to combination therapy?,” *Eur. J. Med. Chem.*, vol. 150, pp. 206–227, 2018.
- [101] J. Herskovitz and H. E. Gendelman, “HIV and the Macrophage: From Cell Reservoirs to Drug Delivery to Viral Eradication,” *J. Neuroimmune Pharmacol.*, pp. 1–16, 2018.
- [102] A. Dembri, M. J. Montisci, J. C. Gantier, H. Chacun, and G. Ponchel, “Targeting of 3'-azido 3'-deoxythymidine (AZT)-loaded poly(isohexylcyanoacrylate) nanospheres to the gastrointestinal mucosa and associated lymphoid tissues,” *Pharm. Res.*, vol. 18, no. 4, pp. 467–473, 2001.
- [103] R. Löbenberg, J. Maas, and J. Kreuter, “Improved body distribution of ¹⁴C-labelled AZT bound to nanoparticles in rats determined by radioluminography,” *J. Drug Target.*, vol. 5, no. 3, pp. 171–179, 1998.
- [104] T. Dutta, M. Garg, and N. K. Jain, “Targeting of efavirenz loaded tuftsin conjugated poly(propyleneimine) dendrimers to HIV infected macrophages in vitro,” *Eur. J. Pharm. Sci.*, vol. 34, no. 2–3, pp. 181–189, 2008.
- [105] T. Dutta, H. B. Agashe, M. Garg, P. Balasubramaniam, M. Kabra, and N. K.

- Jain, "Poly (propyleneimine) dendrimer based nanocontainers for targeting of efavirenz to human monocytes/macrophages in vitro," *J. Drug Target.*, vol. 15, no. 1, pp. 89–98, 2007.
- [106] K. Pham, D. Li, S. Guo, S. Penzak, and X. Dong, "Development and in vivo evaluation of child-friendly lopinavir/ritonavir pediatric granules utilizing novel in situ self-assembly nanoparticles," *J. Control. Release*, vol. 226, pp. 88–97, 2016.
- [107] N. J. Liptrott, M. Giardiello, T. O. McDonald, S. P. Rannard, and A. Owen, "Assessment of interactions of efavirenz solid drug nanoparticles with human immunological and haematological systems," *J. Nanobiotechnology*, vol. 16, no. 1, pp. 1–15, 2018.
- [108] T. Govender, E. Ojewole, P. Naidoo, and I. Mackraj, "Polymeric nanoparticles for enhancing antiretroviral drug therapy," *Drug Deliv.*, vol. 15, no. 8, pp. 493–501, 2008.
- [109] L. K. Shah and M. M. Amiji, "Intracellular delivery of saquinavir in biodegradable polymeric nanoparticles for HIV/AIDS," *Pharm. Res.*, vol. 23, no. 11, pp. 2638–2645, 2006.
- [110] M. Garg, A. Asthana, H. B. Agashe, G. P. Agrawal, and N. K. Jain, "Stavudine-loaded mannosylated liposomes: in-vitro anti-HIV-I activity, tissue distribution and pharmacokinetics," *J. Pharm. Pharmacol.*, vol. 58, no. 5, pp. 605–616, 2006.
- [111] I. N. et Al., "The Cardiovascular and Metabolic Heterogeneity of Obesity: Clinical Challenges and Implications for Management," *Circulation*, vol. 137, no. 13, pp. 1391–1406, 2018.
- [112] A. Haeri *et al.*, "Effective attenuation of vascular restenosis following local delivery of chitosan decorated sirolimus liposomes," *Carbohydr. Polym.*, vol. 157, pp. 1461–1469, 2017.
- [113] G. Arzani, A. Haeri, M. Daeihamed, H. Bakhtiari-Kaboutaraki, and S. Dadashzadeh, "Niosomal carriers enhance oral bioavailability of carvedilol: Effects of bile salt-enriched vesicles and carrier surface charge," *Int. J. Nanomedicine*, vol. 10, pp. 4797–4813, 2015.

- [114] F. R. Formiga *et al.*, “Sustained release of VEGF through PLGA microparticles improves vasculogenesis and tissue remodeling in an acute myocardial ischemia-reperfusion model,” *J. Control. Release*, vol. 147, no. 1, pp. 30–37, 2010.
- [115] T. Simón-Yarza, F. R. Formiga, E. Tamayo, B. Pelacho, F. Prosper, and M. J. Blanco-Prieto, “PEGylated-PLGA microparticles containing VEGF for long term drug delivery,” *Int. J. Pharm.*, vol. 440, no. 1, pp. 13–18, 2013.
- [116] A. R. Neves, L. Marlene, S. Martins, J. L. C. Lima, and S. Reis, “Novel resveratrol nanodelivery systems based on lipid nanoparticles to enhance its oral bioavailability Novel resveratrol nanodelivery systems based on lipid nanoparticles to enhance its oral bioavailability,” no. January 2013, pp. 177–187, 2016.
- [117] M. A. Phillips, M. L. Gran, and N. A. Peppas, “Targeted nanodelivery of drugs and diagnostics,” *Nano Today*, vol. 5, no. 2, pp. 143–159, 2010.
- [118] W. M. Pardridge, “Drug transport across the blood-brain barrier,” *J. Cereb. Blood Flow Metab.*, vol. 32, no. 11, pp. 1959–1972, 2012.
- [119] S. Wohlfart, S. Gelperina, and J. Kreuter, “Transport of drugs across the blood-brain barrier by nanoparticles,” *J. Control. Release*, vol. 161, no. 2, pp. 264–273, 2012.
- [120] H. L. Liu, C. H. Fan, C. Y. Ting, and C. K. Yeh, “Combining microbubbles and ultrasound for drug delivery to brain tumors: Current progress and overview,” *Theranostics*, vol. 4, no. 4, pp. 432–444, 2014.
- [121] H.-W. Klafki, M. Staufienbiel, J. Kornhuber, and J. Wiltfang, “Therapeutic approaches to Alzheimer’s disease,” *Brain*, vol. 129, no. 11, pp. 2840–2855, 2006.
- [122] B. Wilson, M. K. Samanta, K. Santhi, K. P. S. Kumar, N. Paramakrishnan, and B. Suresh, “Poly(n-butylcyanoacrylate) nanoparticles coated with polysorbate 80 for the targeted delivery of rivastigmine into the brain to treat Alzheimer’s disease,” *Brain Res.*, vol. 1200, pp. 159–168, 2008.
- [123] H. N. Patel and P. M. Patel, “Dendrimer applications - A review,” *Int. J. Pharma*

Bio Sci., vol. 4, no. 2, pp. 454–463, 2013.

- [124] S. Laserra *et al.*, “Solid lipid nanoparticles loaded with lipoyl-memantine codrug: Preparation and characterization,” *Int. J. Pharm.*, vol. 485, no. 1–2, pp. 183–191, 2015.
- [125] C. Saraiva, C. Praça, R. Ferreira, T. Santos, L. Ferreira, and L. Bernardino, “Nanoparticle-mediated brain drug delivery: Overcoming blood-brain barrier to treat neurodegenerative diseases,” *J. Control. Release*, vol. 235, pp. 34–47, 2016.
- [126] H. Hu, Y. Qiao, F. Meng, X. Liu, and C. Ding, “Enhanced apatite-forming ability and cytocompatibility of porous and nanostructured TiO₂/CaSiO₃ coating on titanium,” *Colloids Surfaces B Biointerfaces*, vol. 101, pp. 83–90, 2013.
- [127] S. A. Joshi, S. S. Chavhan, and K. K. Sawant, “Rivastigmine-loaded PLGA and PBCA nanoparticles: Preparation, optimization, characterization, in vitro and pharmacodynamic studies,” *Eur. J. Pharm. Biopharm.*, vol. 76, no. 2, pp. 189–199, 2010.
- [128] C. Tapeinos, M. Battaglini, and G. Ciofani, “Advances in the design of solid lipid nanoparticles and nanostructured lipid carriers for targeting brain diseases,” *J. Control. Release*, vol. 264, no. July, pp. 306–332, 2017.
- [129] D. Silva Adaya, L. Aguirre-Cruz, J. Guevara, and E. Ortiz-Islas, “Nanobiomaterials’ applications in neurodegenerative diseases,” *J. Biomater. Appl.*, vol. 31, no. 7, pp. 953–984, 2017.
- [130] F. HH, “Updates in the medical management of Parkinson disease,” *Cleve Clin J Med*, vol. 79, no. 1, pp. 28–35, 2012.
- [131] P. A. MacDonald *et al.*, “The effect of dopamine therapy on ventral and dorsal striatum-mediated cognition in Parkinson’s disease: Support from functional MRI,” *Brain*, vol. 134, no. 5, pp. 1447–1463, 2011.
- [132] A. D. Kulkarni, Y. H. Vanjari, K. H. Sancheti, V. S. Belgamwar, S. J. Surana, and C. V. Pardeshi, “Nanotechnology-mediated nose to brain drug delivery for Parkinson’s disease: A mini review,” *J. Drug Target.*, vol. 23, no. 9, pp. 775–788, 2015.

- [133] A. Azeem, S. Talegaonkar, L. M. Negi, F. J. Ahmad, R. K. Khar, and Z. Iqbal, "Oil based nanocarrier system for transdermal delivery of ropinirole: A mechanistic, pharmacokinetic and biochemical investigation," *Int. J. Pharm.*, vol. 422, no. 1–2, pp. 436–444, 2012.
- [134] M. D. Shadab *et al.*, "Bromocriptine loaded chitosan nanoparticles intended for direct nose to brain delivery: Pharmacodynamic, Pharmacokinetic and Scintigraphy study in mice model," *Eur. J. Pharm. Sci.*, vol. 48, no. 3, pp. 393–405, 2013.
- [135] S. K. Gendelman, Howard E. Anantharam, Vellareddy Bronich, Tatiana Ghaisas, Shivani Jin, Huajun Kanthasamy, Anumantha G. Liu, Xinming McMillan, JoEllyn Mosley, R. Lee Narasimhan, Balaji Mallapragada, "Nanoneuromedicines for Degenerative, Inflammatory, and Infectious Nervous System Diseases," *Nanomedicine*, vol. 11, no. 3, pp. 751–767, 2015.
- [136] E. V Batrakova *et al.*, "NIH Public Access," vol. 18, no. 5, pp. 1498–1506, 2009.
- [137] S. Crotty *et al.*, "Neuroprotective effects of novel phosphatidylglycerol-based phospholipids in the 6-hydroxydopamine model of Parkinson's disease," *Eur. J. Neurosci.*, vol. 27, no. 2, pp. 294–300, 2008.
- [138] P. W. Xia CF, Boado RJ, Zhang Y, Chu C, "Intravenous glial-derived neurotrophic factor gene therapy of experimental Parkinson's disease with Trojan horse liposomes and a tyrosine hydroxylase promoter," *J Gene Med*, vol. 10, no. 3, pp. 306–315, 2008.
- [139] R. Huang *et al.*, "Neuroprotection in a 6-hydroxydopamine-lesioned Parkinson model using lactoferrin-modified nanoparticles," *J. Gene Med.*, vol. 11, no. 9, pp. 754–763, 2009.
- [140] R. Huang *et al.*, "Gene therapy using lactoferrin-modified nanoparticles in a rotenone-induced chronic Parkinson model," *J. Neurol. Sci.*, vol. 290, no. 1–2, pp. 123–130, 2010.
- [141] O. Lindvall and A. Björklund, "Cell Therapeutics in Parkinson's Disease," *Neurotherapeutics*, vol. 8, no. 4, pp. 539–548, 2011.

- [142] S. S. Davis, "Biomedical applications of nanotechnology--implications for drug targeting and gene therapy.," *Trends Biotechnol.*, vol. 15, no. 6, pp. 217–24, 1997.
- [143] D. M. Yurek, A. M. Fletcher, T. H. Kowalczyk, L. Padegimas, and J. Cooper, "NIH Public Access," vol. 18, no. 10, pp. 1183–1196, 2011.
- [144] D. F. Bondi ML, Craparo EF, Giammona G, "Brain-targeted solid lipid nanoparticles containing riluzole: preparation, characterization and biodistribution," *Nanomedicine (Lond)*, vol. 5, no. 1, pp. 25–32, 2010.
- [145] V. Mazibuko, Zamanzima Choonara, Yahya E. Kumar, Pradeep Du Toit, Lisa C. Modi, Girish Naidoo, Dinesh Pillay, "A review of the potential role of nano-enabled drug delivery technologies in amyotrophic lateral sclerosis: lessons learned from other neurodegenerative disorders.," *Pharm Sci.*, vol. 104, no. 4, pp. 1213–1229, 2015.
- [146] A. Basso and D. Frenkel, "Reversal of axonal loss and disability in a mouse model of progressive multiple sclerosis," *J. Clin. Invest.*, vol. 118, no. 4, pp. 1532–43, 2008.
- [147] Y. Diebold and M. Calonge, "Progress in Retinal and Eye Research Applications of nanoparticles in ophthalmology," *Prog. Retin. Eye Res.*, vol. 29, no. 6, pp. 596–609, 2010.
- [148] P. G. Puglia C, Offerta A, Carbone C, Bonina F, Pignatello R, "Lipid nanocarriers (LNC) and their applications in ocular drug delivery," *Curr Med Chem*, vol. 22, no. 13, pp. 1589–1602, 2015.
- [149] Y. Weng, J. Liu, S. Jin, W. Guo, X. Liang, and Z. Hu, "Nanotechnology-based strategies for treatment of ocular disease," *Acta Pharm. Sin. B*, vol. 7, no. 3, pp. 281–291, 2017.
- [150] G. Abrego *et al.*, "Biopharmaceutical profile of pranoprofen-loaded PLGA nanoparticles containing hydrogels for ocular administration," *Eur. J. Pharm. Biopharm.*, vol. 95, pp. 261–270, 2015.
- [151] R. Asasutjarit, T. Theerachayanan, P. Kewsuwan, S. Veeranodha, A.

- Fuongfuchat, and G. C. Ritthidej, "Development and Evaluation of Diclofenac Sodium Loaded-N-Trimethyl Chitosan Nanoparticles for Ophthalmic Use," *AAPS PharmSciTech*, vol. 16, no. 5, pp. 1013–1024, 2015.
- [152] A. Fabiano, P. Chetoni, and Y. Zambito, "Mucoadhesive nano-sized supramolecular assemblies for improved pre-corneal drug residence time," *Drug Dev. Ind. Pharm.*, vol. 41, no. 12, pp. 2069–2076, 2015.
- [153] N. S. El-salamounia and R. M. Farida, "SM Gr up Recent Drug Delivery Systems for Treatment," pp. 1–13, 2016.
- [154] M. M. Ibrahim, A.-E. H. Abd-Elgawad, O. A.-E. Soliman, and M. M. Jablonski, "Natural Bioadhesive Biodegradable Nanoparticle-Based Topical Ophthalmic Formulations for Management of Glaucoma," *Transl. Vis. Sci. Technol.*, vol. 4, no. 3, p. 12, 2015.
- [155] et al. Pan Q, Xu Q, Boylan NJ, "Corticosteroid-loaded biodegradable nanoparticles for prevention of corneal allograft rejection in rats," *J Control Release*, vol. 201, pp. 32–40, 2015.
- [156] R. R. Joseph and S. S. Venkatraman, "Drug delivery to the eye: what benefits do nanocarriers offer?," *Nanomedicine*, vol. 12, no. 6, pp. 683–702, 2017.
- [157] World Health Organisation, "Global Tuberculosis Report 2013," *Glob. Tuberc. Rep.*, vol. 1, 2013.
- [158] and R. S. N. Ji Young Yhee, Jintaek Im, "Advanced Therapeutic Strategies for Chronic Lung Disease Using Nanoparticle-Based Drug Delivery," *J Clin Med*, vol. 5, no. 9, p. 82, 2016.
- [159] Y. H. Lim, K. M. Tiemann, D. A. Hunstad, M. Elsabahy, and K. L. Wooley, "Polymeric nanoparticles in development for treatment of pulmonary infectious diseases," *Wiley Interdiscip. Rev. Nanomedicine Nanobiotechnology*, vol. 8, no. 6, pp. 842–871, 2016.
- [160] M. Nasr, M. Najlah, A. D'Emanuele, and A. Elhissi, "PAMAM dendrimers as aerosol drug nanocarriers for pulmonary delivery via nebulization," *Int. J. Pharm.*, vol. 461, no. 1–2, pp. 242–250, 2014.

- [161] R. Mohamud *et al.*, “The effects of engineered nanoparticles on pulmonary immune homeostasis,” *Drug Metab. Rev.*, vol. 46, no. 2, pp. 176–190, 2014.
- [162] S. Gera, Sonia; Sampathi, Sunitha; Dodoala, “Role of Nanoparticles in Drug Delivery and Regenerative Therapy for Bone Diseases,” *Curr. Drug Deliv.*, vol. 14, no. 7, pp. 904–916, 2017.
- [163] D. Alves Cardoso, J. A. Jansen, and S. C. G. Leeuwenburgh, “Synthesis and application of nanostructured calcium phosphate ceramics for bone regeneration,” *J. Biomed. Mater. Res. Part B Appl. Biomater.*, vol. 100B, no. 8, pp. 2316–2326, 2012.
- [164] Y. Ding, Xiaochu Wang, “Weak Bond-Based Injectable and Stimuli Responsive Hydrogels for Biomedical Applications,” *J Mater Chem B Mater Biol Med.*, vol. 5, no. 5, pp. 887–906, 2017.
- [165] O. Unal, Semra Ekren, Nazmi Sengil, Ahmet Z. Oktar, Faik N. Irmak, Ster Oral, Ozlem Sahin, Yesim M. Kilic, Osman Agathopoulos, Simeon Gunduz, “Synthesis, characterization, and biological properties of composites of hydroxyapatite and hexagonal boron nitride,” *J. Biomed. Mater. Res. Part B Appl. Biomater.*, vol. 00, pp. 000–000, 2017.
- [166] I. Ortega-Oller, M. Padiál-Molina, P. Galindo-Moreno, F. O’Valle, A. B. Jódar-Reyes, and J. M. Peula-García, “Bone Regeneration from PLGA Micro-Nanoparticles,” *Biomed Res. Int.*, vol. 2015, no. 1, 2015.
- [167] P. K. Park JS, Yi SW, Kim HJ, Kim SM, “Regulation of Cell Signaling Factors Using PLGA Nanoparticles Coated/Loaded with Genes and Proteins for Osteogenesis of Human Mesenchymal Stem Cells evaluations,” *ACS Appl Mater Interfaces*, vol. 8, no. 44, pp. 30387–30397, 2016.
- [168] W. H. Kong ZQ, Lin J, Yu M, Yu L, Li J, Weng W, Cheng K, “Enhanced loading and controlled release of rhBMP-2 in thin mineralized collagen coatings with the aid of chitosan nanospheres and its biological evaluations,” *J. Mater. Chem*, vol. 2, pp. 4572–4582, 2014.
- [169] U. H. Zhang SF, Kucharski C, Doschak MR, Sebald W, “Polyethylenimine-PEG coated albumin nanoparticles for BMP-2 delivery,” *Biomaterials*, vol. 31, pp.

952–963, 2010.

- [170] E. V. Giger, B. Castagner, and J. C. Leroux, “Biomedical applications of bisphosphonates,” *J. Control. Release*, vol. 167, no. 2, pp. 175–188, 2013.
- [171] X. J. Loh, T.-C. Lee, Q. Dou, and G. R. Deen, “Utilising inorganic nanocarriers for gene delivery,” *Biomater. Sci.*, vol. 4, no. 1, pp. 70–86, 2016.
- [172] S. Warabi, Y. Tachibana, M. Kumegawa, and Y. Hakeda, “Dexamethasone inhibits bone resorption by indirectly inducing apoptosis of the bone-resorbing osteoclasts via the action of osteoblastic cells,” *Cytotechnology*, vol. 35, no. 1, pp. 25–34, 2001.
- [173] B. M. A. Goncalves RM, Pereira ACL, Pereira IO, Oliveira MJ, “Macrophage response to chitosan/poly-(gamma-glutamic acid) nanoparticles carrying an anti-inflammatory drug,” *J. Mater. Sci. Mater.*, vol. 26, p. 81, 2015.
- [174] M. Hofmann-Antenbrink, D. W. Grainger, and H. Hofmann, “Nanoparticles in medicine : Current challenges facing inorganic nanoparticle toxicity assessments and standardizations,” *Nanomedicine Nanotechnology, Biol. Med.*, vol. 11, no. 7, pp. 1689–1694, 2015.
- [175] D. Alcantara and L. Josephson, “Magnetic nanoparticles for application in biomedical sensing,” *Front. Nanosci.*, vol. 4, no. 1, pp. 269–289, 2012.
- [176] D. K. Kim and J. Dobson, “Nanomedicine for targeted drug delivery,” *J. Mater. Chem.*, vol. 19, pp. 6294–9307, 2009.
- [177] P. Stepp, F. Thomas, P. R. Lockman, H. Chen, and A. J. Rosengart, “In vivo interactions of magnetic nanoparticles with the blood-brain barrier,” *J. Magn. Magn. Mater.*, vol. 321, no. 10, pp. 1591–1593, 2009.
- [178] V. Mailander and K. Landfester, “Interaction of nanoparticles with cells,” *Biomacromolecules*, vol. 10, no. 9, pp. 2379–2400, 2009.
- [179] D. K. Bandgar, S. T. Navale, M. Naushad, R. S. Mane, F. J. Stadler, and V. B. Patil, “Ultra-sensitive polyaniline-iron oxide nanocomposite room temperature flexible ammonia sensor,” *RSC Adv.*, vol. 5, no. 84, pp. 68964–68971, 2015.
- [180] K. Hola, Z. Markova, G. Zoppellaro, J. Tucek, and R. Zboril, “Tailored

functionalization of iron oxide nanoparticles for MRI, drug delivery, magnetic separation and immobilization of biosubstances,” *Biotechnol. Adv.*, vol. 33, no. 6, pp. 1162–1176, 2015.

- [181] S. D. Steichen, M. Caldorera-Moore, and N. A. Peppas, “A review of current nanoparticle and targeting moieties for the delivery of cancer therapeutics,” *Eur. J. Pharm. Sci.*, vol. 48, no. 3, pp. 416–427, 2013.
- [182] J. Xie and S. Jon, “Magnetic Nanoparticle-Based Theranostics,” *Theranostics*, vol. 2, no. 1, pp. 122–124, 2012.
- [183] G. Subbiahdoss *et al.*, “Acta Biomaterialia Magnetic targeting of surface-modified superparamagnetic iron oxide nanoparticles yields antibacterial efficacy against biofilms of gentamicin-resistant staphylococci,” *Acta Biomater.*, vol. 8, no. 6, pp. 2047–2055, 2012.
- [184] M. Mahmoudi, S. Sant, B. Wang, S. Laurent, and T. Sen, “Superparamagnetic iron oxide nanoparticles (SPIONs): Development, surface modification and applications in chemotherapy,” *Adv. Drug Deliv. Rev.*, vol. 63, no. 1–2, pp. 24–46, 2011.
- [185] H. L. Karlsson, J. Gustafsson, P. Cronholm, and L. Möller, “Size-dependent toxicity of metal oxide particles-A comparison between nano- and micrometer size,” *Toxicol. Lett.*, vol. 188, no. 2, pp. 112–118, 2009.
- [186] S. Laurent and M. Mahmoudi, “Superparamagnetic iron oxide nanoparticles: Promises for diagnosis and treatment of cancer,” *Int. J. Mol. Epidemiol. Genet.*, vol. 2, no. 4, pp. 367–390, 2011.
- [187] Z. Bakhtiary, A. A. Saei, M. J. Hajipour, M. Raoufi, O. Vermesh, and M. Mahmoudi, “Targeted superparamagnetic iron oxide nanoparticles for early detection of cancer: Possibilities and challenges,” *Nanomedicine Nanotechnology, Biol. Med.*, vol. 12, no. 2, pp. 287–307, 2016.
- [188] A. Espinosa, R. Di Corato, J. Kolosnjaj-Tabi, P. Flaud, T. Pellegrino, and C. Wilhelm, “Duality of Iron Oxide Nanoparticles in Cancer Therapy: Amplification of Heating Efficiency by Magnetic Hyperthermia and Photothermal Bimodal Treatment,” *ACS Nano*, vol. 10, no. 2, pp. 2436–2446,

2016.

- [189] S. Zanganeh *et al.*, “Iron oxide nanoparticles inhibit tumour growth by inducing pro-inflammatory macrophage polarization in tumour tissues,” *Nat. Nanotechnol.*, vol. 11, no. 11, pp. 986–994, 2016.
- [190] S. M. Moghimi, A. C. Hunter, and J. C. Murray, “Long-Circulating and Target-Specific Nanoparticles : Theory to Practice,” *Pharmacol. Rev.*, vol. 53, no. 2, pp. 283–318, 2001.
- [191] A. Curtis and C. Wilkinson, “Nanotechniques and approaches in biotechnology,” *Trends Biotechnol.*, vol. 19, no. 3, pp. 97–101, 2001.
- [192] J. Panyam and V. Labhasetwar, “Biodegradable nanoparticles for drug and gene delivery to cells and tissue,” *Adv. Drug Deliv. Rev.*, vol. 55, no. 3, pp. 329–347, 2003.
- [193] R. Hachani *et al.*, “Polyol synthesis, functionalisation, and biocompatibility studies of superparamagnetic iron oxide nanoparticles as potential MRI contrast agents,” *Nanoscale*, vol. 8, no. 6, pp. 3278–3287, 2016.
- [194] Y.-X. J. Wang, “Superparamagnetic iron oxide based MRI contrast agents: Current status of clinical application.,” *Quant. Imaging Med. Surg.*, vol. 1, no. 1, pp. 35–40, 2011.
- [195] A. Szpak *et al.*, “T1–T2Dual-modal MRI contrast agents based on superparamagnetic iron oxide nanoparticles with surface attached gadolinium complexes,” *J. Nanoparticle Res.*, vol. 16, no. 11, pp. 1–11, 2014.
- [196] P. Parhi, C. Mohanty, and S. K. Sahoo, “Nanotechnology-based combinational drug delivery: an emerging approach for cancer therapy,” *Drug Discovery Today*, vol. 17, no. 17–18. Elsevier Ltd, pp. 1044–1052, 2012.
- [197] W. Wu, C. Jiang, and V. A. L. Roy, “Recent progress in magnetic iron oxide-semiconductor composite nanomaterials as promising photocatalysts,” *Nanoscale*, vol. 7, no. 1, pp. 38–58, 2015.
- [198] W. Wu, Z. Wu, T. Yu, C. Jiang, and W. S. Kim, “Recent progress on magnetic iron oxide nanoparticles: Synthesis, surface functional strategies and biomedical

- applications,” *Sci. Technol. Adv. Mater.*, vol. 16, no. 2, 2015.
- [199] A. K. Gupta and M. Gupta, “Synthesis and surface engineering of iron oxide nanoparticles for biomedical applications,” *Biomaterials*, vol. 26, no. 18, pp. 3995–4021, 2005.
- [200] A. K. Gupta, R. R. Naregalkar, V. D. Vaidya, and M. Gupta, “Recent advances on surface engineering of magnetic iron oxide nanoparticles and their biomedical applications,” *Nanomedicine*, vol. 2, no. 1, pp. 23–39, 2007.
- [201] J. R. McCarthy, K. a Kelly, E. Y. Sun, and R. Weissleder, “Targeted delivery of multifunctional magnetic nanoparticles,” *Nanomedicine (Lond)*, vol. 2, no. 2, pp. 153–167, 2007.
- [202] E. Duguet, S. Vasseur, S. Mornet, and J.-M. Devoisselle, “Magnetic nanoparticles and their applications in medicine,” *Nanomedicine (Lond)*, vol. 1, no. 2, pp. 157–168, 2006.
- [203] L. Douziech-Eyrolles *et al.*, “Nanovectors for anticancer agents based on superparamagnetic iron oxide nanoparticles,” *Int J Nanomedicine*, vol. 2, no. 4, pp. 541–550, 2007.
- [204] John Dobson, “Magnetic Nanoparticles for Drug Delivery,” *Drug Dev. Resarch*, vol. 67, pp. 55–60, 2006.
- [205] C. Sun, J. Lee, and M. Zhang, “Magnetic nanoparticles in MR imaging and drug delivery,” *Adv. Drug Deliv. Rev.*, vol. 60, no. 11, pp. 1252–1265, 2008.
- [206] X.-H. Peng *et al.*, “Targeted magnetic iron oxide nanoparticles for tumor imaging and therapy,” *Int. J. Nanomedicine*, vol. 3, no. 3, pp. 311–321, 2008.
- [207] A. Ito, Y. Kuga, H. Honda, H. Kikkawa, and A. Horiuchi, “Magnetite nanoparticle-loaded anti-HER2 immunoliposomes for combination of antibody therapy with hyperthermia,” *Cancer Lett.*, vol. 212, pp. 167–175, 2004.
- [208] K. Bourzac, “Carrying drugs,” *Nature*, vol. 491, 2012.
- [209] M. L. Etheridge and J. C. Bischof, “Optimizing magnetic nanoparticle based thermal therapies within the physical limits of heating,” *Ann. Biomed. Eng.*, vol. 41, no. 1, pp. 78–88, 2013.

- [210] V. Zavisova *et al.*, “Encapsulation of indomethacin in magnetic biodegradable polymer nanoparticles,” *J. Magn. Magn. Mater.*, vol. 311, no. 1 SPEC. ISS., pp. 379–382, 2007.
- [211] S. Purushotham and R. V. Ramanujan, “Thermoresponsive magnetic composite nanomaterials for multimodal cancer therapy,” *Acta Biomater.*, vol. 6, no. 2, pp. 502–510, 2010.
- [212] O. Oral *et al.*, “Effect of Varying Magnetic Fields on Targeted Gene Delivery of Nucleic Acid-Based Molecules,” *Ann. Biomed. Eng.*, vol. 43, no. 11, pp. 2816–2826, 2015.
- [213] C. Plank, F. Scherer, U. Schillinger, C. Bergemann, and M. Anton, “Magnetofection: enhancing and targeting gene delivery with superparamagnetic nanoparticles and magnetic fields,” *J. Liposome Res.*, vol. 13, no. 1, pp. 29–32, 2003.
- [214] S. C. McBain, H. H. P. Yiu, and J. Dobson, “Magnetic nanoparticles for gene and drug delivery,” *Int. J. Nanomedicine*, vol. 3, no. 2, pp. 169–180, 2008.
- [215] A. Ito, M. Shinkai, H. Honda, and T. Kobayashi, “Medical application of functionalized magnetic nanoparticles,” *J. Biosci. Bioeng.*, vol. 100, no. 1, pp. 1–11, 2005.
- [216] M. Babincova, P. Babinec, and C. Bergemann, “High-Gradient Magnetic Capture of Ferrofluids: Implications for Drug Targeting and Tumor Embolization,” vol. 56, no. Z.Naturforsch., pp. 909–911, 2001.
- [217] Y. X. J. Wang, S. M. Hussain, and G. P. Krestin, “Superparamagnetic iron oxide contrast agents: Physicochemical characteristics and applications in MR imaging,” *Eur. Radiol.*, vol. 11, no. 11, pp. 2319–2331, 2001.
- [218] R. R. T. Ragheb *et al.*, “Induced clustered nanoconfinement of superparamagnetic iron oxide in biodegradable nanoparticles enhances transverse relaxivity for targeted theranostics,” *Magn. Reson. Med.*, vol. 70, no. 6, pp. 1748–1760, 2013.
- [219] S. Prijic and G. Sersa, “Magnetic nanoparticles as targeted delivery systems in

- oncology,” *Radiol. Oncol.*, vol. 45, no. 1, pp. 1–16, 2011.
- [220] M. Caldorera-Moore, N. Guimard, L. Shi, and K. Roy, “Designer nanoparticles: Incorporating size, shape, and triggered release into nanoscale drug carriers,” *Expert Opin Drug Deliv*, vol. 7, no. 4, pp. 479–495, 2010.
- [221] L. T. Lu *et al.*, “Synthesis of magnetic cobalt ferrite nanoparticles with controlled morphology, monodispersity and composition: The influence of solvent, surfactant, reductant and synthetic conditions,” *Nanoscale*, vol. 7, no. 46, pp. 19596–19610, 2015.
- [222] Y. Jun, J. Choi, and J. Cheon, “Heterostructured magnetic nanoparticles: their versatility and high performance capabilities,” *Chem. Commun. (Camb)*, no. 12, pp. 1203–1214, 2007.
- [223] N. Sahiner, N. Pekel, P. Akkas, and O. Güven, “Amidoximation and Characterization of New Complexing Hydrogels Prepared From N-Vinyl 2-Pyrrolidone/Acrylonitrile Systems,” *J. Macromol. Sci. Part A*, vol. 37, no. 10, pp. 1159–1172, 2000.
- [224] D. Kandasamy, Ganeshlenin; Maity, “Recent advances in superparamagnetic iron oxide nanoparticles (SPIONs) for in vitro and in vivo cancer nanotheranostics,” *Int. J. Pharm.*, no. 496, pp. 191–218, 2015.
- [225] J. S. Weinstein *et al.*, “Superparamagnetic iron oxide nanoparticles: diagnostic magnetic resonance imaging and potential therapeutic applications in neurooncology and central nervous system inflammatory pathologies, a review,” *J. Cereb. blood flow Metab.*, vol. 30, no. 1, pp. 15–35, 2010.
- [226] Z. Wu, Y. Du, H. Xue, Y. Wu, and B. Zhou, “Aluminum induces neurodegeneration and its toxicity arises from increased iron accumulation and reactive oxygen species (ROS) production,” *Neurobiol. Aging*, vol. 33, no. 1, pp. 1–12, 2012.
- [227] P. B. Santhosh and N. P. Ulrih, “Multifunctional superparamagnetic iron oxide nanoparticles: Promising tools in cancer theranostics,” *Cancer Lett.*, vol. 336, no. 1, pp. 8–17, 2013.

- [228] S. Laurent *et al.*, “Magnetic Iron Oxide Nanoparticles: Synthesis, Stabilization, Vectorization, Physicochemical Characterizations, and Biological Applications,” *Chem. Rev.*, vol. 108, pp. 2064–2110, 2008.
- [229] L. H. Reddy, J. L. Arias, J. Nicolas, and P. Couvreur, “magnetic nanoparticles: Design and Characterization, toxicity and biocompatibility, pharmaceutical and biomedical applications,” *Chem. Rev.*, vol. 112, pp. 5818–5878, 2012.
- [230] J. H. Park, G. Saravanakumar, K. Kim, and I. C. Kwon, “Targeted delivery of low molecular drugs using chitosan and its derivatives,” *Adv. Drug Deliv. Rev.*, vol. 62, no. 1, pp. 28–41, 2010.
- [231] A. H. Faraji and P. Wipf, “Nanoparticles in cellular drug delivery,” *Bioorganic Med. Chem.*, vol. 17, no. 8, pp. 2950–2962, 2009.
- [232] R. Singh and J. W. Lillard, “Nanoparticle-based targeted drug delivery,” *Exp. Mol. Pathol.*, vol. 86, no. 3, pp. 215–223, 2009.
- [233] M. O. Aviles, A. D. Ebner, and J. a. Ritter, “In vitro study of magnetic particle seeding for implant-assisted-magnetic drug targeting: Seed and magnetic drug carrier particle capture,” *J. Magn. Magn. Mater.*, vol. 321, no. 10, pp. 1586–1590, 2009.
- [234] L. Xu, M.-J. Kim, K.-D. Kim, Y.-H. Choa, and H.-T. Kim, “Surface modified Fe₃O₄ nanoparticles as a protein delivery vehicle,” *Colloids Surfaces A Physicochem. Eng. Asp.*, vol. 350, no. 1–3, pp. 8–12, 2009.
- [235] A. K. Gupta and A. S. Curtis, “Surface modified superparamagnetic nanoparticles for drug delivery: interaction studies with human fibroblasts in culture,” *J Mater Sci Mater Med*, vol. 15, no. 4, pp. 493–496, 2004.
- [236] H. Cao, J. He, L. Deng, and X. Gao, “Fabrication of cyclodextrin-functionalized superparamagnetic Fe₃O₄/amino-silane core-shell nanoparticles via layer-by-layer method,” *Appl. Surf. Sci.*, vol. 255, no. 18, pp. 7974–7980, 2009.
- [237] J. J. Lin *et al.*, “Folic acid-Pluronic F127 magnetic nanoparticle clusters for combined targeting, diagnosis, and therapy applications,” *Biomaterials*, vol. 30, no. 28, pp. 5114–5124, 2009.

- [238] J. Cheng *et al.*, “Formulation of functionalized PLGA-PEG nanoparticles for in vivo targeted drug delivery,” *Biomaterials*, vol. 28, no. 5, pp. 869–876, 2007.
- [239] M. Nadeem, M. Ahmad, M. S. Akhtar, and A. Shaari, “Magnetic Properties of Polyvinyl Alcohol and Doxorubicine Loaded Iron Oxide Nanoparticles for Anticancer Drug Delivery Applications,” *PLoS One*, vol. 11, no. 6, pp. 1–12, 2016.
- [240] M. Khalkhali, K. Rostamizadeh, S. Sadighian, F. Khoeini, and M. Naghibi, “The impact of polymer coatings on magnetite nanoparticles performance as MRI contrast agents : a comparative study,” *DARU J. Pharm. Sci.*, pp. 1–12, 2015.
- [241] F. Dilnawaz, A. Singh, C. Mohanty, and S. K. Sahoo, “Dual drug loaded superparamagnetic iron oxide nanoparticles for targeted cancer therapy,” *Biomaterials*, vol. 31, no. 13, pp. 3694–3706, 2010.
- [242] K. Chatterjee, S. Sarkar, K. Jagajjanani Rao, and S. Paria, “Core/shell nanoparticles in biomedical applications,” *Adv. Colloid Interface Sci.*, vol. 209, pp. 8–39, 2014.
- [243] S. Yu *et al.*, “Magnetic and pH-sensitive nanoparticles for antitumor drug delivery,” *Colloids Surfaces B Biointerfaces*, vol. 103, pp. 15–22, 2013.
- [244] L. M. Lacava *et al.*, “Use of magnetic resonance to study biodistribution of dextran-coated magnetic fluid intravenously administered in mice,” *J. Magn. Magn. Mater.*, vol. 252, no. 1–3 SPEC. ISS., pp. 367–369, 2002.
- [245] J. Chomoucka, J. Drbohlavova, D. Huska, V. Adam, R. Kizek, and J. Hubalek, “Magnetic nanoparticles and targeted drug delivering,” *Pharmacol. Res.*, vol. 62, no. 2, pp. 144–149, 2010.
- [246] J. Drbohlavova, R. Hrdy, V. Adam, R. Kizek, O. Schneeweiss, and J. Hubalek, “Preparation and properties of various magnetic nanoparticles,” *Sensors*, vol. 9, no. 4, pp. 2352–2362, 2009.
- [247] P. J. Cregg, K. Murphy, and A. Mardinoglu, “Calculation of nanoparticle capture efficiency in magnetic drug targeting,” *J. Magn. Magn. Mater.*, vol. 320, no. 23, pp. 3272–3275, 2008.

- [248] D. S. Wang, J. G. Li, H. P. Li, and F. Q. Tang, "Preparation and drug releasing property of magnetic chitosan-5-fluorouracil nano-particles," *Trans. Nonferrous Met. Soc. China (English Ed.)*, vol. 19, no. 5, pp. 1232–1236, 2009.
- [249] S. Parvin, J. Matsui, E. Sato, and T. Miyashita, "Side-chain effect on Langmuir and Langmuir-Blodgett film properties of poly(N-alkylmethacrylamide)-coated magnetic nanoparticle," *J. Colloid Interface Sci.*, vol. 313, no. 1, pp. 128–134, 2007.
- [250] I. Cicha, L. Scheffler, A. Ebenau, S. Lyer, C. Alexiou, and M. Goppelt-Struebe, "Mitoxantrone-loaded superparamagnetic iron oxide nanoparticles as drug carriers for cancer therapy: Uptake and toxicity in primary human tubular epithelial cells," *Nanotoxicology*, vol. 5390, no. February 2016, pp. 1–10, 2015.
- [251] N. Lee, D. Yoo, D. Ling, M. H. Cho, T. Hyeon, and J. Cheon, "Iron Oxide Based Nanoparticles for Multimodal Imaging and Magneto-responsive Therapy," *Chem. Rev.*, vol. 115, pp. 10637–10689, 2015.
- [252] D. Ling, N. Lee, and T. Hyeon, "Chemical Synthesis and Assembly of Uniformly Sized Iron Oxide Nanoparticles for Medical Applications," *Acc. Chem. Res.*, vol. 48, pp. 1276–1285, 2015.
- [253] S. H. Koenig and K. E. Kellar, "Theory of $1/T_1$ and $1/T_2$ NMRD profiles of solutions of magnetic nanoparticles," *Magn. Reson. Med.*, vol. 34, no. 2, pp. 227–233, 1995.
- [254] A. Masoudi, H. R. Madaah Hosseini, S. M. Seyed Reyhani, M. A. Shokrgozar, M. A. Oghabian, and R. Ahmadi, "Long-term investigation on the phase stability, magnetic behavior, toxicity, and MRI characteristics of superparamagnetic Fe/Fe-oxide core/shell nanoparticles," *Int. J. Pharm.*, vol. 439, no. 1–2, pp. 28–40, 2012.
- [255] T. K. Jain, J. Richey, M. Strand, D. L. Leslie-Pelecky, C. a. Flask, and V. Labhasetwar, "Magnetic nanoparticles with dual functional properties: Drug delivery and magnetic resonance imaging," *Biomaterials*, vol. 29, no. 29, pp. 4012–4021, 2008.
- [256] H. Xie *et al.*, "Lactoferrin-conjugated superparamagnetic iron oxide

- nanoparticles as a specific MRI contrast agent for detection of brain glioma in vivo,” *Biomaterials*, vol. 32, no. 2, pp. 495–502, 2011.
- [257] C. Rūmenapp, B. Gleich, and A. Haase, “Magnetic nanoparticles in magnetic resonance imaging and diagnostics,” *Pharm. Res.*, vol. 29, no. 5, pp. 1165–1179, 2012.
- [258] F. Yazdani, B. Fattahi, and N. Azizi, “Journal of Magnetism and Magnetic Materials Synthesis of functionalized magnetite nanoparticles to use as liver targeting MRI contrast agent,” vol. 406, pp. 207–211, 2016.
- [259] Y. Huang, K. Mao, B. Zhang, and Y. Zhao, “Superparamagnetic iron oxide nanoparticles conjugated with folic acid for dual target-specific drug delivery and MRI in cancer theranostics,” *Mater. Sci. Eng. C*, vol. 70, pp. 763–771, 2017.
- [260] J. E. Rosen, L. Chan, D. Shieh, and F. X. Gu, “Iron oxide nanoparticles for targeted cancer imaging and diagnostics,” *Nanomedicine Nanotechnology, Biol. Med.*, vol. 8, no. 3, pp. 275–290, 2012.
- [261] A. E. Deatsch and B. A. Evans, “Heating efficiency in magnetic nanoparticle hyperthermia,” *J. Magn. Magn. Mater.*, vol. 354, pp. 163–172, 2014.
- [262] R. Ghosh *et al.*, “Induction heating studies of Fe₃O₄ magnetic nanoparticles capped with oleic acid and polyethylene glycol for hyperthermia,” *J. Mater. Chem.*, vol. 21, p. 13388, 2011.
- [263] D. Chang *et al.*, “Biologically targeted magnetic hyperthermia: Potential and limitations,” *Front. Pharmacol.*, vol. 9, no. AUG, 2018.
- [264] V. M. Khot, A. B. Salunkhe, N. D. Thorat, R. S. Ningthoujam, and S. H. Pawar, “Induction heating studies of dextran coated MgFe₂O₄ nanoparticles for magnetic hyperthermia,” *Dalt. Trans.*, vol. 42, no. 4, pp. 1249–1258, 2013.
- [265] Suriyanto, E. Y. K. Ng, and S. D. Kumar, “Physical mechanism and modeling of heat generation and transfer in magnetic fluid hyperthermia through Néelian and Brownian relaxation: a review,” *Biomed. Eng. Online*, vol. 16, no. 1, p. 36, 2017.
- [266] I. Obaidat, B. Issa, and Y. Haik, “Magnetic Properties of Magnetic Nanoparticles for Efficient Hyperthermia,” *Nanomaterials*, vol. 5, no. 1, pp. 63–89, 2015.

- [267] J. van der Zee, Z. Vujaskovic, M. Kondo, and T. Sugahara, "The Kadota Fund International Forum 2004 - Clinical group consensus," *Int. J. Hyperth.*, vol. 24, no. 2, pp. 111–122, 2008.
- [268] R. A. C. A. Dias A.M.G.C. , Hussain A. , Marcos A.S., "A biotechnological perspective on the application of iron oxide magnetic colloids modified with polysaccharides," *Biotechnol. Adv.*, vol. 29, pp. 142–155, 2011.
- [269] R. Hergt and S. Dutz, "Magnetic particle hyperthermia-biophysical limitations of a visionary tumour therapy," *J. Magn. Magn. Mater.*, vol. 311, no. 1 SPEC. ISS., pp. 187–192, 2007.
- [270] S. Laurent, S. Dutz, U. O. Häfeli, and M. Mahmoudi, "Magnetic fluid hyperthermia: Focus on superparamagnetic iron oxide nanoparticles," *Adv. Colloid Interface Sci.*, vol. 166, no. 1–2, pp. 8–23, 2011.
- [271] S. Balivada *et al.*, "A/C magnetic hyperthermia of melanoma mediated by iron(0)/iron oxide core/shell magnetic nanoparticles: a mouse study.," *BMC Cancer*, vol. 10, p. 119, 2010.
- [272] E. Ruiz-Hernández, A. Baeza, and M. Vallet-Regí, "Smart Drug Delivery through DNA / Magnetic Nanoparticle Gates," *ACS Nano*, vol. 5, no. 2, pp. 1259–1266, 2011.
- [273] J. L. Hood, M. J. Scott, and S. A. Wickline, "Maximizing exosome colloidal stability following electroporation," *Anal. Biochem.*, vol. 448, no. 1, pp. 41–49, 2014.
- [274] R. S. Rachakatla *et al.*, "Attenuation of Mouse Melanoma by A/C Magnetic Field after Delivery of Bi- Magnetic Nanoparticles by Neural Progenitor Cells," *ACS Nano*, vol. 4, no. 12, pp. 7093–7104, 2010.
- [275] J. Hamzehalipour Almaki, R. Nasiri, A. Idris, M. Nasiri, F. A. Abdul Majid, and D. Losic, "Trastuzumab-decorated nanoparticles for in vitro and in vivo tumor-targeting hyperthermia of HER2+ breast cancer," *J. Mater. Chem. B*, vol. 5, no. 35, pp. 7369–7383, 2017.
- [276] P. Kumari, B. Ghosh, and S. Biswas, "Nanocarriers for cancer-targeted drug

- delivery,” *J. Drug Target.*, vol. 24, no. 3, pp. 179–191, 2016.
- [277] D. Vainauska, S. Kozireva, A. Karpovs, M. Cistjakovs, and M. Barisevs, “A novel approach for nucleic acid delivery into cancer cells A Novel Approach for Nucleic Acid Delivery Into Cancer Cells,” *Med.*, vol. 48, no. 6, pp. 324–9, 2012.
- [278] J. D. Byrne, T. Betancourt, and L. Brannon-Peppas, “Active targeting schemes for nanoparticle systems in cancer therapeutics,” *Adv. Drug Deliv. Rev.*, vol. 60, pp. 1615–1626, 2008.
- [279] A. Beduneau, P. Saulnier, and J.-P. Benoit, “Active targeting of brain tumors using nanocarriers,” *Biomaterials*, vol. 28, pp. 4947–4967, 2007.
- [280] F. Scherer *et al.*, “Magnetofection: enhancing and targeting gene delivery by magnetic force in vitro and in vivo,” *Gene Ther.*, vol. 9, pp. 102–109, 2002.
- [281] R. Bazak, M. Hourri, S. El Achy, S. Kamel, and T. Refaat, “Cancer active targeting by nanoparticles: a comprehensive review of literature,” *J. Cancer Res. Clin. Oncol.*, vol. 141, no. 5, pp. 769–784, 2015.
- [282] J. Wang *et al.*, “Quantitative Examination of the Active Targeting Effect: The Key Factor for Maximal Tumor Accumulation and Retention of Short-Circulated Biopolymeric Nanocarriers,” *Bioconjug. Chem.*, vol. 28, no. 5, pp. 1351–1355, 2017.
- [283] J. Fang, H. Nakamura, and H. Maeda, “The EPR effect : Unique features of tumor blood vessels for drug delivery , factors involved , and limitations and augmentation of the effect ☆,” *Adv. Drug Deliv. Rev.*, vol. 63, no. 3, pp. 136–151, 2011.
- [284] H. Maeda, J. Wu, T. Sawa, Y. Matsumura, and K. Hori, “Tumor vascular permeability and the EPR effect in macromolecular therapeutics: A review,” *J. Control. Release*, vol. 65, no. 1–2, pp. 271–284, 2000.
- [285] S. K. Sahoo *et al.*, “Pegylated zinc protoporphyrin: A water-soluble heme oxygenase inhibitor with tumor-targeting capacity,” *Bioconjug. Chem.*, vol. 13, no. 5, pp. 1031–1038, 2002.
- [286] T. Stylianopoulos, “EPR-effect: utilizing size-dependent nanoparticle delivery to

- solid tumors,” *Ther. Deliv.*, vol. 4, no. 4, pp. 421–423, 2013.
- [287] Y. Sato *et al.*, “Innovative Technologies in Nanomedicines: From Passive Targeting to Active Targeting/From Controlled Pharmacokinetics to Controlled Intracellular Pharmacokinetics,” *Macromol. Biosci.*, vol. 17, no. 1, pp. 1–16, 2017.
- [288] R. Bazak, M. Houri, S. El Achy, W. Hussein, and T. Refaat, “Passive targeting of nanoparticles to cancer: A comprehensive review of the literature,” *Mol. Clin. Oncol.*, pp. 904–908, 2014.
- [289] K. Cho, X. Wang, S. Nie, Z. Chen, and D. M. Shin, “Therapeutic nanoparticles for drug delivery in cancer,” *Clin. Cancer Res.*, vol. 14, no. 5, pp. 1310–1316, 2008.
- [290] Z. M. Yigit, Mehmet V, Anna Moore, “Magnetic Nanoparticles for Cancer Diagnosis and Therapy,” *Pharm. Res.*, vol. 29, pp. 1180–1188, 2012.
- [291] J. L. Arias, V. Gallardo, M. A. Ruiz, and Á. V. Delgado, “Magnetite/poly(alkylcyanoacrylate) (core/shell) nanoparticles as 5-Fluorouracil delivery systems for active targeting,” *Eur. J. Pharm. Biopharm.*, vol. 69, no. 1, pp. 54–63, 2008.
- [292] E. Gravel, J. Ogier, T. Arnauld, N. MacKiewicz, F. Ducongé, and E. Doris, “Drug delivery and imaging with polydiacetylene micelles,” *Chem. - A Eur. J.*, vol. 18, no. 2, pp. 400–408, 2012.
- [293] A. J. Cole, V. C. Yang, and A. E. David, “Cancer theranostics: The rise of targeted magnetic nanoparticles,” *Trends Biotechnol.*, vol. 29, no. 7, pp. 323–332, 2011.
- [294] A. J. Cole, A. E. David, J. Wang, C. J. Galbán, and V. C. Yang, “Magnetic brain tumor targeting and biodistribution of long-circulating PEG-modified, cross-linked starch-coated iron oxide nanoparticles,” *Biomaterials*, vol. 32, no. 26, pp. 6291–6301, 2011.
- [295] J. Park *et al.*, “Biomaterials Polymer e iron oxide composite nanoparticles for EPR-independent drug delivery,” *Biomaterials*, vol. 101, pp. 285–295, 2016.

- [296] A. S. Lübbe, C. Bergemann, W. Huhnt, T. Fricke, and H. Riess, "Predinical Experiences Drug Targeting : Tolerance and Efficacy," *Cancer Res.*, vol. 56, pp. 4694–4701, 1996.
- [297] B. Chertok *et al.*, "Iron oxide nanoparticles as a drug delivery vehicle for MRI monitored magnetic targeting of brain tumors," *Biomaterials*, vol. 29, no. 4, pp. 487–496, 2008.
- [298] T. N. Ito, Ritsuko, Yoshiharu Machida, Takanori Sannan, "Magnetic granules: a novel system for specific drug delivery to esophageal mucosa in oral administration," *Int. J. Pharm.*, vol. 61, no. 1–2, pp. 109–117, 1990.
- [299] A. S. Lübbe *et al.*, "Clinical Experiences with Magnetic Drug Targeting: A Phase I Study with 4'-Epidoxorubicin in 14 Patients with Advanced Solid Tumors in 14 Patients with Advanced Solid Tumors," *Cancer Res.*, pp. 4686–4693, 1996.
- [300] M. A. Busquets, R. Sabaté, and J. Estelrich, "Potential applications of magnetic particles to detect and treat Alzheimer's disease," pp. 1–10, 2014.
- [301] H. Amiri, K. Saeidi, P. Borhani, A. Manafirad, M. Ghavami, and V. Zerbi, "Alzheimer's disease: Pathophysiology and applications of magnetic nanoparticles as MRI theranostic agents," *ACS Chem. Neurosci.*, vol. 4, no. 11, pp. 1417–1429, 2013.
- [302] S. Niu *et al.*, "Inhibition by multifunctional magnetic nanoparticles loaded with alpha-synuclein RNAi plasmid in a Parkinson's disease model," *Theranostics*, vol. 7, no. 2, pp. 344–356, 2017.
- [303] R. Jurgons, C. Seliger, a Hilpert, L. Trahms, S. Odenbach, and C. Alexiou, "Drug loaded magnetic nanoparticles for cancer therapy," *J. Phys. Condens. Matter*, vol. 18, no. 38, pp. S2893–S2902, 2006.
- [304] M. A. Erickson and W. A. Banks, "Blood-brain barrier dysfunction as a cause and consequence of Alzheimer's disease.," *J. Cereb. Blood Flow Metab.*, vol. 33, no. 10, pp. 1500–13, 2013.
- [305] J. Kreuter, "Nanoparticulate systems for brain delivery of drugs," *Adv. Drug Deliv. Rev.*, vol. 64, no. SUPPL., pp. 213–222, 2012.

- [306] P. R. Lockman, R. J. Mumper, M. A. Khan, and D. D. Allen, "Nanoparticle technology for drug delivery across the blood-brain barrier.," *Drug Dev. Ind. Pharm.*, vol. 28, no. 1, pp. 1–13, 2002.
- [307] W. M. Pardridge, "Drug and Gene Delivery to the BrainThe Vascular Route," *Neuron*, vol. 36, no. 4, pp. 555–558, 2002.
- [308] C. Wang, L. Qiao, Q. Zhang, H. Yan, and K. Liu, "Enhanced cell uptake of superparamagnetic iron oxide nanoparticles through direct chemisorption of FITC-Tat-PEG600-b-poly(glycerol monoacrylate)," *Int. J. Pharm.*, vol. 430, no. 1–2, pp. 372–380, 2012.
- [309] A. K. Gupta and S. Wells, "Surface-Modified Superparamagnetic Nanoparticles for Drug Delivery: Preparation, Characterization, and Cytotoxicity Studies," *IEEE Trans. Nanobioscience*, vol. 3, no. 1, pp. 66–73, 2004.
- [310] C. Fonseca, S. Simões, and R. Gaspar, "Paclitaxel-loaded PLGA nanoparticles: Preparation, physicochemical characterization and in vitro anti-tumoral activity," *J. Control. Release*, vol. 83, no. 2, pp. 273–286, 2002.
- [311] J. M. Chan *et al.*, "PLGA-lecithin-PEG core-shell nanoparticles for controlled drug delivery," *Biomaterials*, vol. 30, no. 8, pp. 1627–1634, 2009.
- [312] D. Couto *et al.*, "Biodistribution of polyacrylic acid-coated iron oxide nanoparticles is associated with proinflammatory activation and liver toxicity," *J. Appl. Toxicol.*, vol. 36, pp. 1321–1331, 2016.
- [313] D. Lachowicz *et al.*, "Biocompatible and fluorescent superparamagnetic iron oxide nanoparticles with superior magnetic properties coated with charged polysaccharide derivatives," *Colloids Surfaces B Biointerfaces*, vol. 150, pp. 402–407, 2017.
- [314] C. Janko *et al.*, "Strategies to optimize the biocompatibility of iron oxide nanoparticles ??? ???SPIONs safe by design???", *J. Magn. Magn. Mater.*, vol. 431, pp. 281–284, 2017.
- [315] G. Cordova, S. Attwood, R. Gaikwad, F. Gu, and Z. Leonenko, "Magnetic Force Microscopy Characterization of Superparamagnetic Iron Oxide Nanoparticles,"

Nano Biomed Eng, vol. 6, no. 1, pp. 31–39, 2014.

- [316] F. Xiong *et al.*, “A Functional Iron Oxide Nanoparticles Modified with PLA-PEG-DG as Tumor-Targeted MRI Contrast Agent,” *Pharm. Res.*, vol. 34, no. 8, pp. 1683–1692, 2017.
- [317] C. Alexiou *et al.*, “Targeting cancer cells: Magnetic nanoparticles as drug carriers,” *Eur. Biophys. J.*, vol. 35, no. 5, pp. 446–450, 2006.
- [318] N. Cui and S.-H. Zhu, “Monoclonal antibody-tagged polyethylenimine (PEI)/poly(lactide) (PLA) nanoparticles for the enhanced delivery of doxorubicin in HER-positive breast cancers,” *RSC Adv.*, vol. 6, pp. 79822–79829, 2016.
- [319] R. Vivek *et al.*, “HER2 Targeted Breast Cancer Therapy with Switchable ‘off/On’ Multifunctional ‘smart’ Magnetic Polymer Core-Shell Nanocomposites,” *ACS Appl. Mater. Interfaces*, vol. 8, no. 3, pp. 2262–2279, 2016.
- [320] K. Pala, A. Serwotka, F. Jeleń, P. Jakimowicz, and J. Otlewski, “Tumor-specific hyperthermia with aptamer-tagged superparamagnetic nanoparticles,” *Int. J. Nanomedicine*, vol. 9, no. 1, pp. 67–76, 2013.
- [321] N. V. Jadhav *et al.*, “Synthesis of oleic acid functionalized Fe₃O₄ magnetic nanoparticles and studying their interaction with tumor cells for potential hyperthermia applications,” *Colloids Surfaces B Biointerfaces*, vol. 108, pp. 158–168, 2013.
- [322] A. C. Silva *et al.*, “Application of hyperthermia induced by superparamagnetic iron oxide nanoparticles in glioma treatment,” *Int. J. Nanomedicine*, vol. 6, pp. 591–603, 2011.
- [323] C. M. Curtin, E. G. Tierney, K. Mcsorley, S. A. Cryan, G. P. Duffy, and F. J. O’Brien, “Combinatorial gene therapy accelerates bone regeneration: Non-viral dual delivery of VEGF and BMP2 in a collagen-nanohydroxyapatite scaffold,” *Adv. Healthc. Mater.*, vol. 4, no. 2, pp. 223–227, 2015.
- [324] K. L. Jackson *et al.*, “Preservation of forelimb function by UPF1 gene therapy in a rat model of TDP-43-induced motor paralysis,” *Gene Ther.*, vol. 22, no. 1, pp.

20–28, 2015.

- [325] A. Mangraviti *et al.*, “Polymeric nanoparticles for nonviral gene therapy extend brain tumor survival in vivo,” *ACS Nano*, vol. 9, no. 2, pp. 1236–1249, 2015.
- [326] A. Georgiadis *et al.*, “Development of an optimized AAV2/5 gene therapy vector for Leber congenital amaurosis owing to defects in RPE65,” *Gene Ther.*, vol. 23, no. 12, pp. 857–862, 2016.
- [327] S. Palfi *et al.*, “Long-term safety and tolerability of ProSavin, a lentiviral vector-based gene therapy for Parkinson’s disease: A dose escalation, open-label, phase 1/2 trial,” *Lancet*, vol. 383, no. 9923, pp. 1138–1146, 2014.
- [328] R. G. Crystal, “Adenovirus: The First Effective *In Vivo* Gene Delivery Vector,” *Hum. Gene Ther.*, vol. 25, no. 1, pp. 3–11, 2014.
- [329] R. E. MacLaren *et al.*, “Retinal gene therapy in patients with choroideremia: Initial findings from a phase 1/2 clinical trial,” *Lancet*, vol. 383, no. 9923, pp. 1129–1137, 2014.
- [330] P. Agrawal *et al.*, “Fast, Efficient, and Gentle Transfection of Human Adherent Cells in Suspension,” *ACS Appl. Mater. Interfaces*, vol. 8, no. 14, pp. 8870–8874, 2016.
- [331] H. Yin, R. L. Kanasty, A. A. Eltoukhy, A. J. Vegas, J. R. Dorkin, and D. G. Anderson, “Non-viral vectors for gene-based therapy,” *Nat. Rev. Genet.*, vol. 15, no. 8, pp. 541–555, 2014.
- [332] M. Ramamoorth and A. Narvekar, “Non viral vectors in gene therapy - An overview,” *J. Clin. Diagnostic Res.*, vol. 9, no. 1, pp. GE01-GE06, 2015.
- [333] A. A. M. Elsherbini, M. Saber, M. Aggag, A. El-Shahawy, and H. A. A. Shokier, “Magnetic nanoparticle-induced hyperthermia treatment under magnetic resonance imaging,” *Magn. Reson. Imaging*, vol. 29, no. 2, pp. 272–280, 2011.
- [334] S. Majidi *et al.*, “Magnetic nanoparticles: Applications in gene delivery and gene therapy,” *Artif. Cells, Nanomedicine, Biotechnol.*, vol. 43, no. November, pp. 1–8, 2015.
- [335] A. M. Eslaminejad Touba, Nouredin Nematollahi-Mahani Seyed, “Glioblastoma

- Targeted Gene Therapy Based on pEGFP/p53-Loaded Superparamagnetic Iron Oxide Nanoparticles,” *Curr. Gene Ther.*, vol. 17, no. 11, pp. 59–69, 2017.
- [336] P. I.-K. Uthaman Saji , Lee Sang Joon, Cherukula Kondareddy, Cho Chong-Su, “Polysaccharide-Coated Magnetic Nanoparticles for Imaging and Gene Therapy,” *Biomed Res. Int.*, 2015.
- [337] T. H. Xiao Shili, Castro Rita, Rodrigues João, Shi Xiangyang, “PAMAM Dendrimer/pDNA Functionalized-Magnetic Iron Oxide Nanoparticles for Gene Delivery,” *J. Biomed. Nanotechnol.*, vol. 11, no. 15, pp. 1370–1384, 2015.
- [338] Z. R. Stephen *et al.*, “Approach to Rapid Synthesis and Functionalization of Iron Oxide Nanoparticles for High Gene Transfection,” *ACS Appl. Mater. Interfaces*, vol. 8, no. 10, pp. 6320–6328, 2016.
- [339] W. Wu, Z. Wu, T. Yu, C. Jiang, and W. S. Kim, “Recent progress on magnetic iron oxide nanoparticles: Synthesis, surface functional strategies and biomedical applications,” *Sci. Technol. Adv. Mater.*, vol. 16, no. 2, pp. 59–69, 2015.
- [340] Wahajuddin and S. Arora, “Superparamagnetic iron oxide nanoparticles: Magnetic nanoplatforms as drug carriers,” *Int. J. Nanomedicine*, vol. 7, pp. 3445–3471, 2012.
- [341] F. Scherer *et al.*, “Magnetofection: Enhancing and targeting gene delivery by magnetic force in vitro and in vivo,” *Gene Ther.*, vol. 9, no. 2, pp. 102–109, 2002.
- [342] L. Zhang, Y. Li, J. C. Yu, Y. Y. Chen, and K. M. Chan, “Assembly of polyethylenimine-functionalized iron oxide nanoparticles as agents for DNA transfection with magnetofection technique,” *J. Mater. Chem. B*, vol. 2, no. 45, pp. 7936–7944, 2014.
- [343] M. Subramanian, A.-J. Tyler, E. Luther, E. Daniel, J. Lim, and J. Dobson, “Oscillating Magnet Array–Based Nanomagnetic Gene Transfection: A Valuable Tool for Molecular Neurobiology Studies,” *Nanomaterials*, vol. 7, no. 2, p. 28, 2017.
- [344] V. Camacho, J. M. ; Sosa, “Alternative method to calculate the magnetic field of

- permanent magnets with azimuthal symmetry,” *Rev. Mex. fisica E*, vol. 59, no. 1, pp. 8–17, 2013.
- [345] P. P. Askeland, D.R. ; Phule, *The Science and Engineering of Materials*. .
- [346] S. C. McBain *et al.*, “Magnetic nanoparticles as gene delivery agents: Enhanced transfection in the presence of oscillating magnet arrays,” *Nanotechnology*, vol. 19, no. 40, pp. 59–69, 2008.
- [347] Y. C. Lu, F. Y. Chang, S. J. Tu, J. P. Chen, and Y. H. Ma, “Cellular uptake of magnetite nanoparticles enhanced by NdFeB magnets in staggered arrangement,” *J. Magn. Magn. Mater.*, vol. 427, no. June 2016, pp. 71–80, 2017.
- [348] V. Kozlov, D. Avotina, V. Kasyanov, and M. Baryshev, “The Effect of Cyclic Movement of Magnets on the Sedimentation of Magnetic Nanoparticles in Magnetofection Devices: Computer Simulation,” *Sep. Sci. Technol.*, vol. 50, no. 5, pp. 767–771, 2015.
- [349] S. Huth *et al.*, “Insights into the mechanism of magnetofection using PEI-based magnetofectins for gene transfer,” *J. Gene Med.*, vol. 6, no. 8, pp. 923–936, 2004.